

Full-Wave Field Interactions of Nonuniform Transmission Lines

Dissertation

zur Erlangung des akademischen Grades

**Doktoringenieur
(Dr.-Ing.)**

von **Dipl.-Ing. Heiko Haase**

geb. am 30.01.1974 in Magdeburg

genehmigt durch die Fakultät für Elektrotechnik und Informationstechnik
der Otto-von-Guericke-Universität Magdeburg

Gutachter:

Univ.-Prof. Dr. rer. nat. habil. Jürgen Nitsch

Univ.-Prof. Dr.-Ing. Günter Wollenberg

Dr. Dr. E.h. Carl E. Baum

Prof. Dr.-Ing. habil. Albrecht Reibiger

Promotionskolloquium am 02.03.2005

“Just because something doesn’t do what you planned it to do doesn’t mean it’s useless.”

Thomas A. Edison (1847 - 1931)

Contents

Acknowledgment	9
Abstract	13
Zusammenfassung	15
List of Symbols	17
1 Introduction	21
2 Review of Maxwell's Theory and the Classical Transmission-Line Theory	27
2.1 Maxwell's Theory	27
2.1.1 Formulation of Maxwell's Equations	27
2.1.2 Retarded Electromagnetic Potentials	30
2.1.3 Calculating the Current and Charge Distributions	32
2.2 Classical Transmission-Line Theory	33
2.2.1 Properties of the TEM Mode	34
2.2.2 Telegrapher Equations	35
2.2.3 Field Coupling	37
2.2.4 Losses and Dielectrics	39
2.2.5 Nonuniformity and Multiconductor Lines	39
2.2.6 Different Representations	40
2.2.7 Solution	41
3 Equations for Nonuniform Transmission Lines	43
3.1 Conductor Geometry	44
3.1.1 Local Coordinate System	44
3.1.2 Tangential Surface Vector	46
3.1.3 Volume and Surface Integrals	47
3.2 Equations from Electrodynamics	47
3.2.1 Continuity Equation	48
3.2.2 Integral Equation	49

3.3	Representation as Matrix Equations	51
3.4	Current and Charge Trial Function	51
3.5	Generalized Telegrapher Equations	52
3.6	Parameters and Source Term Determination	54
3.6.1	Parameters	54
3.6.2	Source Terms	55
3.7	Solution of the Extended Telegrapher Equations	56
3.8	Going Back to Voltages ?	57
3.9	Discussion of the New Parameters	59
3.9.1	Wave Equation	59
3.9.2	Radiation Losses	59
3.9.3	Asymmetric Parameter Matrices	60
4	Numerical Evaluation of the Parameters	63
4.1	Starting Values for the Iteration	63
4.2	First Iteration	65
4.2.1	Taylor Series Expansion of the Product Integral	66
4.2.2	Eigenvalue Decomposition	68
4.3	Discussion of the Numerical Methods	69
5	Application	71
5.1	The Straight, Finite-Length Wire Above Ground	71
5.2	The Semi-Infinite Line	77
5.3	Field Coupling to an Infinite Line	78
5.4	The Skewed Wire Transmission Line	82
5.5	The Periodic Transmission Line	85
5.6	Cross Talk in a Nonuniform Multiconductor Transmission Line	90
6	Conclusion and Perspectives	93
	Appendices	95
A	Adaption of the Integral Equations to the Conductor Geometry	95
B	The Product Integral	99
B.1	The Differential Equation and its Solution	99
B.2	The Determination of the Product Integral	99
B.3	Inverse Operation	101
B.4	Calculation Rules for the Product Integral	101
C	Solutions for Some Important Integrals	103
C.1	Integrals Involving Powers of $\sqrt{x^2 + b^2}$	103

C.2	Integrals Involving Exponential and Power Functions	104
C.3	Integrals Involving Trigonometric and Exponential Functions	105
	Bibliography	107
	Curriculum Vitae	117

Acknowledgment

Someone who reads this thesis or only a part of it, will realize that it is almost impossible to handle all the work without a productive scientific environment. Therefore, I would like to thank all friends and colleagues who helped with many interesting discussions and helpful suggestions to let this thesis become reality.

First of all I would like to express my thanks to all members of our EMC group and the Institute of Fundamental Electrical Engineering and Electromagnetic Compatibility at the Otto-von-Guericke University in Magdeburg. In particular, I would like to thank my Professor J. Nitsch for his guidance, support, and for his constant stimulation for new scientific results. I would also like to thank my colleagues T. Steinmetz, Dr. H. G. Krauthäuser, Dr. F. Gronwald, and Dr. S. Tkachenko for fruitful discussions and valuable hints.

My thanks also goes to our colleagues abroad for their interest in the topic, their helpful remarks, criticism and precious insights. This includes Dr. C. Baum from the AFRL at Kirtland Air Force Base, USA, Dr. D. Giri from Pro-Tech, USA, Prof. F. Tesche from Clemson University, USA, and Dr. J.P. Parmantier from Onera, France.

I would also like to thank Prof. A. Stone, Prof. E. Schamiloglu, and Prof. S. Tyo for making my stay abroad at the Department of Electrical and Computer Engineering at the University of New Mexico, Albuquerque, USA a valuable and pleasant experience.

Furthermore, I am thankful for the financial support from the WIS, Munster (Federal Office of Defense Technology and Procurement) and for the support from the Helmut-Schmidt-Universität Hamburg, especially Prof. Lunderstädt and his staff. I also like to thank the Summa Foundation for the Summa Fellowship Award which allowed me to conduct my research at the University of New Mexico, Albuquerque, USA for eight months.

I appreciate the thorough reviews of the jury members, Dr. C. Baum, Prof. J. Nitsch, Prof. A. Reibiger, and Prof. G. Wollenberg.

Last but not least this all would not be possible without the care and backing from my family, especially from my parents Karin and Rainer Haase, my sister Tina Haase and my girlfriend Anja Baier.

A **transmission line** is the material medium or structure that forms all or part of a path from one place to another for directing the transmission of energy, such as electromagnetic waves or acoustic waves. Examples of transmission lines include wires, coaxial cables, dielectric slabs, optical fibers, and circular or rectangular closed waveguides.

Wikipedia – The Free Encyclopedia ([wikipedia.org](https://www.wikipedia.org))

Abstract

This thesis presents a new method to derive a generalized transmission-line theory, the *Transmission-Line Supertheory* (TLST). Besides a new kind of telegrapher equations, one also gets equations for the determination of the per-unit-length parameters and the source terms. The theory is directly based on Maxwell's theory. There are no restrictions (like the exclusive TEM mode) or simplifications, although a transition from the current and charge densities to the conductor currents and charges is performed.

The new theory is applicable to nonuniform transmission lines consisting of one or more wire-like conductors. It describes the propagation of electromagnetic waves along those lines as well as the coupling of external electromagnetic fields to the lines. It automatically includes all field modes and thus, covers all physical effects, including radiation losses, that can occur on a nonuniform transmission line. The principal structure of the telegrapher equations, which is known from the classical transmission-line theory, is preserved. The generalized telegrapher equations are still a system of first-order differential equations.

The per-unit-length parameters not only depend on the cross-sectional shape of the line but also depend on the whole geometry of the conductors and are determined by the solution of an integral equation. Due to frequency-dependent field modes and radiation losses the parameters become complex valued and frequency dependent, even for a perfectly conducting line.

The theoretical derivations are supported by several examples demonstrating the capabilities of the new theory.

Zusammenfassung

Diese Arbeit widmet sich der Aufstellung einer verallgemeinerten Leitungstheorie, der Transmission-Line Supertheory (Leitungssupertheorie). Neben einer neuen Art von Telegraphengleichungen erhält man Bestimmungsgleichungen für die verallgemeinerten Leitungsbeläge und Quellterme. Die Theorie basiert direkt auf den Maxwellschen Gleichungen. Es werden keine Einschränkungen und Vereinfachungen (z.B. ein exklusiver TEM Mode) vorgenommen. Es wird jedoch ein Übergang von Strom- und Ladungsdichten zu den Leiterströmen und -ladungen vollzogen.

Die neue Theorie ist auf beliebig ungleichförmige, aus einem oder mehreren drahtähnlichen Leitern bestehende Leitungen anwendbar. Es wird sowohl die Ausbreitung elektromagnetischer Wellen auf den Leitern als auch die Einkopplung externer Felder in die Leiter beschrieben. Alle relevanten Feldmoden sind automatisch berücksichtigt, d.h. alle wichtigen physikalischen Effekte, inklusive Abstrahlungsverluste werden korrekt modelliert. Dabei bleibt die von der klassischen Leitungstheorie her bekannte Struktur der Telegraphengleichungen erhalten, es handelt sich immer noch um ein System von Differentialgleichungen erster Ordnung.

Die Leitungsbeläge hängen nicht nur von dem jeweiligen Querschnitt ab, sondern von den geometrischen Charakteristika der gesamten Leitung. Sie werden durch die Lösung einer Integralgleichung berechnet. Wegen der frequenzabhängigen Feldmoden und der Strahlungsverluste sind die entsprechenden Leitungsbeläge komplexwertig und frequenzabhängig.

Die theoretischen Ausführungen werden durch Beispiele untermauert, die die neuen Möglichkeiten der Theorie aufzeigen.

List of Symbols

Here we list all symbols that are used throughout the thesis. Some symbols are used twice with different meaning. This is only in parts of single sections. The meaning of the symbols is also explained in the text.

\mathbf{A}	vector potential
\mathcal{B}, \mathbf{B}	magnetic field strength
\mathbf{B}^u	binormal unit vector
C', \mathbf{C}'	per-unit-length capacitance, per-unit-length capacitance matrix
\mathcal{C}	integration path
\mathbf{C}	spatial vector to conductor “center”
\mathcal{D}, \mathbf{D}	electric excitation
\mathbf{D}	damping coefficient
\mathbf{D}	diagonal matrix of eigenvalues
\mathcal{E}, \mathbf{E}	electric field strength
\mathcal{F}	Lorentz force
G', \mathbf{G}'	per-unit-length conductance, per-unit-length conductance matrix
G_1, G_2, G_3	integrals of the Green’s function
$H_0^{(2)}$	Hankel function of second kind
\mathcal{H}, \mathbf{H}	magnetic excitation
\mathbf{I}	matrix or vector, result of an integration
$\bar{\mathbf{I}}$	supermatrix, result of an integration
J_0	Bessel function of first kind
\mathcal{J}, \mathbf{J}	current density
K_0	modified Bessel function of second kind
L', \mathbf{L}'	per-unit-length inductance, per-unit-length inductance matrix
N	number of conductors in transmission lines
\mathbf{N}^u	normal unit vector
\mathbf{P}, \mathbf{P}^*	per-unit-length parameter matrix, blocks of a supermatrix
$\bar{\mathbf{P}}, \bar{\mathbf{P}}^*$	per-unit-length parameter supermatrix
Q	charge
R	distance between two points
R', \mathbf{R}'	per-unit-length resistance, per-unit-length resistance matrix

$S, \partial S$	open surface and its boundary
\mathbf{T}	tangential vector
\mathbf{T}^u	tangential unit vector
$V, \partial V$	volume and its closed surface
\mathbf{W}	dyadic product of eigenvectors
Y_0	Bessel function of second kind
a	wire radius, distance
b	spatial distance
d	eigenvalues of parameter matrix
$d_{\mathbf{J}}, d_{\rho}$	current density distribution, charge density distribution
$d\mathbf{a}, da$	vectorial surface element, scalar surface element
$d\mathbf{s}$	line element
dv	volume element
$\mathbf{e}_x, \mathbf{e}_y, \mathbf{e}_z$	unit vectors in Cartesian coordinates
f	frequency
f_{c_i}	geometric correction factor
h	wire height
i	index variable
i, \mathbf{i}	current and current vector
j	imaginary unit, $j^2 = -1$
j	index variable
k	wave number
$\overline{\mathbf{K}}$	supermatrix of integral kernel matrices
$k_c, k_l, \mathbf{k}_c, \mathbf{k}_l$	integral kernels and corresponding matrices
l	segment length
m	index variable
n	index variable
p	index variable
p	power
q, \mathbf{q}	per-unit-length charge and per-unit-length charge vector
r	radius, distance
t	time
u	length of tangential vector
v, \mathbf{v}	voltage and voltage vector
\mathbf{w}	eigenvector of parameter matrix
$\hat{\mathbf{x}}$	spatial vector to the surface of a conductor
\mathbf{x}, \mathbf{x}'	spatial vectors to observation and source points
z, \mathbf{z}	surface impedance and corresponding matrix
Γ	propagation matrix
α	angle
$\varepsilon, \varepsilon_0, \varepsilon_r$	permittivity (absolute, vacuum, relative)

κ	curvature
λ	wavelength
μ, μ_0, μ_r	permeability (absolute, vacuum, relative)
ω	angular frequency
φ	scalar potential
φ, Φ	quasivoltage
ρ	charge density
σ	electric conductivity
ζ	coordinate, curve parameter
$()^{(i)}$	incident
$()^{(k)}, ()^{(k+1)}$	quantity after the k -th or $(k + 1)$ -th iteration
$()^{\text{scat}}$	scattered
$()^u$	unit vector
$()_s$	source term
$()_t$	coefficient of trial function
$()_{\text{rad}}$	radiated

Chapter 1

Introduction

Since at least the 18th century electrical transmission lines are a fascinating as well as challenging object of scientists and engineers. In that period *Sir William Watson* tried to determine the speed of electricity. For this he conducted experiments involving a 6.4 km (12276 feet) long wire line, as shown in his sketch in Figure 1.1. Within the accuracy of the measuring equipment of that time, he found that the “velocity of electricity was instantaneous”. However, he noticed the electric resistance. His results were published in [Wat46, Wat48].

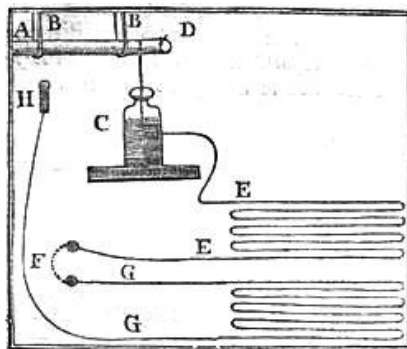


Figure 1.1: Illustration of Watsons experiments to determine the velocity of electricity.

Driven by the development of telegraphs and the desire for overseas communication, a mathematical description of the signal propagation along transmission lines was indispensable. A cornerstone was the contribution from *Sir William Thomson* a.k.a. Lord Kelvin. He established the “Law of retardation” in 1854. However, he only took into account the capacity and the resistance of the cable [Kel55].

In 1857 *Gustav Kirchhoff* published two papers [Kir57b, Kir57c] (see also [Kir57a, GA94] for an English translation) where he set up equations describing the motion of electricity in wires and conductors. In the first paper he formulated equations for the current and the charge based on an electric and a magnetic potential, which are

comparable to today's telegrapher equations. He also found that in a wire with negligible resistance, electricity propagates at the speed of light.

Later on, in 1874 *Oliver Heaviside* developed the well known transmission-line theory and the telegrapher equations [Hea51]. These equations are valid for a broad range of transmission lines. After these pioneering achievements numerous scientists contributed to the transmission-line theory and it was published in numerous excellent text books and reviews, e.g., [Mie00, Som64, KS64, Sch55, Kin55, DSH87, Col91, Pau94, Ung96, Fra97, TIK97, Rei02]. The theory was successfully applied to several fields in electrical engineering.

Although, the transmission-line theory is around for more than 130 years, it did not lose its relevance to current situations. High operating frequencies of modern electronic equipment turn even the smallest piece of wire into a transmission line with signal retardation, dispersion, attenuation, and distortion. Moreover, in today's electromagnetic environment transmission lines can pick up external electromagnetic fields which generate noise currents which are superimposed on the useful signals. The lines act not only as receiving antennas but can also radiate parts of the signal energy into the environment. Some of these effects are covered by the "classical transmission-line theory" (cTTL), some are not.

Heaviside showed that the transmission-line theory is a special case of Maxwell's theory. The key is the transverse electromagnetic mode (TEM mode), where the electric and magnetic fields are perpendicular to each other and perpendicular to the direction of propagation. With the assumption of an exclusive TEM mode propagating along a transmission line, one can, without any further approximations, find the telegrapher equations.

The exclusive TEM mode is only possible on an ideal transmission line. This line would be infinitely long, lossless, with parallel conductors, and would be excited at infinity. Already an excitation at a finite position produces other modes in the vicinity of the excitation and thus invalidates the cTTL. The same is true for finite lines, where usually other modes occur close to the terminations. Also losses in the conductors destroy the exclusive TEM mode, because longitudinal components of the electric field are present.

Nonetheless, for many applications, at least when the wavelength is much larger than the cross-sectional size of the line, the other modes decay exponentially, do not propagate and hence are negligible compared to the dominant TEM mode. In this case one speaks of a quasi-TEM mode. The cTTL gives excellent results that are in very good agreement with experiments as well as with analytical calculations which take into account all modes.

The TEM mode allows us to split the solution procedure into two separate steps. First, the so-called per-unit-length parameters of the transmission line are determined. For a uniform line these parameters only depend on the cross-sectional geometry of

the line. They describe the coupling between individual conductors as well as the propagation properties and thus fully characterize the transmission line. The second step is the solution of the governing equations, the telegrapher equations which are coupled partial first-order differential equations. The procedure for the computation of the results for these kinds of equations are very well known. For some important cases analytical solutions exist, for other cases usually numerical methods are used.

Things become much more complicated, if the transmission lines become nonuniform, i.e., if the conductors are not in parallel anymore and the cross section changes along the line. One can imagine that the field distributions become much more involved than for uniform lines. In the literature there is a host of publications concerning nonuniform transmission lines. Already Heaviside made some contributions [Hea25].

The majority of these papers discusses the solution procedure for the telegrapher equations with position-dependent parameters. Often the dependence is described by some simple mathematical function, e.g. linearly or exponentially varying parameters. Most papers do not clearly specify where these parameters come from, usually a TEM mode on the nonuniform transmission line is assumed. Recent publications on this topic include [BNS96, BNS97, Nit98, NG99] where the product integral [Gan84, DF79] is applied to formulate analytical solutions of the telegrapher equations for nonuniform multiconductor transmission lines.

There are several approaches to broaden the scope of the classical transmission-line theory, see [HNS03] and references therein, however, most of them work only in a certain low-frequency range. Many works [Kin55, Lam76, Lam77, GCT78, GC86, Get93, DZ88, TB94, LK99] are dedicated to the correction of the telegrapher equations when transmission lines with nonuniformities or discontinuities are under investigation. The models encompass abrupt bends, round bends, vertical risers, or the cross coupling between two skewed lines. For low frequencies (quasi-static case) the additional effects are modeled with the aid of lumped elements (L,C) or additional transmission lines that are connected to the actual line. Sometimes nonuniform lines are treated as if they were built of uniform segments, i.e., within each section the line is regarded to be uniform [OKH97].

There have been attempts to solve nonuniform transmission-line problems with higher mode effects using the cTTL. This is done by modeling a physical effect, e.g. radiation, which was beforehand excluded from the theory, by some additional term in the telegrapher equation [WtH97].

In the past few years considerable effort was put into the development of an extended transmission-line theory, which is not restricted to the TEM mode nor any other mode. Instead of extending the existing theory, the preferred way to go is to derive generalized equations directly from Maxwell's theory. Some of the approaches deal with special geometric characteristics of the conductors like sharp bends, vertical termination wires,

or field excitations that generate non-TEM modes [NHFY95, TRI99, TRI01, TN02, TRNS03, NT02, NT04c, NT04b]. Although these works show great improvements compared to the cTTL, they do not provide a general procedure to handle arbitrary nonuniform transmission lines; they concentrate on one specific problem.

In [Stu98] and [Stu99] two different approaches for the development of a generalized transmission-line theory, with interesting ideas are shown. Unfortunately, only the theoretical derivation is considered and no practical examples are presented.

A different approach is shown in [Mei03]. There a proof is given that the current distribution of a nonuniform transmission line is governed by a second-order differential equation. Then from known linearly independent solutions for the currents for different terminations it is possible to construct the coefficients of the differential equations which then become the per-unit-length parameters. The required solutions can be obtained numerically, e.g. with the method of moments (MoM).

The most recent contribution to this topic is [NT04a], where a modal decomposition based on a spatial Fourier series is used to formulate modal telegrapher equations, i.e. one for every current component. After solving these equations one needs to sum up the infinite Fourier series to get the real current. In [NT05] these results are compared with the results obtained with the procedures introduced in this thesis and a very good agreement can be observed.

This thesis presents a new method to derive a generalized transmission-line theory, the **Transmission-Line SuperTheory** (TLST) [Bau02]. Besides new telegrapher equations, one also gets equations for the determination of the per-unit-length parameters and the source terms. The theory is directly based on Maxwell's theory. There are no restrictions (like an exclusive TEM mode) or simplifications, although a transition from the current and charge densities to the conductor currents and charges is performed.

The new theory is applicable to nonuniform transmission lines consisting of one or more wire-like conductors. It describes the propagation of electromagnetic waves along those lines as well as the coupling of external electromagnetic fields to the lines. It automatically includes all field modes and thus, covers all physical effects, including radiation losses, that can occur on a nonuniform transmission line. The principal structure of the telegrapher equations is preserved; the generalized telegrapher equations are still a system of first-order differential equations. However, because, in the general case, the voltage is not the difference of two values of the scalar potential anymore, it is the path-dependent integral of the electric field strength, this quantity is replaced by the charge per unit length. The telegrapher equations are formulated in terms of the current and the charge per unit length. The parameters not only depend on the cross-sectional shape of the line but also depend on the whole geometry of the conductors and are determined by the solution of an integral equation. Due to frequency-dependent field modes and radiation losses the parameters become complex valued and frequency

dependent, even for a simple superconducting line.

The chapter following this introduction is dedicated to a short review of Maxwell's theory and the classical transmission-line equations with emphasis on the expressions related to the transmission-line supertheory. This theory is covered in Chapter 3 where an in-depth derivation is shown. Moreover, this chapter includes details on the computation of the parameters and the source terms. Possible numerical implementations of the algorithms are the subject of Chapter 4. The next chapter shows some interesting applications of the theory. Eventually in Chapter 6 the achievements of this work are summarized and conclusions are drawn.

Chapter 2

Review of Maxwell's Theory and the Classical Transmission-Line Theory

***Abstract** — In this chapter we will shortly review Maxwell's theory. Furthermore, we will provide equations for the electromagnetic potentials and derive an integral equation for the calculation of the current and charge density. These are prerequisites for the later development of the transmission-line supertheory. This chapter also covers a variant of the derivation of the classical transmission-line theory for a two-conductor line. It is based on the formulation of the fields of a TEM mode.*

2.1 Maxwell's Theory

2.1.1 Formulation of Maxwell's Equations

Electromagnetic phenomena are governed by a set of partial differential equations, named after *James Clerk Maxwell*. He refined the ideas of *Michael Faraday*, *André Marie Ampère* and others about electromagnetism. The first publication related to these equations dates back to 1864/65 [Max65], however, the most cited reference is his treatise [Max73] from 1873. Other scientists, such as *Oliver Heaviside*, purified the equations and formulated the theory in an axiomatic way. *Heinrich Hertz* experimentally verified the theoretical results.

The source of all electromagnetic fields clearly are charged particles. Some components of the fields arise already from static charges, others only exist if the charged particles are in motion, i.e. a current is flowing.

From a modern point of view there are only a few experimental observations like the conservation of charge, the conservation of the magnetic flux, the absence of magnetic monopoles, the Lorentz covariance of electromagnetics, and the existence of a force on fixed or moving charged particles, that are sufficient to formulate Maxwell's equations.

The former is usually expressed by the continuity equation

$$\operatorname{div} \mathcal{J} + \frac{\partial \rho}{\partial t} = 0. \quad (2.1)$$

Here \mathcal{J} is the current density and ρ is the charge density.

A direct consequence of this are the inhomogeneous Maxwell equations involving the electric and magnetic excitations \mathcal{D} and \mathcal{H} [HOR99]:

$$\operatorname{div} \mathcal{D} = \rho \quad (2.2)$$

and

$$\operatorname{curl} \mathcal{H} - \frac{\partial \mathcal{D}}{\partial t} = \mathcal{J}. \quad (2.3)$$

Historically these quantities are called dielectric displacement and magnetic field, respectively.

The existence of a force \mathcal{F} on charged particles with charge Q and velocity \mathbf{v} leads to the introduction of the electric and magnetic field strength \mathcal{E} and \mathcal{B} . The so-called Lorentz force is expressed by

$$\mathcal{F} = Q (\mathcal{E} + \mathbf{v} \times \mathcal{B}). \quad (2.4)$$

With the aid of the above mentioned physical observations one can find relations for these field strengths. The equations establish the homogeneous part of Maxwell's equations:

$$\operatorname{div} \mathcal{B} = 0 \quad (2.5)$$

and

$$\operatorname{curl} \mathcal{E} + \frac{\partial \mathcal{B}}{\partial t} = \mathbf{0}. \quad (2.6)$$

Finally, the materials where the fields reside determine the relation between the excitations and the corresponding field strengths. In general these can be rather complicated functions. We will restrict ourself to isotropic media, where the following holds:

$$\mathcal{D} = \varepsilon \mathcal{E} = \varepsilon_r \varepsilon_0 \mathcal{E} \quad (2.7)$$

$$\mathcal{B} = \mu \mathcal{H} = \mu_r \mu_0 \mathcal{H}, \quad (2.8)$$

where ε is the electric permittivity and μ the magnetic permeability.

There is also a relation between the current density and the electric field strength, which usually is a complicated and nonlinear function. The first term of a Taylor series of this function is a good approximation inside good conducting materials. This is also known as Ohm's Law and is written as

$$\mathcal{J} = \sigma \mathcal{E}. \quad (2.9)$$

Besides these equations, which all have a physical background, there are two important expressions originating in vector analysis. The first is the divergence theorem or Gauss' theorem. It connects the divergence of a vector field \mathbf{X} inside a volume V with this vector field \mathbf{X} on the closed surface (∂V) of that volume:

$$\oint_{\partial V} \mathbf{X} \cdot d\mathbf{a} = \int_V (\operatorname{div} \mathbf{X}) dv. \quad (2.10)$$

In this equations $d\mathbf{a}$ is pointing outward. The second expression is the curl theorem or Stokes' theorem. Here the vector field at the boundary ∂S of an open surface S is connected to the curl of that field on that surface:

$$\oint_{\partial S} \mathbf{X} \cdot d\mathbf{s} = \int_S (\operatorname{curl} \mathbf{X}) \cdot d\mathbf{a}. \quad (2.11)$$

If the divergence theorem is applied to the continuity equation one can derive an integral representation of this expression:

$$\oint_{\partial V} \mathcal{J} \cdot d\mathbf{a} + \int_V \frac{\partial \rho}{\partial t} dv = 0. \quad (2.12)$$

In the same manner integral expressions of Maxwell's equations can be found. By applying either the divergence or the curl theorem one gets

$$\oint_{\partial V} \mathcal{D} \cdot d\mathbf{a} = \int_V \rho dv \quad (2.13)$$

$$\oint_{\partial S} \mathcal{H} \cdot d\mathbf{s} - \int_S \frac{\partial \mathcal{D}}{\partial t} \cdot d\mathbf{a} = \int_S \mathcal{J} \cdot d\mathbf{a} \quad (2.14)$$

$$\oint_{\partial V} \mathcal{B} \cdot d\mathbf{a} = 0 \quad (2.15)$$

$$\oint_{\partial S} \mathcal{E} \cdot d\mathbf{s} + \int_S \frac{\partial \mathcal{B}}{\partial t} \cdot d\mathbf{a} = 0. \quad (2.16)$$

These equations must be satisfied for every well behaved volume and surface.

For many applications it is convenient to transform the above equations and quantities from the time domain into the frequency domain using the Fourier transformation

[MF53, Arf85, Kra99]. The transformation from time to frequency domain and back is done by applying the following integrals:

$$F(j\omega, \dots) = \int_{-\infty}^{\infty} \mathcal{F}(t, \dots) e^{-j\omega t} dt \quad (2.17)$$

$$\mathcal{F}(t, \dots) = \frac{1}{2\pi} \int_{-\infty}^{\infty} F(j\omega, \dots) e^{+j\omega t} d\omega. \quad (2.18)$$

This, however, is only possible for linear systems. We assume this linearity. Many equations become considerably simpler and solutions can be computed easier. For the transformation of Maxwell's equations the following rules may be used:

$$\mathcal{F}(t, \dots) \circ\text{--}\bullet F(j\omega, \dots) \quad (2.19)$$

$$\mathcal{F}(t, \dots) \circ\text{--}\bullet \mathbf{F}(j\omega, \dots) \quad (2.20)$$

$$\frac{\partial}{\partial t} \dots \circ\text{--}\bullet j\omega \dots \quad (2.21)$$

Then we get:

$$\operatorname{div} \mathbf{D} = \varrho \quad \oint_{\partial V} \mathbf{D} \cdot d\mathbf{a} = \int_V \varrho dv \quad (2.22)$$

$$\operatorname{div} \mathbf{B} = 0 \quad \oint_{\partial V} \mathbf{B} \cdot d\mathbf{a} = 0 \quad (2.23)$$

$$\operatorname{curl} \mathbf{H} - j\omega \mathbf{D} = \mathbf{J} \quad \oint_{\partial S} \mathbf{H} \cdot d\mathbf{s} - j\omega \int_S \mathbf{D} \cdot d\mathbf{a} = \int_S \mathbf{J} \cdot d\mathbf{a} \quad (2.24)$$

$$\operatorname{curl} \mathbf{E} + j\omega \mathbf{B} = \mathbf{0} \quad \oint_{\partial S} \mathbf{E} \cdot d\mathbf{s} + j\omega \int_S \mathbf{B} \cdot d\mathbf{a} = 0. \quad (2.25)$$

Furthermore, the continuity equation becomes

$$\operatorname{div} \mathbf{J} + j\omega \varrho = 0 \quad \oint_{\partial V} \mathbf{J} \cdot d\mathbf{a} + j\omega \int_V \varrho dv = 0. \quad (2.26)$$

Throughout the whole document we will stay in the frequency domain. The representation of the $j\omega$ dependence of the respective quantities will be omitted.

2.1.2 Retarded Electromagnetic Potentials

A common way to find solutions to Maxwell's equations is to express the field with the aid of potentials. The Helmholtz theorem [MF53] states that every, at infinity vanishing vector field can be expressed as the sum of the gradient of a scalar field and

the curl of a vector field. In the special case of the magnetic field \mathbf{B} the scalar field must be zero to satisfy (2.23). Thus we can write

$$\mathbf{B} = \text{curl } \mathbf{A}, \quad (2.27)$$

where \mathbf{A} is the vector potential. Inserting this into (2.25) gives the expression

$$\text{curl}(\mathbf{E} + j\omega\mathbf{A}) = \mathbf{0}, \quad (2.28)$$

which means that the term inside the parenthesis is a curl-free field. According to the Helmholtz theorem those fields can be represented by the gradient of a scalar potential or

$$\mathbf{E} = -\text{grad } \varphi - j\omega\mathbf{A}. \quad (2.29)$$

The homogeneous equations (2.23) and (2.25) are automatically fulfilled by the fields (2.27) and (2.29). If we insert these fields into the inhomogeneous equations (2.22) and (2.24) we get

$$\Delta\varphi + j\omega \text{div } \mathbf{A} = -\frac{\varrho}{\varepsilon} \quad (2.30)$$

$$\Delta\mathbf{A} - (j\omega)^2 \mu\varepsilon\mathbf{A} - \text{grad}(\text{div } \mathbf{A} + j\omega\mu\varepsilon\varphi) = -\mu\mathbf{J}. \quad (2.31)$$

Due to the gauge invariance of the fields [GN99] we are free to choose a condition for $\text{div } \mathbf{A}$. Usually the Coulomb gauge $\text{div } \mathbf{A} = 0$ or the Lorenz¹ gauge $\text{div } \mathbf{A} + j\omega\mu\varepsilon\varphi = 0$ is used. For our purposes the latter is more suitable. This condition decouples (2.30) and (2.31) and yields inhomogeneous wave equations for the potentials:

$$(\Delta + k^2) \varphi = -\frac{\varrho}{\varepsilon} \quad (2.32)$$

$$(\Delta + k^2) \mathbf{A} = -\mu\mathbf{J}. \quad (2.33)$$

The quantity $k = \omega\sqrt{\mu\varepsilon}$ is called the wave number. A solution of the above equations, which are elliptical partial differential equations, is, in general, obtained by finding appropriate Green's functions [Lin95, Dud94, Bal89]. The solutions can then be written as

$$\varphi(\mathbf{x}) = \frac{1}{\varepsilon} \int_V G(\mathbf{x}, \mathbf{x}') \varrho(\mathbf{x}') dv' \quad (2.34)$$

and

$$\mathbf{A}(\mathbf{x}) = \mu \int_V G(\mathbf{x}, \mathbf{x}') \mathbf{J}(\mathbf{x}') dv'. \quad (2.35)$$

¹Ludvig Lorenz published these equations in [Lor67b, Lor67a] first; some authors erroneously give credit to Hendrik A. Lorentz for this, see [vB91, NS01]

For the rather simple case of free space the Green's function can be found to be (see e.g. [Jac98])

$$G(\mathbf{x}, \mathbf{x}') = \frac{e^{-jkR}}{4\pi R} \quad (2.36)$$

with the distance $R = |\mathbf{x} - \mathbf{x}'|$. Because the Green's function contains the phase factor e^{-jkR} , which in time domain is a time delay, the potentials are called retarded potentials.

More complicated boundaries than free space with corresponding boundary conditions can be taken into account with the appropriate Green's function. Often this function is very complicated. For some cases, e.g., for an ideal ground plane with or without a dielectric layer or a corner, closed-form formulae of this function can be given. Mostly, these are linear combinations of terms of the type of the free-space Green's function. We will concentrate on those, however, whenever necessary also more complicated Green's functions can be used.

In (2.34) and (2.35) the integration must be carried out over the whole volume. The vector \mathbf{x}' points to the elementary volume element, where the integration is currently performed. The observation point, where the electromagnetic potentials and fields are computed is denoted by \mathbf{x} .

With the above equations the fields can be calculated when the field sources, i.e. the current and the charge densities, are known. However, the sources and the fields interact with each other, which usually makes the determination of the sources and fields a difficult problem [RW44].

2.1.3 Calculating the Current and Charge Distributions

In order to solve Maxwell's equations for real world problems often an integral equation is formulated. For this the total electric field strength \mathbf{E} is divided into two parts:

$$\mathbf{E} = \mathbf{E}^{\text{scat}} + \mathbf{E}^{(i)}. \quad (2.37)$$

The first is the scattered field \mathbf{E}^{scat} , generated by the currents and charges in the conductors of the structure under investigation. The second part is an external incident field $\mathbf{E}^{(i)}$ that is known. According to (2.29), the scattered field can be expressed with the aid of the scalar potential φ and the vector potential \mathbf{A} :

$$\mathbf{E} = -\text{grad } \varphi - j\omega\mathbf{A} + \mathbf{E}^{(i)}. \quad (2.38)$$

The terms for the potentials may now be replaced into this equation yielding an equation involving the total electric field, the current density and the charge density. The observation point \mathbf{x} , where the electric field strength is computed, is moved inside a

conductor, where a current is flowing. Then Ohm's law can be applied to eliminate the electric field strength. In combination with the continuity relation we get two equations with two unknowns:

$$\text{grad} \frac{1}{\varepsilon} \int_V G(\mathbf{x}, \mathbf{x}') \varrho(\mathbf{x}') dv' + j\omega\mu \int_V G(\mathbf{x}, \mathbf{x}') \mathbf{J}(\mathbf{x}') dv' + \frac{\mathbf{J}(\mathbf{x})}{\sigma} = \mathbf{E}^{(i)}(\mathbf{x}) \quad (2.39)$$

$$j\omega\varrho(\mathbf{x}) + \text{div} \mathbf{J}(\mathbf{x}) = 0. \quad (2.40)$$

These can be solved for \mathbf{J} and ϱ either analytically for special cases or in the general case numerically.

2.2 Classical Transmission-Line Theory

Contrary to the previously shown solution method for Maxwell's equations, a certain class of problems is solved by decomposing the fields into so-called modes. In particular this is done for cavities and closed waveguides. Every mode exhibits a certain pattern while the sum of all modes gives the actual field distribution. One of these modes is the **T**ransverse **E**lectro**M**agnetic (TEM) mode. There the field vectors are orthogonal to each other and to the propagation direction. This mode is very important because it occurs in many configurations, either alone or as the dominant mode.

Transmission lines are such configurations. In the ideal case they only support TEM modes. Those lines consist of two or more infinitely long and lossless conductors, with a constant cross section. Simple examples are, e.g., the two-wire line or a coaxial cable.

In this section we will derive equations for those lines, consisting of two conductors. In principle it is possible to perform the derivation for N conductors. However, this will complicate matters and not give any more information on fundamental principles of the transmission-line theory. The new equations are the so-called telegrapher equations, which describe the field propagation along the conductors with the aid of the voltage and the current.

For realistic conductors with losses and terminations other field modes are excited as well and usually exist on the transmission line. For low frequencies these modes are small, such that one can assume an "almost" TEM mode or quasi-TEM mode.

There are many different ways to derive these equations from Maxwell's theory, e.g., [Kin55, Pau94, Rei02]. Our approach requires a pure TEM mode on the line. With this assumption Maxwell's equations can be cast into the telegrapher equations. A completely different approach, based on the retarded potentials is shown by King [Kin55]. This derivation is a special case of our new theory presented in detail in Chapter 3.

2.2.1 Properties of the TEM Mode

Before we start, we will discuss some properties of the TEM mode. As mentioned already, the primary characteristic of this mode is the mutual orthogonality of the electric and magnetic fields and the propagation direction. We will give only a short overview over this field mode; reference [Col91] is an excellent source for more information on this subject.

Without loss of generality, let us assume that the propagation direction is along the z axis of a Cartesian coordinate system. Then the z components of the electric field strength and of the magnetic excitation vanish. For source free regions (i.e. $\mathbf{J} = \mathbf{0}$, $\rho = 0$) Maxwell's equations become

$$\operatorname{div} \mathbf{D} = 0 \quad (2.41)$$

$$\operatorname{div} \mathbf{B} = 0 \quad (2.42)$$

$$\operatorname{curl} \mathbf{E} + j\omega\mu\mathbf{H} = \mathbf{0} \quad (2.43)$$

$$\operatorname{curl} \mathbf{H} - j\omega\varepsilon\mathbf{E} = \mathbf{0}. \quad (2.44)$$

Taking into account the vanishing z components of the fields, the equations (2.43) and (2.44) reduce to

$$(\operatorname{curl} \mathbf{E}) \cdot \mathbf{e}_z = 0 \quad (2.45)$$

$$(\operatorname{curl} \mathbf{H}) \cdot \mathbf{e}_z = 0 \quad (2.46)$$

when dot multiplied with \mathbf{e}_z . This means both fields are curl free in a plane $z = \text{const}$ and thus can be represented by the product of scalar z -dependent functions g_e and g_h and transverse gradient fields:

$$\mathbf{E} = -g_e(z) \operatorname{grad} \varphi_e(x, y) \quad (2.47)$$

$$\mathbf{H} = -g_h(z) \operatorname{grad} \varphi_h(x, y). \quad (2.48)$$

One could say that the scalar, real valued functions determine the intensity of transverse field pattern which is given by the gradient expression. Furthermore, if (2.43) and (2.44) are cross multiplied with \mathbf{e}_z one gets

$$\frac{\partial \mathbf{E}}{\partial z} + j\omega\mu\mathbf{H} \times \mathbf{e}_z = \mathbf{0} \quad (2.49)$$

$$\frac{\partial \mathbf{H}}{\partial z} - j\omega\varepsilon\mathbf{E} \times \mathbf{e}_z = \mathbf{0} \quad (2.50)$$

which are the equations describing the propagation of the fields along the z axis. Note that (2.45) and (2.49) as well as (2.46) and (2.50) are identical to (2.43) and (2.44), respectively. They are decompositions into the transverse and longitudinal components.

With (2.49) the magnetic excitation can also be represented with the aid of the electric potential

$$\mathbf{H} = \frac{1}{j\omega\mu} (\mathbf{e}_z \times \text{grad } \varphi_e) \frac{\partial g_e}{\partial z}. \quad (2.51)$$

Thus both fields are given by the function g_e and the scalar potential φ_e .

It is quite simple to eliminate either \mathbf{H} or \mathbf{E} in (2.49) and (2.50). In both cases one gets a homogeneous wave equation, that can be solved with standard techniques. However, instead of doing this we will convert the equations into telegrapher equations, which represent the physical problem with the aid of the voltage and the current and then solve for these quantities.

2.2.2 Telegrapher Equations

Figure 2.1 shows an exemplary transmission line with two conductors. The cross-sectional shape of the conductors is arbitrary. If there is a pure TEM mode outside

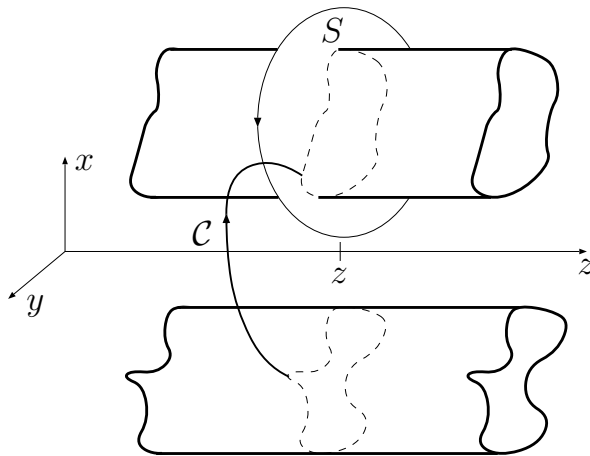


Figure 2.1: A uniform transmission line with integration paths.

of the conductors, the longitudinal component of the curl of the fields vanishes. The current in the conductors must be z directed. The conductor surface at $z = \text{const.}$ is an equipotential line. We can define a path independent electric voltage v as

$$v := \int_C \mathbf{E} \cdot d\mathbf{s}. \quad (2.52)$$

The path C is arbitrary and runs from the surface of one conductor to the other in the plane $z = \text{const.}$ We can also define an electric current as the closed path integral of

the magnetic excitation on the boundary of the open surface S

$$i := \oint_{\partial S} \mathbf{H} \cdot d\mathbf{s}. \quad (2.53)$$

Equation (2.49) is now integrated over the path \mathcal{C} , which yields

$$\frac{\partial v}{\partial z} + j\omega\mu \int_{\mathcal{C}} (\mathbf{H} \times \mathbf{e}_z) \cdot d\mathbf{s} = 0. \quad (2.54)$$

In this expression \mathbf{H} is replaced by (2.51) and we get

$$\frac{\partial v}{\partial z} + \frac{\partial g_e}{\partial z} \int_{\mathcal{C}} \text{grad } \varphi_e \cdot d\mathbf{s} = 0. \quad (2.55)$$

In order to derive an formula for $\frac{\partial g_e}{\partial z}$ we insert (2.51) into (2.53). After some simple rearrangements this gives

$$\frac{\partial g_e}{\partial z} = j\omega\mu \frac{i(z)}{\oint_{\partial S} (\mathbf{e}_z \times \text{grad } \varphi_e) \cdot d\mathbf{s}}, \quad (2.56)$$

which can be inserted into (2.55). This yields the first of the two telegrapher equations:

$$\frac{\partial v}{\partial z} + j\omega L' i(z) = 0 \quad (2.57)$$

where L' is the z -independent per-unit-length inductance defined by:

$$L' := \mu \frac{\int_{\mathcal{C}} \text{grad } \varphi_e \cdot d\mathbf{s}}{\oint_{\partial S} (\mathbf{e}_z \times \text{grad } \varphi_e) \cdot d\mathbf{s}}. \quad (2.58)$$

In order to get the second equation we integrate (2.50) over the boundary of the open surface S , which results in

$$\frac{\partial i}{\partial z} - j\omega\varepsilon \oint_{\partial S} (\mathbf{E} \times \mathbf{e}_z) \cdot d\mathbf{s} = 0. \quad (2.59)$$

Here \mathbf{E} is replaced by (2.47) giving

$$\frac{\partial i}{\partial z} - j\omega\varepsilon g_e \oint_{\partial S} (\mathbf{e}_z \times \text{grad } \varphi_e) \cdot d\mathbf{s} = 0. \quad (2.60)$$

An formula for g_e is obtained by either integrating (2.56) or by inserting (2.47) into (2.52):

$$g_e(z) = \frac{v(z)}{\int_{\mathcal{C}} \text{grad } \varphi_e \cdot d\mathbf{s}}. \quad (2.61)$$

If this is used to replace g_e in (2.60) we eventually get the second telegrapher equation

$$\frac{\partial i}{\partial z} + j\omega C' v(z) = 0, \quad (2.62)$$

where C' is the z -independent per-unit-length capacitance. This quantity is given by

$$C' := \varepsilon \frac{\oint_{\partial S} (\mathbf{e}_z \times \text{grad } \varphi_e) \cdot d\mathbf{s}}{\int_C \text{grad } \varphi_e \cdot d\mathbf{s}}. \quad (2.63)$$

The two telegrapher equations (2.57) and (2.62) are a system of coupled ordinary first-order differential equations which can be solved with standard algorithms. For the solution the per-unit-length parameters must be known. These coefficients can be determined with the aid of (2.58) and (2.63), which requires the knowledge of the two-dimensional potential field φ_e . To get an equation for the calculation of this function we take the divergence of (2.47), which must vanish in source free regions:

$$\text{div } \mathbf{E} = \text{div} (g_e \text{grad } \varphi_e) = 0 \quad (2.64)$$

$$\Delta \varphi_e = 0 \quad (2.65)$$

This means, at an arbitrary position z we have to solve the above Laplace equation. We have to take into account appropriate boundary conditions. At surfaces of the conductors the potential is the same everywhere, thus we may assign a potential of 1 V to the surface of one conductor and a potential of 0 V to the other. For the solution there are many different ways to go. Often the potential is regarded as the real or imaginary part of an analytic function $f(w)$ with $w = u + jv$, where the Laplace equation is automatically fulfilled. Then one needs to find a suitable function $f(w)$, where the equipotential lines coincide with the conductor boundaries. Often the conformal mapping approach is used.

One remarkable result of the derivation is that the above equations are valid for all frequencies, there are no restrictions.

2.2.3 Field Coupling

The prescribed approach does not include field coupling to the transmission lines. In general, external fields disturb the propagating TEM modes and excite additional modes. However, when the distance between the conductors is much smaller than the wavelength, one can assume a quasi-TEM mode which leads to coupling models for the transmission lines. There are three different models known in the literature [APG79, TSH65, Rac93] that all describe the same physics with different quantities. At least for a uniform surrounding medium they all give the same results. A good summary and discussion of all three models is published in [NR95], [Tes95], and [TIK97].

The telegrapher equations are extended by inhomogeneous terms v'_s and i'_s , which represent distributed current and voltage sources along the line and directly depend on the exciting fields. The telegrapher equations then become

$$\frac{\partial v}{\partial z} + j\omega L' i = v'_s \quad (2.66)$$

$$\frac{\partial i}{\partial z} + j\omega C' v = i'_s. \quad (2.67)$$

Depending on the used coupling model v and i represent either the total or the scattered voltage or current and the source terms depend on different components of the electric and magnetic fields. Figure 2.2 shows a uniform transmission line with field coupling. Details for the computation are shown in Table 2.1.

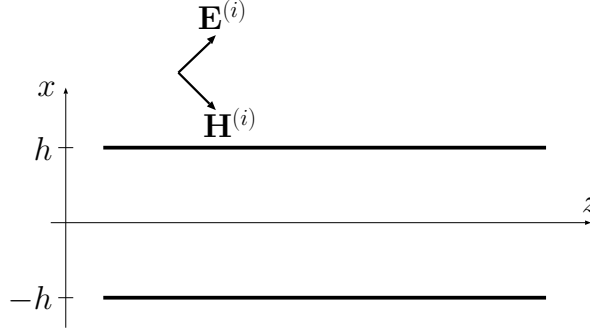


Figure 2.2: A uniform transmission line with field coupling.

Table 2.1: The field to transmission line coupling models.

Model	v	i	v'_s	i'_s
Agrawal [APG79]	scat.	tot.	$E_z^{(i)}(h, z) - E_z^{(i)}(-h, z)$	0
Taylor [TSH65]	tot.	tot.	$j\omega \int_{-h}^h B_y^{(i)} dx$	$-j\omega C' \int_{-h}^h E_x^{(i)} dx$
Rachidi [Rac93]	tot.	scat.	0	$-\frac{1}{L'} \int_{-h}^h \frac{\partial B_z^{(i)}}{\partial y} dx$

In the following we will restrict us to the Agrawal model, because it is closely related to the source terms in the integral equation for the electric field (2.39). Also it will occur in the generalized telegrapher equations in a generalized variant.

2.2.4 Losses and Dielectrics

The derivation for the telegrapher equations is done for a rather ideal case with lossless, infinitely long conductors embedded into a homogeneous, lossless medium. But almost all practical transmission lines have losses. If these losses are small one can speak of a quasi-TEM mode and introduce new quantities in the telegrapher equations:

$$\frac{\partial v}{\partial z} + (j\omega L' + R') i = v'_s \quad (2.68)$$

$$\frac{\partial i}{\partial z} + (j\omega C' + G') v = 0. \quad (2.69)$$

The quantities R' and G' are the per-unit-length resistance and the per-unit-length conductance and represent the losses in the conductor and in the surrounding media, respectively. In a very simple case the per-unit-length resistance is the DC resistance per unit length of the conductor. In general the determination of the loss terms is complicated and goes beyond the scope of this work. The reader is referred to the various, earlier mentioned publications on the transmission-line theory.

2.2.5 Nonuniformity and Multiconductor Lines

Already Heaviside [Hea25] recognized the possibility to make the parameters z dependent. This broadens the scope of the transmission-line theory and allows to apply it to nonuniform transmission lines. Many authors refined these ideas up to recent publications, e.g., [NBS92, BNS96, BS03, Ste05].

Note that these nonuniform transmission lines are different from those that are subject of this work. In the prescribed approach only a quasi-TEM mode is allowed whereas in this work a full-wave description is derived and thus all modes are allowed. Care must be taken because the term nonuniform transmission lines is used in both contexts. It refers to the geometrical nonuniformity, which is present in both cases.

The classical telegrapher equations can also be established for (nonuniform) multiconductor transmission lines (see e.g. [BLT78, KS64, Rei02]). We will, without any derivation, just give the results. The equations can be written in supermatrix notation:

$$\frac{\partial}{\partial z} \begin{bmatrix} \mathbf{v} \\ \mathbf{i} \end{bmatrix} + j\omega \underbrace{\begin{bmatrix} \mathbf{0} & \mathbf{L}'(z) + \frac{1}{j\omega} \mathbf{R}'(z) \\ \mathbf{C}'(z) + \frac{1}{j\omega} \mathbf{G}'(z) & \mathbf{0} \end{bmatrix}}_{\mathbf{P}_c} \begin{bmatrix} \mathbf{v} \\ \mathbf{i} \end{bmatrix} = \begin{bmatrix} \mathbf{v}'_s \\ \mathbf{0} \end{bmatrix}. \quad (2.70)$$

Here, for an N -conductor line, \mathbf{v} and \mathbf{i} are N -element column vectors of the conductor voltages and currents, respectively and \mathbf{v}'_s is the column vector of the distributed source terms. The $N \times N$ (z -dependent) matrices \mathbf{L}' , \mathbf{C}' , \mathbf{R}' , and \mathbf{G}' contain the per-unit-length inductances, capacitances, resistances, and conductances, respectively. Thus, for

an N -conductor transmission line we have $2N$ coupled ordinary differential equations of first order.

2.2.6 Different Representations

The telegrapher equations for (nonuniform) multiconductor transmission lines can be represented in many different forms [HNS03]. In addition to the one already shown, two more are of interest here. Instead of using the voltage and the current we might as well use the charge per unit length and the current. The first is connected to the latter by the continuity equation (see also (3.24)):

$$\frac{\partial}{\partial z} \mathbf{i}(z) + j\omega \mathbf{q}(z) = 0, \quad (2.71)$$

where \mathbf{q} is the column vector of the per-unit-length charges of the conductors. This relation can be inserted into (2.70) giving

$$\frac{\partial}{\partial z} \begin{bmatrix} \mathbf{q} \\ \mathbf{i} \end{bmatrix} + j\omega \begin{bmatrix} \mathbf{P}_{11} & \mathbf{P}_{12} \\ \mathbf{1} & \mathbf{0} \end{bmatrix} \begin{bmatrix} \mathbf{q} \\ \mathbf{i} \end{bmatrix} = \begin{bmatrix} \mathbf{q}'_s \\ \mathbf{0} \end{bmatrix} \quad (2.72)$$

with

$$\mathbf{P}_{11} = \left(\frac{\partial}{\partial z} \left(\mathbf{C}' + \frac{1}{j\omega} \mathbf{G}' \right) \right) \left(\mathbf{C}' + \frac{1}{j\omega} \mathbf{G}' \right)^{-1} \quad (2.73)$$

$$= \mathcal{D}_z \left(\mathbf{C}' + \frac{1}{j\omega} \mathbf{G}' \right) \quad (\text{see Appendix B.3}) \quad (2.74)$$

$$\mathbf{P}_{12} = \left(\mathbf{C}' + \frac{1}{j\omega} \mathbf{G}' \right) \left(\mathbf{L}' + \frac{1}{j\omega} \mathbf{R}' \right) \quad (2.75)$$

and

$$\mathbf{q}'_s = \left(\mathbf{C}' + \frac{1}{j\omega} \mathbf{G}' \right) \mathbf{v}'_s. \quad (2.76)$$

If the line is uniform and the parameters do not depend on z the matrix \mathbf{P}_{11} vanishes.

Instead with $2N$ differential equations of first order, the telegrapher equations can also be represented as N differential equations of second order. If we eliminate \mathbf{q} in (2.72) we get the wave equation for the current:

$$\left(\frac{\partial^2}{\partial z^2} - \mathbf{D} \frac{\partial}{\partial z} - \mathbf{\Gamma}^2 \right) \mathbf{i} = -j\omega \mathbf{q}_s \quad (2.77)$$

with

$$\mathbf{\Gamma}^2 = -\omega^2 \mathbf{P}_{12} \quad \text{and} \quad \mathbf{D} = -j\omega \mathbf{P}_{11}. \quad (2.78)$$

The matrix $\mathbf{\Gamma}$ is called the propagation matrix. For uniform lines it is independent of z ; for nonuniform lines it is a function of z . \mathbf{D} is a damping factor. The waves are damped when they propagate along the line because a part of the wave energy is reflected back to the beginning due to the nonuniformity. This coefficient vanishes for uniform lines because there are no reflections. Note that this damping is not caused by losses.

2.2.7 Solution

The solution of the telegrapher equations can be easily obtained by using standard methods for solving differential equations (e.g. [Pau94]). One common method in the frequency domain is to construct the solution with the aid of the matrix exponential. This is a special case of the product integral (Appendix B). See also Section 3.7 for more details on the solution of the telegrapher equations.

Chapter 3

Equations for Nonuniform Transmission Lines

Abstract — *This chapter deals with the development of the transmission-line supertheory. This theory describes the wave propagation along as well as the field coupling to nonuniform transmission lines. Starting from a geometrical description of the transmission-line conductors, in the course of the derivation, Maxwell's equations are cast into telegrapher equations with position-dependent per-unit-length parameters. The wave propagation is described with the aid of the current and the per-unit-length charge or the quasivoltage. There is no restriction to the (quasi-) TEM mode. Even radiation is accounted for.*

Preliminary Remarks Concerning Voltage, Potential, and Charge

The classical transmission-line theory connects the *voltage* and the *current* on a transmission line by a system of first-order differential equations. Although the voltage is a physical, measurable quantity it is not very well suited for generalized telegrapher equations. In the general case, the voltage does not only depend on the two points where it is measured or calculated, but also on the path taken to get from one point to the other. Only in special cases, e.g. in a plane perpendicular to a TEM-mode transmission line, the voltage is independent from that path. For a nonuniform line which supports arbitrary modes there is no such plane. Thus a replacement for the voltage is needed. There are at least two possibilities.

One of these possibilities is to choose the *scalar potential*. This quantity can be calculated at every point and depends only on the point itself. However, the scalar potential is a purely mathematical aid to calculate electromagnetic fields, has no physical meaning, and can not be measured. Moreover, it is a gauge-dependent value. The advantage is that the unit of the voltage remains in the telegrapher equations and the generalized telegrapher equations “feel” like the classical equations. Furthermore, the potential can be used to easily calculate the voltage on sections of the transmission line where only a TEM mode is supported.

The second possibility is to choose the *charge*. This is a physical quantity and the natural supplement to the current. One of the telegrapher equations would then become the adapted continuity equation, which is one of the fundamental laws of electrodynamics. Because only physical quantities are used the latter is the better choice. However, we will show how to convert the resulting equations to a form using the current and the scalar potential.

3.1 Conductor Geometry

Before we actually start deriving the theory we need a way to precisely specify the geometry of the nonuniform transmission lines. For that we borrow some techniques from differential geometry (see e.g. [O’N66]).

The position of a conductor i is given by a general space curve. The vector $\mathbf{C}_i(\zeta)$ points to that curve, which must be well behaved and two-times differentiable. For all conductors we choose the curve parameter to be the same. One side of the conductors, e.g. the beginning of the line, corresponds to the curve parameter ζ_0 and the other side coincides with the ζ_i . The conductors can have different lengths, can be bent or can have loops. There is no restriction on the shape of the conductor, as long as it can be described by a space curve.

One may raise the question, how to determine the space curve for a given conductor. There is no unique way, in fact, there are infinite possibilities. The most favorable way is to find a circular tube that tightly surrounds the conductor and choose the center line of this tube.

3.1.1 Local Coordinate System

A local coordinate system (see Figure 3.1) can be constructed using the so-called *Frenet* frame. This frame is composed of three vectors, the tangential unit vector $\mathbf{T}_i^u(\zeta)$, the normal unit vector $\mathbf{N}_i^u(\zeta)$ and the binormal unit vector $\mathbf{B}_i^u(\zeta)$. The tangential vector can be calculated by differentiating $\mathbf{C}_i(\zeta)$ with respect to ζ :

$$\mathbf{T}_i = \frac{\partial \mathbf{C}_i}{\partial \zeta}. \quad (3.1)$$

This vector is not a unit vector because the curve parameter is not the arc length, instead the unit vector \mathbf{T}_i^u is

$$\mathbf{T}_i^u(\zeta) = \frac{\mathbf{T}_i(\zeta)}{u_{ii}(\zeta)}, \quad (3.2)$$

where u_{ii} is the length of the tangential vector at the location ζ .

$$u_{ii}(\zeta) = |\mathbf{T}_i(\zeta)| \quad (3.3)$$

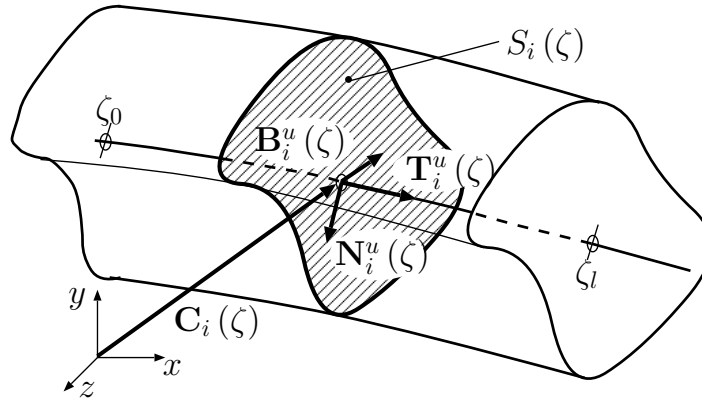


Figure 3.1: A conductor with the central space curve and the tangential, normal, and binormal vectors.

The normal and binormal unit vectors are given by

$$\mathbf{N}_i^u = \frac{1}{\kappa_i u_{ii}} \frac{\partial \mathbf{T}_i^u}{\partial \zeta} \quad (3.4)$$

and

$$\mathbf{B}_i^u = \mathbf{T}_i^u \times \mathbf{N}_i^u, \quad (3.5)$$

with the quantity κ_i being the curvature

$$\kappa_i = \left| \frac{\partial \mathbf{T}_i^u}{\partial \zeta} \right| \frac{1}{u_{ii}}. \quad (3.6)$$

We might note here that for straight conductors the derivative of the tangential vector vanishes and one can not uniquely define a normal vector. Under this circumstances we choose a direction which is most convenient for us.

Now a polar coordinate system in the plane spanned by \mathbf{N}_i^u and \mathbf{B}_i^u is introduced. Every point \mathbf{x}_i inside the conductor volume V_i can then be addressed by the coordinates (ζ, r, α) (see Figure 3.2):

$$\mathbf{x}_i(\zeta, r, \alpha) = \mathbf{C}_i(\zeta) + \mathbf{N}_i^u(\zeta) r \cos \alpha + \mathbf{B}_i^u(\zeta) r \sin \alpha. \quad (3.7)$$

For all conductors the coordinate ζ is in the interval $[\zeta_0, \zeta_l]$. The upper and lower bounds coincide with the two ends of the conductors. The angle α can have values between 0 and 2π . The radius r is bounded by $\hat{r}_i(\zeta, \alpha)$, which describes the surface of the conductor. This way of specifying the conductor volume does not allow all surface shapes, however, the most interesting shapes are covered.

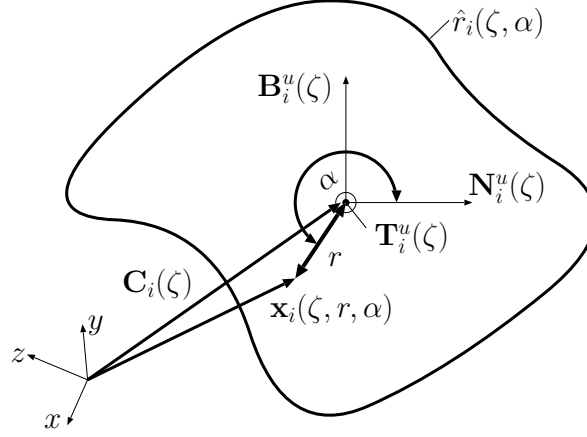


Figure 3.2: The conductor cross section with the polar coordinate system.

3.1.2 Tangential Surface Vector

In order to apply a boundary condition for the electric field the tangential vector on the surface of a conductor must be known. With the above coordinates the surface of the conductor is given by

$$\hat{\mathbf{x}}_i(\zeta, \alpha) = \mathbf{C}_i(\zeta) + \mathbf{N}_i^u(\zeta) \hat{r}(\zeta, \alpha) \cos \alpha + \mathbf{B}_i^u(\zeta) \hat{r}(\zeta, \alpha) \sin \alpha. \quad (3.8)$$

The tangential vector on the surface in the direction of the conductor is then

$$\frac{\partial \hat{\mathbf{x}}_i(\zeta, \alpha)}{\partial \zeta} = \mathbf{T}_i(\zeta) + \frac{\partial (\mathbf{N}_i^u(\zeta) \hat{r}(\zeta, \alpha))}{\partial \zeta} \cos \alpha + \frac{\partial (\mathbf{B}_i^u(\zeta) \hat{r}(\zeta, \alpha))}{\partial \zeta} \sin \alpha. \quad (3.9)$$

To simplify matters, we require that the length of the last two vectors in this sum is small compared to the first one. Thus if

$$|\mathbf{T}_i(\zeta)| \gg \left| \frac{\partial (\mathbf{N}_i^u(\zeta) \hat{r}(\zeta, \alpha))}{\partial \zeta} \cos \alpha + \frac{\partial (\mathbf{B}_i^u(\zeta) \hat{r}(\zeta, \alpha))}{\partial \zeta} \sin \alpha \right| \quad (3.10)$$

we can write

$$\frac{\partial \hat{\mathbf{x}}_i(\zeta, \alpha)}{\partial \zeta} \approx \mathbf{T}_i(\zeta). \quad (3.11)$$

This restricts the theory to conductors where the cross-sectional shape is varying very slowly along ζ , which is true for many configurations. For a constant cross section the last two terms even vanish. If the above condition is not fulfilled the correct tangential vector must be taken into account. This does not influence our derivation, however, it would make the equations more complicated.

3.1.3 Volume and Surface Integrals

It will be necessary to integrate a function $F(\dots, \mathbf{x}')$ over the conductor volume V_i , e.g.

$$\int_{V_i} F(\dots, \mathbf{x}') dv' \quad (3.12)$$

With the just established coordinate system the volume element dv' becomes

$$dv' = \left| \frac{\partial(x, y, z)}{\partial(\zeta, r, \alpha)} \right| dr d\alpha d\zeta \quad (3.13)$$

$$= (1 - r\kappa_i(\zeta) \cos \alpha) r dr d\alpha u_{ii}(\zeta) d\zeta \quad (3.14)$$

$$= f_{c_i}(\zeta, r, \alpha) r dr d\alpha u_{ii}(\zeta) d\zeta, \quad (3.15)$$

where

$$f_{c_i}(\zeta, r, \alpha) = (1 - r\kappa_i(\zeta) \cos \alpha) \quad (3.16)$$

and the integral can be written as

$$\int_{V_i} F(\dots, \mathbf{x}') dv' = \int_{\zeta_0}^{\zeta_i} \int_0^{2\pi} \int_0^{\hat{r}_i(\zeta, \alpha)} F(\dots, \mathbf{x}') f_{c_i} r' dr' d\alpha' u_{ii} d\zeta'. \quad (3.17)$$

The two inner integrals correspond to an integration over the cross section of the conductor. This will be abbreviated as

$$\int_0^{2\pi} \int_0^{\hat{r}_i(\zeta', \alpha')} F(\dots, \mathbf{x}') f_{c_i} r' dr' d\alpha' = \int_{S_i(\zeta')} F(\dots, \mathbf{x}') f_{c_i} da'. \quad (3.18)$$

3.2 Equations from Electrodynamics

Based on the continuity equation we will derive the first of the two telegrapher equations. This step is rather simple because it only involves the adaption of the continuity equation to the conductor geometry.

The second telegrapher equation is then derived from an integral equation for the electric field. This step requires some more advanced techniques. The basic idea is to formulate a trial function for the current which corresponds to a solution of a second-order differential equation. If this trial function is inserted into the integral equation it becomes the second telegrapher equation.

3.2.1 Continuity Equation

The continuity equation connects the charge density with the current density. To adapt this equation to the conductor geometry, one can define a conductor current and a per-unit-length charge.

We start with the application of the integral form of (2.26) to a volume enclosing a part of conductor i . The two cross-sectional surfaces $S_i(\zeta_0)$ at the beginning of the conductor and $S_i(\zeta)$ at position ζ somewhere on the conductor, must belong to this volume surface. Then we can write

$$\oint_{\partial V_{i\zeta_0\cdots\zeta}} \mathbf{J} \, da + j\omega \int_{V_{i\zeta_0\cdots\zeta}} \varrho \, dv = 0. \quad (3.19)$$

Because there is no current through the surface of the conductor, except at the cross sections, we may also write

$$\int_{S_i(\zeta)} \mathbf{J} \cdot \mathbf{T}_i^u(\zeta) \, da - \int_{S_i(\zeta_0)} \mathbf{J} \cdot \mathbf{T}_i^u(\zeta_0) \, da + j\omega \int_{\zeta_0}^{\zeta} u_{ii} \int_{S_i(\zeta')} \varrho f_{c_i} \, da \, d\zeta' = 0. \quad (3.20)$$

This expression is differentiated with respect to ζ resulting in

$$\frac{\partial}{\partial \zeta} \int_{S_i(\zeta)} \mathbf{J} \cdot \mathbf{T}_i^u(\zeta) \, da + j\omega u_{ii} \int_{S_i(\zeta')} \varrho f_{c_i} \, da = 0. \quad (3.21)$$

The first term is the derivative of the conductor current and the second term is a per-unit-length charge multiplied with $j\omega$. With the definitions

$$i_i(\zeta) := \int_{S_i(\zeta)} \mathbf{J}(\mathbf{x}_i) \cdot \mathbf{T}_i^u(\zeta) \, da \quad (3.22)$$

and

$$q_i(\zeta) := \int_{S_i(\zeta)} \varrho(\mathbf{x}_i) f_{c_i} \, da u_{ii}(\zeta) \quad (3.23)$$

(3.21) becomes

$$\frac{\partial i_i}{\partial \zeta} + j\omega q_i = 0, \quad (3.24)$$

which is the continuity equation tailored for the current and the per-unit-length charge in a conductor and is named the first extended telegrapher equation.

Reconstruction of the Densities

For the calculation of electromagnetic fields the current density and the charge density are required. With a given current and per-unit-length charge, respectively, the densities can be reconstructed with the aid of distribution functions as follows:

$$\mathbf{J}(\mathbf{x}_i) = \mathbf{T}_i^u(\zeta) i_i(\zeta) d_{\mathbf{J}_i}(\mathbf{x}_i) \quad (3.25)$$

$$\varrho(\mathbf{x}_i) = q_i(\zeta) \frac{d_{\varrho_i}(\mathbf{x}_i)}{u_{ii}(\zeta)}. \quad (3.26)$$

The distribution functions are defined as

$$d_{\mathbf{J}_i}(\mathbf{x}_i) := \frac{\mathbf{J}(\mathbf{x}_i) \cdot \mathbf{T}_i^u(\zeta)}{i_i(\zeta)} \quad (3.27)$$

and

$$d_{\varrho_i}(\mathbf{x}_i) := \frac{\varrho(\mathbf{x}_i)}{q_i(\zeta)} u_{ii}(\zeta). \quad (3.28)$$

Our theory is not able to predict these functions, rather it is necessary to specify them before any calculations are made. In many cases it is sufficient to either select some simple function or by “guessing” the current and charge distribution. For thin wires, for instance, the thin-wire approximation can be used (see below).

In general, this approach allows us to take into account current and charge displacement effects, such as the skin effect, however, most of the time the solutions for the current and charge distribution inside the conductors are unknown.

There are also several publications dealing with the solution for the fields and source distributions inside straight wires, e.g. [Mie00, Som64, KS64]. Unfortunately, it is not possible to directly transfer the results to our nonuniform lines. In [NT04a] a Fourier series approach was used to calculate the azimuthal current distribution in a straight thick wire above ground.

This seems to be one possible solution to this problem. One could expand the distribution functions in a combination of a Fourier (for α) and a Taylor series (for r). Then one would get a system of telegrapher equations for every coefficient of these series expansions.

3.2.2 Integral Equation

The second equation arises from the integral equation (2.39). If this equation is applied to the geometry of a multiconductor transmission line the volume integrals can be split into a sum of volume integrals over the conductor volumina. The observation point \mathbf{x}

is on the surface of the conductor j and thus becomes $\hat{\mathbf{x}}_j$. Furthermore, we substitute (3.25) and (3.26) for \mathbf{J} and ϱ . Now the equation is multiplied with the tangential vector \mathbf{T}_j^u , to extract the tangential component of the current and fields along the conductors. Eventually, the average on the surface is computed by performing the operation

$$\frac{1}{2\pi} \int_0^{2\pi} f(\dots, \alpha) d\alpha. \quad (3.29)$$

After this we get an adapted version of the integral equation (2.39) for a nonuniform multiconductor transmission line. A detailed derivation is shown in Appendix A, which yields the equation

$$\frac{\partial}{\partial \zeta} \sum_{i=1}^N \int_{\zeta_0}^{\zeta_i} k_{c_{ji}}(\zeta, \zeta') q_i(\zeta') d\zeta' + j\omega \sum_{i=1}^N \int_{\zeta_0}^{\zeta_i} k_{l_{ji}}(\zeta, \zeta') i_i(\zeta') d\zeta' + z_{jj}(\zeta) i_j(\zeta) = v_j^{(i)'}(\zeta), \quad (3.30)$$

where the source term

$$v_j^{(i)'}(\zeta) := \frac{1}{2\pi} \int_0^{2\pi} \mathbf{T}_j(\zeta) \cdot \mathbf{E}^{(i)}(\hat{\mathbf{x}}_j) d\alpha \quad (3.31)$$

is the averaged incident electric field. The variable z_{jj} represents the per-unit-length surface impedance of conductor j and is calculated from

$$z_{jj}(\zeta) := \frac{u_{jj}}{2\pi} \int_0^{2\pi} \frac{d_{\mathbf{J}_i}(\hat{\mathbf{x}}_i)}{\sigma} d\alpha. \quad (3.32)$$

The integral kernels are composed of Green's functions, current or charge distribution functions, and geometrical factors and read

$$k_{l_{ji}}(\zeta, \zeta') = \frac{\mu}{2\pi} \mathbf{T}_j(\zeta) \cdot \mathbf{T}_i(\zeta') \int_0^{2\pi} \int_{S_i(\zeta')} G(\hat{\mathbf{x}}_j, \mathbf{x}'_i) d_{\mathbf{J}_i}(\mathbf{x}_i) f_{c_i} da' d\alpha \quad (3.33)$$

and

$$k_{c_{ji}}(\zeta, \zeta') = \frac{1}{2\pi\epsilon} \int_0^{2\pi} \int_{S_i(\zeta')} G(\hat{\mathbf{x}}_j, \mathbf{x}'_i) d_{\varrho_i}(\mathbf{x}_i) f_{c_i} da' d\alpha. \quad (3.34)$$

Thin-Wire Approximation

Very often it is sufficient to think of the conductors as thin wires with a circular cross section. The thin-wire approximation then assumes that the currents and charges are

concentrated at the center of the wires. In this situation the integral kernels can be significantly simplified:

$$k_{l_{ji}}(\zeta, \zeta') := \mu \mathbf{T}_j(\zeta) \cdot \mathbf{T}_i(\zeta') G(\mathbf{C}_j(\zeta), \mathbf{C}_i(\zeta')), \quad (3.35)$$

$$k_{c_{ji}}(\zeta, \zeta') := \frac{1}{\varepsilon} G(\mathbf{C}_j(\zeta), \mathbf{C}_i(\zeta')). \quad (3.36)$$

If \mathbf{C}_j and \mathbf{C}_i point to the center of the same conductor, \mathbf{C}_i must be moved from the center to the surface.

With this approximation many problems can be solved. However, the current and charge distributions inside the conductors are fixed and effects such as the skin effect or the proximity effect can not be taken into account.

3.3 Representation as Matrix Equations

For a transmission line with N conductors we now have $2N$ equations (N equations of type (3.24) and N equations of type (3.30)). We also have $2N$ unknowns ($q_1 \dots q_N, i_1 \dots i_N$). We may now combine this system of equations into two matrix equations. The first set of telegrapher equations (3.24) may then be written as

$$\frac{\partial}{\partial \zeta} \mathbf{i} + j\omega \mathbf{q} = \mathbf{0}. \quad (3.37)$$

The column vectors $\mathbf{i} = [i_1 \dots i_N]^T$ and $\mathbf{q} = [q_1 \dots q_N]^T$ contain the conductor currents and the per-unit-length charges, respectively. The second equation (3.30) becomes

$$\frac{\partial}{\partial \zeta} \int_{\zeta_0}^{\zeta} \mathbf{k}_c(\zeta, \zeta') \mathbf{q}(\zeta') d\zeta' + j\omega \int_{\zeta_0}^{\zeta} \mathbf{k}_l(\zeta, \zeta') \mathbf{i}(\zeta') d\zeta' + \mathbf{z}(\zeta) \mathbf{i}(\zeta) = \mathbf{v}^{(i)'}(\zeta). \quad (3.38)$$

The elements of the matrix functions \mathbf{k}_c and \mathbf{k}_l are the integral kernels (3.33) and (3.34), while the column vector $\mathbf{v}^{(i)'}$ contains the distributed sources. The diagonal matrix \mathbf{z} accommodates the per-unit-length surface impedances.

3.4 Current and Charge Trial Function

Equation (3.38) already shows some similarities to the telegrapher equation. However, the unknown quantities \mathbf{i} and \mathbf{q} are inside integrals. We need to find a way to pull the current and the per-unit-length charge out of the integrals. This can be achieved by introducing trial functions for the current and the per-unit-length charge.

King presented similar equations for uniform lines in [Kin55]. His trial function is a Taylor series expansion of the current, truncated after the linear term. He shows that

only these terms are important, which is due to the TEM mode. Since we do not have an exclusive TEM mode anymore, our trial function is more complicated.

On an excited transmission line there are usually forward and backward traveling waves. These waves are governed by wave equations. Also the currents in the conductors obey wave equations. Thus it is obvious to use the solution of a wave equation as a trial function for the current. In frequency domain a wave equation usually is a second-order ordinary differential equation (ODE), with, in the most general case, nonconstant coefficients. For our N -conductor system we get N coupled ODEs, which are most conveniently written as a matrix equation:

$$\left(\frac{\partial^2}{\partial \zeta^2} + j\omega \mathbf{P}_{t11}(\zeta) \frac{\partial}{\partial \zeta} + \omega^2 \mathbf{P}_{t12}(\zeta) \right) \mathbf{i}(\zeta) = -j\omega \mathbf{q}'_t(\zeta). \quad (3.39)$$

The matrices \mathbf{P}_{t11} and \mathbf{P}_{t12} are the coefficient matrices, and the column vector \mathbf{q}'_t is the excitation. With the aid of (3.37) we may convert this equation into a system of coupled first-order differential equations. In supermatrix notation this becomes

$$\frac{\partial}{\partial \zeta} \begin{bmatrix} \mathbf{q}(\zeta) \\ \mathbf{i}(\zeta) \end{bmatrix} + j\omega \underbrace{\begin{bmatrix} \mathbf{P}_{t11} & \mathbf{P}_{t12} \\ \mathbf{1} & \mathbf{0} \end{bmatrix}}_{\bar{\mathbf{P}}_t} \begin{bmatrix} \mathbf{q}(\zeta) \\ \mathbf{i}(\zeta) \end{bmatrix} = \begin{bmatrix} \mathbf{q}'_t(\zeta) \\ \mathbf{0} \end{bmatrix}. \quad (3.40)$$

The general solution of (3.40) can be written in a very compact form:

$$\begin{bmatrix} \mathbf{q}(\zeta') \\ \mathbf{i}(\zeta') \end{bmatrix} = \mathcal{M}_{\zeta}^{\zeta'} \{ -j\omega \bar{\mathbf{P}}_t \} \begin{bmatrix} \mathbf{q}(\zeta) \\ \mathbf{i}(\zeta) \end{bmatrix} + \int_{\zeta}^{\zeta'} \mathcal{M}_{\xi}^{\zeta'} \{ -j\omega \bar{\mathbf{P}}_t \} \begin{bmatrix} \mathbf{q}'_t(\xi) \\ \mathbf{0} \end{bmatrix} d\xi, \quad (3.41)$$

where $\mathcal{M}_{\zeta}^{\zeta'} \{ -j\omega \bar{\mathbf{P}}_t \}$ is the product integral [Gan84, DF79] (see also Appendix B). This expression is the desired trial function. Although, the supermatrix $\bar{\mathbf{P}}_t$ and the excitation vector \mathbf{q}'_t are unknown, this expression gives us a very general relation for the currents and per-unit-length charges at two different positions along the transmission lines.

3.5 Generalized Telegrapher Equations

In the next step to the generalized telegrapher equations, this trial function (3.41) is substituted into (3.38). For this (3.38) may be rearranged to

$$\left[\mathbf{1}j\omega \quad \mathbf{1} \frac{\partial}{\partial \zeta} \right]_{(N,2N)} \int_{\zeta_0}^{\zeta} \bar{\mathbf{K}}(\zeta, \zeta') \begin{bmatrix} \mathbf{q}(\zeta') \\ \mathbf{i}(\zeta') \end{bmatrix} d\zeta' + \mathbf{z}(\zeta) \mathbf{i}(\zeta) = \mathbf{v}^{(i)'}(\zeta), \quad (3.42)$$

where the supermatrix $\bar{\mathbf{K}}$ is given by

$$\bar{\mathbf{K}} := \begin{bmatrix} \mathbf{0} & \mathbf{k}_l \\ \mathbf{k}_c & \mathbf{0} \end{bmatrix}. \quad (3.43)$$

Now (3.41) can be directly inserted and after some minor rearrangements the result becomes

$$\mathbf{I}_{21} \frac{\partial \mathbf{q}}{\partial \zeta} + \mathbf{I}_{22} \frac{\partial \mathbf{i}}{\partial \zeta} + \left(j\omega \mathbf{I}_{11} + \frac{\partial \mathbf{I}_{21}}{\partial \zeta} \right) \mathbf{q} + \left(j\omega \mathbf{I}_{12} + \frac{\partial \mathbf{I}_{22}}{\partial \zeta} + \mathbf{z} \right) \mathbf{i} + j\omega \mathbf{I}_{01} + \frac{\partial \mathbf{I}_{02}}{\partial \zeta} = \mathbf{v}^{(i)'}. \quad (3.44)$$

The new matrices and vectors \mathbf{I}_{ij} are the blocks of the supermatrix

$$\bar{\mathbf{I}}(\zeta) = \int_{\zeta_0}^{\zeta_t} \bar{\mathbf{K}}(\zeta, \zeta') \mathcal{M}_{\zeta'}^{\zeta'} \{ -j\omega \bar{\mathbf{P}}_t \} d\zeta' \quad (3.45)$$

and of the supervector

$$\begin{bmatrix} \mathbf{I}_{10}(\zeta) \\ \mathbf{I}_{20}(\zeta) \end{bmatrix} = \int_{\zeta_0}^{\zeta_t} \bar{\mathbf{K}}(\zeta, \zeta') \int_{\zeta}^{\zeta'} \mathcal{M}_{\xi}^{\zeta'} \{ -j\omega \bar{\mathbf{P}}_t \} \begin{bmatrix} \mathbf{q}'_t(\xi) \\ \mathbf{0} \end{bmatrix} d\xi d\zeta'. \quad (3.46)$$

We now can combine (3.37) and (3.44) into a supermatrix equation

$$\frac{\partial}{\partial \zeta} \begin{bmatrix} \mathbf{q}(\zeta) \\ \mathbf{i}(\zeta) \end{bmatrix} + j\omega \bar{\mathbf{P}}(\zeta) \begin{bmatrix} \mathbf{q}(\zeta) \\ \mathbf{i}(\zeta) \end{bmatrix} = \begin{bmatrix} \mathbf{q}'_s(\zeta) \\ \mathbf{0} \end{bmatrix} \quad (3.47)$$

where

$$\bar{\mathbf{P}} = \begin{bmatrix} \mathbf{I}_{21} & \mathbf{I}_{22} \\ \mathbf{0} & \mathbf{1} \end{bmatrix}^{-1} \begin{bmatrix} \mathbf{I}_{11} + \frac{1}{j\omega} \frac{\partial \mathbf{I}_{21}}{\partial \zeta} & \mathbf{I}_{12} + \frac{1}{j\omega} \left(\frac{\partial \mathbf{I}_{22}}{\partial \zeta} + \mathbf{z} \right) \\ \mathbf{1} & \mathbf{0} \end{bmatrix} \quad (3.48)$$

and

$$\mathbf{q}'_s = \mathbf{I}_{21}^{-1} \left(\mathbf{v}^{(i)'} - j\omega \mathbf{I}_{10} - \frac{\partial \mathbf{I}_{20}}{\partial \zeta} \right). \quad (3.49)$$

This is a remarkable result! With the introduction of the trial function we were able to cast the integral equation together with the continuity relation into a system of first-order ODEs. These equations are identical with the ODEs, the solution of which is the trial function. Thus the current is indeed governed by a second-order ODE.

The equation (3.47) has the same structure as the telegrapher equations, although it encompasses the full integral equations which come directly from Maxwell's theory. No restricting assumptions are made, apart from assumptions about the current and charge distribution inside the conductors.

The equations are valid for a nonuniform multiconductor transmission line and take into account all field modes and physical effects that might occur, including radiation losses. It surpasses the classical transmission-line theory, which is a special case. Thus we call our new theory the **Transmission-Line Superttheory (TLST)**.

3.6 Parameters and Source Term Determination

Before we can solve the above generalized telegrapher equations, the parameters and source terms must be determined. This is the most complicated part because it involves the solution of integral equations.

3.6.1 Parameters

During the derivation of the generalized telegrapher equations we also got a formula for the determination of the parameters (see (3.48)). In order to evaluate this we must compute $\bar{\mathbf{I}}$ which depends on the parameters of the trial function $\bar{\mathbf{P}}_t$. Unfortunately these parameters are unknown. However, (3.40) and (3.47) contain the same physical quantities, and thus the coefficients as well as the source terms must be identical. Therefore we can set

$$\bar{\mathbf{P}}_t = \bar{\mathbf{P}} = \begin{bmatrix} \mathbf{I}_{21}^{-1} \left(\mathbf{I}_{11} - \mathbf{I}_{22} + \frac{1}{j\omega} \frac{\partial \mathbf{I}_{21}}{\partial \xi} \right) & \mathbf{I}_{21}^{-1} \left(\mathbf{I}_{12} + \frac{1}{j\omega} \left(\mathbf{z} + \frac{\partial \mathbf{I}_{22}}{\partial \xi} \right) \right) \\ \mathbf{1} & \mathbf{0} \end{bmatrix}. \quad (3.50)$$

If we now insert (3.50) into (3.45) we get an integral equation for $\bar{\mathbf{I}}$:

$$\bar{\mathbf{I}}(\zeta) = \int_{\zeta_0}^{\zeta_t} \bar{\mathbf{K}}(\zeta, \zeta') \mathcal{M}_{\zeta'}^{\zeta'} \{ -j\omega \bar{\mathbf{P}} \} d\zeta'. \quad (3.51)$$

There is no known way to us, to explicitly solve for $\bar{\mathbf{I}}$ in the general case. Therefore, we will use an iterative procedure to determine $\bar{\mathbf{I}}$:

$$\bar{\mathbf{I}}^{(k+1)} = \mathcal{L}_p \{ \bar{\mathbf{I}}^{(k)} \}. \quad (3.52)$$

The operation \mathcal{L}_p is given by (3.50) and (3.51). $\bar{\mathbf{I}}^{(k)}$ is the approximation for $\bar{\mathbf{I}}$ after the k -th iteration. The final result of this operation is then used to calculate the parameters with the aid of (3.48) or (3.50).

Concerning convergence of the procedure, for several examples we have shown that one can get very good results with only one iteration. Additionally, for line setups, where analytical solutions are possible, the iterative approach gives the same results as other methods (see Section 5). However, currently we can not provide a proof for the general convergence of the iteration procedure.

To start the iteration, we need an $\bar{\mathbf{I}}^{(0)}$ to begin with. For this, we will try to get as much information from (3.51) as possible. One can expand $\bar{\mathbf{I}}$ into a series:

$$\bar{\mathbf{I}} = \bar{\mathbf{I}}_0 + j\omega \bar{\mathbf{I}}_1 + \dots \quad (3.53)$$

As we already know, for a pure TEM mode the parameters are frequency independent. Consequently all but the constant term of this series will vanish. If there are additional modes on the line the higher order terms occur. However, for many cases the constant term will still be dominant. Thus this term should be a quite good starting value for the iteration:

$$\bar{\mathbf{I}}^{(0)} = \bar{\mathbf{I}}_0. \quad (3.54)$$

To calculate $\bar{\mathbf{I}}^{(0)}$ we have to evaluate (3.51) for $\omega = 0$. With some additional approximations this can be done explicitly.

$$\bar{\mathbf{I}}^{(0)}(\zeta) = \int_{\zeta_0}^{\zeta_t} \bar{\mathbf{K}}(\zeta, \zeta')|_{\omega=0} \mathcal{M}_{\zeta'}^{\zeta'} \left\{ - \begin{bmatrix} \mathbf{I}_{21}^{-1} \frac{\partial \mathbf{I}_{21}}{\partial \xi} & \mathbf{I}_{21}^{-1} \left(\mathbf{z} + \frac{\partial \mathbf{I}_{22}}{\partial \xi} \right) \\ \mathbf{1} & \mathbf{0} \end{bmatrix} \right\} d\zeta', \quad (3.55)$$

The product integral can be replaced by its series representation

$$\bar{\mathbf{I}}^{(0)}(\zeta) = \int_{\zeta_0}^{\zeta_t} \bar{\mathbf{K}}(\zeta, \zeta')|_{\omega=0} \left(\bar{\mathbf{I}} - \int_{\zeta}^{\zeta'} \begin{bmatrix} \mathbf{I}_{21}^{-1} \frac{\partial \mathbf{I}_{21}}{\partial \xi} & \mathbf{I}_{21}^{-1} \left(\mathbf{z} + \frac{\partial \mathbf{I}_{22}}{\partial \xi} \right) \\ \mathbf{1} & \mathbf{0} \end{bmatrix} d\xi + \dots \right) d\zeta'. \quad (3.56)$$

We may now argue that the major contribution to the integral arises if $\zeta \approx \zeta'$. Physically this means, that the interaction of regions of the transmission line that are very close to each other is much stronger than the interaction of more distant regions. In this case, the second term of the series representation of the product integral is smaller than the constant term and can be neglected. This argumentation is not necessarily true for a general nonuniform transmission line, but it is a reasonable way to get good starting values. Thus the starting values for the iteration are set to

$$\bar{\mathbf{I}}^{(0)}(\zeta) = \int_{\zeta_0}^{\zeta_t} \bar{\mathbf{K}}(\zeta, \zeta')|_{\omega=0} d\zeta'. \quad (3.57)$$

Note that this expression is frequency independent because it is the constant term of the Taylor expansion of the actual frequency-dependent function. Nonetheless, this result is used as the starting values for the iteration at all frequencies.

3.6.2 Source Terms

Once the parameters are determined we can calculate the source terms \mathbf{q}'_s , which are given by (3.49). For the evaluation we need \mathbf{I}_{10} and \mathbf{I}_{20} . Both depend on the already known $\bar{\mathbf{P}}_t$ and on \mathbf{q}'_t . This second quantity is equal to our unknown source term because (3.40) and (3.47) are identical:

$$\mathbf{q}'_t = \mathbf{q}'_s. \quad (3.58)$$

With this relation we get an implicit expression for the determination of \mathbf{q}'_s . Because an explicit expression is not known, an iterative approach is used to calculate the \mathbf{q}'_s :

$$\mathbf{q}_s^{(k+1)'} = \mathcal{L}_q \left\{ \mathbf{q}_s^{(k)'} \right\}, \quad (3.59)$$

where \mathcal{L}_q consists of (3.49) and (3.46). The iteration is started with vanishing sources, i.e. $\mathbf{q}_s^{(0)'} = \mathbf{0}$. Then we get with (3.46)

$$\mathbf{I}_{10}^{(0)} = \mathbf{0} \quad (3.60)$$

$$\mathbf{I}_{20}^{(0)} = \mathbf{0} \quad (3.61)$$

and with (3.49)

$$\mathbf{q}_s^{(1)'} = \mathbf{I}_{21}^{-1} \mathbf{v}^{(i)'}. \quad (3.62)$$

The result should then be used to calculate $\mathbf{I}_{10}^{(1)}$ and $\mathbf{I}_{20}^{(1)}$, which again is used to calculate $\mathbf{q}^{(2)'}$ and so on. For practical applications often the first iteration already delivers very good results.

3.7 Solution of the Extended Telegrapher Equations

The extended telegrapher equations in frequency domain are a system of first-order ordinary differential equations with nonconstant (i.e. position-dependent) coefficients. The solution method to this kind of equations is very well known and is the subject of many books and publications, e.g., from the mathematical point of view [Gan84, DF79], from the transmission-line-theory point of view [BNS96, NG99], or from the numerical point of view [Zur84]. As was anticipated in the previous section the general solution is

$$\begin{bmatrix} \mathbf{q}(\zeta) \\ \mathbf{i}(\zeta) \end{bmatrix} = \mathcal{M}_{\zeta_0}^{\zeta} \{-j\omega \mathbf{P}\} \begin{bmatrix} \mathbf{q}(\zeta_0) \\ \mathbf{i}(\zeta_0) \end{bmatrix} + \int_{\zeta_0}^{\zeta} \mathcal{M}_{\xi}^{\zeta} \{-j\omega \mathbf{P}\} \begin{bmatrix} \mathbf{q}'_s(\xi) \\ \mathbf{0} \end{bmatrix} d\xi. \quad (3.63)$$

Here $\mathcal{M}_{\zeta_0}^{\zeta} \{-j\omega \mathbf{P}\}$ is the product integral, which often is written as

$$\mathcal{M}_{\zeta_0}^{\zeta} \{\mathbf{X}\} = \prod_{\zeta_0}^{\zeta} e^{\mathbf{X}(\eta)d\eta}. \quad (3.64)$$

In Appendix B more details on the product integral are provided. The column vectors $\mathbf{q}(\zeta_0)$ and $\mathbf{i}(\zeta_0)$ are integration constants and are determined by the boundary conditions at the terminals of the transmission lines.

3.8 Going Back to Voltages ?

In many cases it is much more convenient to deal with a voltage instead of a charge per unit length. For instance if the transmission line is embedded into a circuit and other elements are connected to the line we must know the voltages at the terminals to perform our calculations.

The voltage v_{12} between the two points \mathbf{x}_1 and \mathbf{x}_2 is defined as the integral of the electric field strength \mathbf{E} along a path \mathcal{C} which connects the two points:

$$v_{12} := - \int_{\mathcal{C}_{\mathbf{x}_1 \rightarrow \mathbf{x}_2}} \mathbf{E} \cdot d\mathbf{s}. \quad (3.65)$$

If \mathbf{E} is represented with the aid of potentials one can also write

$$v_{12} = \int_{\mathcal{C}_{\mathbf{x}_1 \rightarrow \mathbf{x}_2}} (\text{grad } \varphi + j\omega \mathbf{A}) \cdot d\mathbf{s} \quad (3.66)$$

$$= \varphi(\mathbf{x}_2) - \varphi(\mathbf{x}_1) + j\omega \int_{\mathcal{C}_{\mathbf{x}_1 \rightarrow \mathbf{x}_2}} \mathbf{A} \cdot d\mathbf{s}. \quad (3.67)$$

In general, the remaining integral depends on the path that is chosen and thus the voltage is different for different paths. For a TEM-mode line, in a plane perpendicular to the conductors, the second integral becomes zero because $\mathbf{A} \perp d\mathbf{s}$ and the voltage can be uniquely defined as $v_{12} := \varphi(\mathbf{x}_2) - \varphi(\mathbf{x}_1)$. For a general nonuniform line this is not the case. Thus in order to compute the voltage we need to know the vector potential along that path. This can be computed, however, it is rather cumbersome to do this calculation along the transmission line.

If the distance between the conductors at the terminals, i.e. the lengths of the integration paths for the voltage computation, is much smaller than the smallest wavelength λ , this region of the transmission line can be regarded to be in the “static” regime. Fortunately, this is quite often the case and the voltage is given by the difference of potentials at the corresponding conductor terminals. For the potential we use the average potential at the surface of the conductors, which is calculated by

$$\varphi_i(\zeta) = \frac{1}{2\pi} \int_0^{2\pi} \varphi(\hat{\mathbf{x}}_i(\zeta, \alpha)) d\alpha. \quad (3.68)$$

[Bau04] suggested to call this potential the quasivoltage. Now (2.34) is inserted into this equation. Then, with some more manipulations (in fact the same as in the derivation of (3.38), which contains the same expression) we arrive at

$$\varphi(\zeta) = \int_{\zeta_0}^{\zeta_i} \mathbf{k}_c(\zeta, \zeta') \mathbf{q}(\zeta') d\zeta'. \quad (3.69)$$

Here $\boldsymbol{\varphi}$ is the column vector of the average conductor potentials. With the aid of (3.41), (3.22), and (3.46) this expression becomes

$$\boldsymbol{\varphi} = \mathbf{I}_{21}\mathbf{q} + \mathbf{I}_{22}\mathbf{i} + \mathbf{I}_{20}, \quad (3.70)$$

which allows us to formulate the following transformation:

$$\begin{bmatrix} \boldsymbol{\varphi} \\ \mathbf{i} \end{bmatrix} = \begin{bmatrix} \mathbf{I}_{21} & \mathbf{I}_{22} \\ \mathbf{0} & \mathbf{1} \end{bmatrix} \begin{bmatrix} \mathbf{q} \\ \mathbf{i} \end{bmatrix} + \begin{bmatrix} \mathbf{I}_{20} \\ \mathbf{0} \end{bmatrix}. \quad (3.71)$$

Because this relation is valid everywhere on the line, not only at the beginning or the end, we can easily convert the telegrapher equation into the quasivoltage-current representation

$$\frac{\partial}{\partial \zeta} \begin{bmatrix} \boldsymbol{\varphi}(\zeta) \\ \mathbf{i}(\zeta) \end{bmatrix} + j\omega \overline{\mathbf{P}}^*(\zeta) \begin{bmatrix} \boldsymbol{\varphi}(\zeta) \\ \mathbf{i}(\zeta) \end{bmatrix} = \begin{bmatrix} \boldsymbol{\varphi}'_s(\zeta) \\ \mathbf{i}'_s(\zeta) \end{bmatrix}, \quad (3.72)$$

where

$$\overline{\mathbf{P}}^* = \begin{bmatrix} \mathbf{I}_{11}\mathbf{I}_{21}^{-1} & \mathbf{I}_{12} - \mathbf{I}_{11}\mathbf{I}_{21}^{-1}\mathbf{I}_{22} + \frac{\mathbf{z}}{j\omega} \\ \mathbf{I}_{21}^{-1} & -\mathbf{I}_{21}^{-1}\mathbf{I}_{22} \end{bmatrix} \quad (3.73)$$

and

$$\begin{bmatrix} \boldsymbol{\varphi}'_s \\ \mathbf{i}'_s \end{bmatrix} = \begin{bmatrix} \mathbf{v}^{(i)'} + j\omega (\mathbf{I}_{11}\mathbf{I}_{21}^{-1}\mathbf{I}_{20} - \mathbf{I}_{10}) \\ j\omega \mathbf{I}_{21}^{-1}\mathbf{I}_{20} \end{bmatrix}. \quad (3.74)$$

Remember, the quasivoltage along the line is still a gauge-dependent quantity with no physical meaning. Only when the prescribed conditions are met, the quasivoltage becomes a real, physical voltage.

In the above equations we can identify $j\omega \mathbf{P}_{12}^*$ as the parameter matrix, which is equivalent to the per-unit-length impedance matrix of the classical transmission-line theory. Moreover, the matrix $j\omega \mathbf{P}_{21}^*$ is equivalent to the per-unit-length admittance matrix. The two other block matrices $j\omega \mathbf{P}_{11}^*$ and $j\omega \mathbf{P}_{22}^*$ vanish in the classical theory and are only nonzero for nonuniform lines. However, when interpreting these parameters, one should keep in mind that they connect the current, which is a physical quantity, and the quasivoltage, which, in general, has no physical meaning.

Also note that unlike the parameters in (3.47) these parameters do not contain any derivatives. This makes the numerical evaluation of the product integral much simpler than for (3.47).

3.9 Discussion of the New Parameters

3.9.1 Wave Equation

In the previous sections we derived a new set of differential equations for nonuniform transmission lines. The equations have new coefficients, the per-unit-length parameters. In order to give some meaning to these parameters we will investigate a different representation. First, let us convert the system of $2N$ first-order differential equations in q - i representation into a system of N second-order differential equations, involving the conductor currents and its first and second derivatives.

$$\left(\frac{\partial^2}{\partial \zeta^2} - \mathbf{D} \frac{\partial}{\partial \zeta} - \mathbf{\Gamma}^2 \right) \mathbf{i} = \mathbf{i}_s \quad (3.75)$$

where

$$\mathbf{\Gamma}^2 = -\omega^2 \mathbf{P}_{12} \quad (3.76)$$

$$= -\omega^2 \mathbf{I}_{21}^{-1} \mathbf{I}_{12} + j\omega \mathbf{I}_{21}^{-1} \left(\frac{\partial}{\partial \zeta} \mathbf{I}_{22} + \mathbf{z} \right) \quad (3.77)$$

$$\mathbf{D} = -j\omega \mathbf{P}_{11} \quad (3.78)$$

$$= -\mathbf{I}_{21}^{-1} \frac{\partial}{\partial \zeta} \mathbf{I}_{21} - j\omega \mathbf{I}_{21}^{-1} (\mathbf{I}_{11} - \mathbf{I}_{22}) \quad (3.79)$$

$$\mathbf{i}_s = -j\omega \mathbf{q}_s \quad (3.80)$$

We can clearly identify $\mathbf{\Gamma}$ as the propagation function, equivalent to the propagation function in the classical theory (cf. Section 2.2.6). In general this is a complex valued matrix, incorporating losses, not only caused by conductor losses but also caused by radiation. The matrix \mathbf{D} describes the damping along the line due to the reflections caused by the nonuniformity.

3.9.2 Radiation Losses

To further investigate the radiation losses [NT05] suggested the establishment of a power balance for the transmission line. Here we will use a simple model, consisting only of a one-conductor transmission line above a ground plane. Equation (3.72) is used to describe this transmission line and we assume that all conditions for the validity of this equation are met. At position ζ_0 the line is fed with a source and there is a load at ζ_l . The real power generated by the source is then given by

$$p(\zeta_0) = \frac{1}{2} \left(\varphi(\zeta_0) \overline{i(\zeta_0)} + \overline{\varphi(\zeta_0)} i(\zeta_0) \right) \quad (3.81)$$

where the line above the variables indicates the complex conjugate. Likewise, the power dissipated in the load is given by

$$p(\zeta_l) = \frac{1}{2} \left(\varphi(\zeta_l) \overline{i(\zeta_l)} + \overline{\varphi(\zeta_l)} i(\zeta_l) \right). \quad (3.82)$$

Then the power balance is $p(\zeta_0) = p_{\text{TL}} + p(\zeta_l)$ or rearranged

$$p_{\text{TL}} = - \left(p(\zeta_l) - p(\zeta_0) \right), \quad (3.83)$$

where p_{TL} is the power dissipated in the transmission line. The expression inside the parenthesis can be regarded as an integral of the form

$$p_{\text{TL}} = - \int_{\zeta_0}^{\zeta_l} \frac{dp(\zeta)}{d\zeta} d\zeta. \quad (3.84)$$

where

$$p(\zeta) = \frac{1}{2} \left(\varphi(\zeta) \overline{i(\zeta)} + \overline{\varphi(\zeta)} i(\zeta) \right). \quad (3.85)$$

After some longer manipulations [NT05] one gets the relation

$$p_{\text{TL}} = - \int_{\zeta_0}^{\zeta_l} \omega \left(\Im(P_{12}^*) |i|^2 + \Im(P_{21}^*) |\varphi|^2 + \Im((P_{11}^* - \overline{P_{22}^*}) \varphi \overline{i}) \right) d\zeta \quad (3.86)$$

which describes the real power dissipated by the transmission line. This includes the power which is converted to heat in the conductors as well as the radiated power. As we can see, the imaginary parts of the per-unit-length parameters \mathbf{P}_{12}^* and \mathbf{P}_{21}^* are the important coefficients here. Multiplied with $j\omega$ these imaginary parts become real and hence, act as a series resistances and a shunt conductance. The above expression can also be obtained for other representations of the generalized telegrapher equations. However, the imaginary parts of the $\overline{\mathbf{P}}^*$ parameters, which are responsible for losses and radiation, are “hidden” in the real and imaginary parts of the corresponding parameters of the other representations and can not be isolated as in (3.86).

3.9.3 Asymmetric Parameter Matrices

In the classical transmission-line theory, reciprocity implies symmetric parameter matrices. Unlike these matrices, the parameter matrices of the supertheory are not necessarily symmetric.

For instance imagine a transmission line, like the one shown in Figure 3.3. In every one of the parameter matrices there will be one coefficient describing the coupling from conductor 1 to conductor 2 and one for the coupling from conductor 2 to conductor 1.

In the classical theory, because of reciprocity, these two coefficients are identical and thus the corresponding matrix is symmetric.

In the supertheory the first coefficient describes the coupling from all parts of conductor 1 to the point ζ on conductor 2 (it is a nonlocal interaction), the other parameter vice versa. It is very reasonable that only in rare cases, these couplings and thus the coefficients are the same. Hence the coefficient matrix is not symmetric.

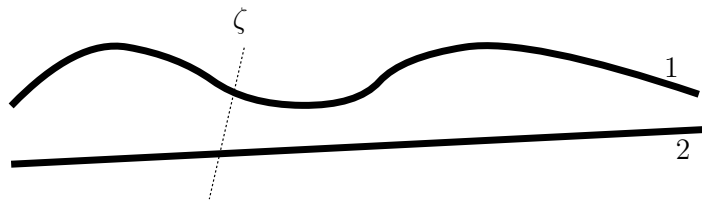


Figure 3.3: Nonuniform transmission lines and asymmetric parameter matrices.

Chapter 4

Numerical Evaluation of the Parameters

***Abstract** — In this chapter we develop methods for the numerical determination of the parameters. This involves the iterative solution of the parameter integral equations. Two methods are discussed. Both require the expansion of the product integral and of the Green's function into series expressions. The first uses the Taylor series, while the second is based on an eigenvalue decomposition of the product integral.*

We will now discuss methods to calculate the parameters of the generalized telegrapher equations. This mainly involves the evaluation of (3.50) and (3.51). For an efficient processing some assumptions must be made, which require a careful preparation of problems to be calculated. The setup should be in free space, an ideal ground plane or a corner can be taken into account with the aid of the method of images [Jac98, Bal89, Lin95]. Also all conductors should be thin wires. This is not strictly necessary for the following derivations, however, some integrals can only be solved in closed form if the thin-wire approximation is used.

The transmission line is divided into M segments. Within each segment, the conductors should be straight, but not necessarily in parallel to the reference conductor. Thus their position can be approximated by a linear function. The parameters are determined at the centers of the segments and are interpolated for positions in between. Therefore, segment length should reflect the nonuniformity of the line, for strongly nonuniform lines a finer segmentation is required.

4.1 Starting Values for the Iteration

The first step is the calculation of $\bar{\mathbf{I}}^{(0)}$ using (3.57). For the segmented transmission line this equation becomes

$$\bar{\mathbf{I}}^{(0)}(\zeta) = \sum_{m=0}^M \int_{\zeta_m}^{\zeta_{m+1}} \bar{\mathbf{K}}(\zeta, \zeta')|_{\omega=0} d\zeta'. \quad (4.1)$$

The integration of the matrix function is performed by the integration of the single elements resulting in

$$\bar{\mathbf{I}}^{(0)}(\zeta) = \sum_{m=0}^M \begin{bmatrix} \mathbf{0} & \mu \left[\mathbf{T}_j(\zeta) \cdot \mathbf{T}_i(\zeta_{c_m}) I_{m_{ij}}^{(0)} \right] \\ \frac{1}{\varepsilon} \left[I_{m_{ij}}^{(0)} \right] & \mathbf{0} \end{bmatrix} \quad (4.2)$$

where

$$I_{m_{ij}}^{(0)}(\zeta) = \int_{\zeta_m}^{\zeta_{m+1}} G(\mathbf{C}_j(\zeta), \mathbf{C}_i(\zeta'))|_{\omega=0} d\zeta'. \quad (4.3)$$

Here the new quantity

$$\zeta_{c_m} = \frac{\zeta_{m+1} + \zeta_m}{2}. \quad (4.4)$$

was introduced to indicate the center of the segments. The above integral can be evaluated in closed form. For a line in free space one can write (see also Figure 4.1)

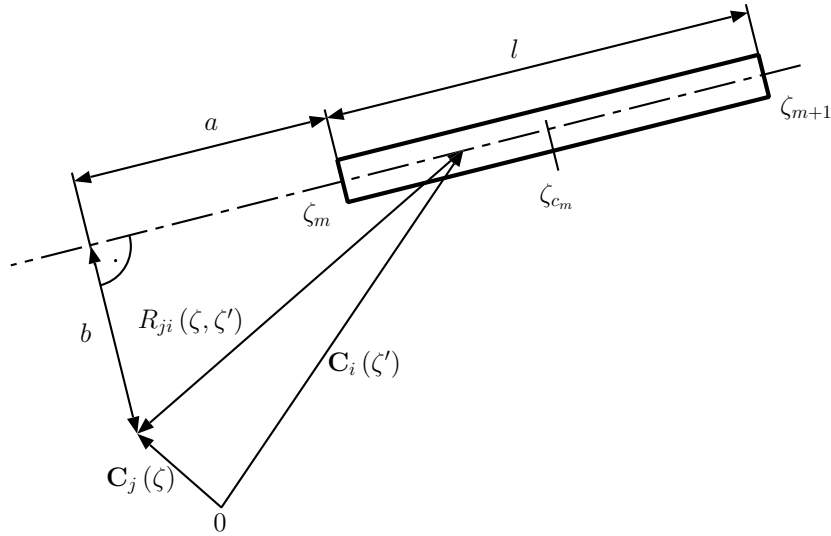


Figure 4.1: One segment of a conductor of a nonuniform transmission line.

$$I_{m_{ij}}^{(0)} = \int_{\zeta_m}^{\zeta_{m+1}} \frac{1}{4\pi |\mathbf{C}_j(\zeta) - \mathbf{C}_i(\zeta')|} d\zeta' \quad (4.5)$$

$$= \int_{\zeta_m}^{\zeta_{m+1}} \frac{1}{4\pi R_{ji}(\zeta, \zeta')} d\zeta' \quad (4.6)$$

with $x = a + l \frac{\zeta - \zeta_m}{\zeta_{m+1} - \zeta_m}$

$$I_{m_{ij}}^{(0)} = \frac{\zeta_{m+1} - \zeta_m}{4\pi l} \int_a^{a+l} \frac{1}{\sqrt{x^2 + b^2}} dx \quad (4.7)$$

$$= \frac{\zeta_{m+1} - \zeta_m}{4\pi l} \begin{cases} \operatorname{arcsinh} \frac{a+l}{b} - \operatorname{arcsinh} \frac{a}{b} & b > 0 \\ \ln \frac{a+l}{a} & b = 0. \end{cases} \quad (4.8)$$

If there is a ground plane or a corner the additional images have to be taken into account. The integrals can be solved similarly to the one for free space. These results are inserted in (3.50) to get the starting parameters $\bar{\mathbf{P}}^{(0)}(\zeta)$ for the first iteration. Note that the parameters are only evaluated at the centers $\zeta = \zeta_m, m = 1 \dots M$ of the segments.

4.2 First Iteration

In the next step (3.51) has to be calculated with the previously determined zeroth-order parameters. Again, the line is divided into segments giving:

$$\bar{\mathbf{I}}^{(1)}(\zeta) = \sum_{m=1}^M \bar{\mathbf{I}}_m^{(1)}(\zeta) \quad (4.9)$$

and

$$\bar{\mathbf{I}}_m^{(1)}(\zeta) = \int_{\zeta_m}^{\zeta_{m+1}} \bar{\mathbf{K}}(\zeta, \zeta') \mathcal{M}_{\zeta}^{\zeta'} \left\{ -j\omega \bar{\mathbf{P}}^{(0)} \right\} d\zeta'. \quad (4.10)$$

The product integral is split into two factors (see (B.15)). One of these factors is independent of the integration variable and can be pulled out of the integral:

$$\bar{\mathbf{I}}_m^{(1)}(\zeta) = \int_{\zeta_m}^{\zeta_{m+1}} \bar{\mathbf{K}}(\zeta, \zeta') \mathcal{M}_{\zeta_{c_m}}^{\zeta'} \left\{ -j\omega \bar{\mathbf{P}}^{(0)} \right\} d\zeta' \mathcal{M}_{\zeta}^{\zeta_{c_m}} \left\{ -j\omega \bar{\mathbf{P}}^{(0)} \right\}. \quad (4.11)$$

We now express the remaining product integral inside the integral as a sum

$$\mathcal{M}_{\zeta_{c_m}}^{\zeta'} \left\{ -j\omega \bar{\mathbf{P}}^{(0)} \right\} = \sum_{n=0}^{\infty} \lambda_{m_n}(\zeta') \bar{\mathbf{M}}_{m_n}, \quad (4.12)$$

where $\lambda_{m_n}(\zeta')$ is a scalar function and $\bar{\mathbf{M}}_{m_n}$ a possibly frequency-dependent super-matrix, which, however, is independent of ζ' . There are several possibilities for the

expansion of the product integral. Below we will discuss two of these, one is a Taylor series and the second is based on an eigenvalue/eigenvector decomposition of the product integral. Equation (4.11) may now be written as

$$\bar{\mathbf{I}}_m^{(1)}(\zeta) = \left(\sum_{n=0}^{\infty} \int_{\zeta_m}^{\zeta_{m+1}} \bar{\mathbf{K}}(\zeta, \zeta') \lambda_{m_n}(\zeta') d\zeta' \bar{\mathbf{M}}_{m_n} \right) \mathcal{M}_{\zeta}^{\zeta_{c_m}} \left\{ -j\omega \bar{\mathbf{P}}^{(0)} \right\}. \quad (4.13)$$

With the previous manipulations we reduced the problem of integrating the product of two matrix functions in (4.10) to the problem of integrating the product of a matrix function and a scalar function in (4.13). This integration can be carried out element wise, yielding

$$\bar{\mathbf{I}}_m^{(1)}(\zeta) = \left(\sum_{n=0}^{\infty} \begin{bmatrix} \mathbf{0} & \left[\mu \mathbf{T}_j(\zeta) \cdot \mathbf{T}_i(\zeta_{m_c}) I_{m_{n_j i}}^{(1)} \right] \\ \left[\frac{1}{\varepsilon} I_{m_{n_j i}}^{(1)} \right] & \mathbf{0} \end{bmatrix} \bar{\mathbf{M}}_{m_n} \right) \mathcal{M}_{\zeta}^{\zeta_{c_m}} \left\{ -j\omega \bar{\mathbf{P}}^{(0)} \right\}, \quad (4.14)$$

with

$$I_{m_{n_j i}}^{(1)} = \int_{\zeta_m}^{\zeta_{m+1}} G(\mathbf{C}_j(\zeta), \mathbf{C}_i(\zeta')) \lambda_{m_n}(\zeta') d\zeta'. \quad (4.15)$$

Depending on the decomposition of the product integral in (4.12) there are several ways to evaluate the last expression. Because of the singularity of the Green's function a numerical integration is rather complicated. In a few cases analytical closed-form formulae can be obtained. However, for the majority of the possible cases a series expansion of the Green's function and λ_{m_n} or of the product of these two is suggested. Some techniques can be adapted from other numerical methods like the MoM. For instance, in [Har67] some techniques for the evaluation of terms involving this Green's function are shown.

4.2.1 Taylor Series Expansion of the Product Integral

The Taylor series expansion of the product integral is given in Appendix B.2. The parameters $\bar{\mathbf{P}}^{(0)}(\zeta)$ are linearly interpolated between the segment centers, and hence are given in segment m by

$$\bar{\mathbf{P}}^{(0)}(\zeta) = \bar{\mathbf{P}}_{m_0} + (\zeta - \zeta_{c_m}) \bar{\mathbf{P}}_{m_1}, \quad \text{for } \zeta_m \leq \zeta \leq \zeta_{m+1}, \quad (4.16)$$

where

$$\bar{\mathbf{P}}_{m_0} = \bar{\mathbf{P}}^{(0)}(\zeta_{c_m}) \quad (4.17)$$

$$\bar{\mathbf{P}}_{m_1} = \begin{cases} \frac{\bar{\mathbf{P}}^{(0)}(\zeta_{c_m}) - \bar{\mathbf{P}}^{(0)}(\zeta_{c_{m-1}})}{\zeta_{c_m} - \zeta_{c_{m-1}}} & \zeta < \zeta_{c_m} \\ \frac{\bar{\mathbf{P}}^{(0)}(\zeta_{c_{m+1}}) - \bar{\mathbf{P}}^{(0)}(\zeta_{c_m})}{\zeta_{c_{m+1}} - \zeta_{c_m}} & \zeta > \zeta_{c_m} \end{cases}. \quad (4.18)$$

Because we use a linear interpolation, the second and all higher order derivatives vanish. That makes the evaluation of the coefficients of the Taylor series (cf. (B.11)) rather simple and we get

$$\lambda_{m_n} = (\zeta' - \zeta_{c_m})^n \quad (4.19)$$

and

$$\bar{\mathbf{M}}_{m_n} = -\frac{j\omega}{n!} \left((n-1) \bar{\mathbf{P}}_{m_1} \bar{\mathbf{M}}_{m_{n-2}} + \bar{\mathbf{P}}_{m_0} \bar{\mathbf{M}}_{m_{n-1}} \right) \quad (4.20)$$

where

$$\bar{\mathbf{M}}_{m_0} = \bar{\mathbf{I}} \quad \text{and} \quad \bar{\mathbf{M}}_{m_1} = -j\omega \bar{\mathbf{P}}_{m_0} \bar{\mathbf{M}}_{m_0}. \quad (4.21)$$

Now, for a line in free space (4.15) becomes

$$I_{m_{n_{ji}}}^{(1)} = \int_{\zeta_m}^{\zeta_{m+1}} \frac{e^{-jkR_{ji}(\zeta, \zeta')} (\zeta' - \zeta_{c_m})^n}{4\pi R_{ji}(\zeta, \zeta')} d\zeta', \quad (4.22)$$

which has no closed-form solution. Similar to the product integral above, the exponential can be split into two factors, where one is independent of the integration:

$$I_{m_{n_{ji}}}^{(1)} = \frac{e^{-jkR_{ji}(\zeta, \zeta_{c_m})}}{4\pi} \int_{\zeta_m}^{\zeta_{m+1}} \frac{e^{-jk(R_{ji}(\zeta, \zeta') - R_{ji}(\zeta, \zeta_{c_m}))} (\zeta' - \zeta_{c_m})^n}{R_{ji}(\zeta, \zeta')} d\zeta'. \quad (4.23)$$

The argument of the remaining exponential function is small if the conductor length within a segment is small compared to the wavelength.

$$|R_{ji}(\zeta, \zeta') - R_{ji}(\zeta, \zeta_{c_m})| \leq |\mathbf{C}_i(\zeta_{m+1}) - \mathbf{C}_i(\zeta_m)| \ll \lambda. \quad (4.24)$$

Thus this function can be expanded into a Taylor series

$$I_{m_{n_{ji}}}^{(1)} = \frac{e^{-jkR_{ji}(\zeta, \zeta_{c_m})}}{4\pi} \sum_{p=0}^{\infty} \frac{(-jk)^p}{p!} \int_{\zeta_m}^{\zeta_{m+1}} \frac{(R_{ji}(\zeta, \zeta') - R_{ji}(\zeta, \zeta_{c_m}))^p (\zeta' - \zeta_{c_m})^n}{R_{ji}(\zeta, \zeta')} d\zeta' \quad (4.25)$$

and truncated after a few terms. The integral can then be modified, similar to (4.7), and becomes

$$\int_{\zeta_m}^{\zeta_{m+1}} \frac{(R_{ji}(\zeta, \zeta') - R_{ji}(\zeta, \zeta_{c_m}))^p (\zeta' - \zeta_{c_m})^n}{R_{ji}(\zeta, \zeta')} d\zeta' = \left(\frac{\zeta_{m+1} - \zeta_m}{l} \right)^{n+1} \int_a^{a+l} \frac{\left(\sqrt{x^2 + b^2} - \sqrt{x_c^2 + b^2} \right)^p}{\sqrt{x^2 + b^2}} (x - x_c)^n dx \quad (4.26)$$

which has a closed-form solution. For small numbers p and n the solutions are given in Appendix C.1. We can now calculate the parameters after the first iteration.

4.2.2 Eigenvalue Decomposition

Instead of representing the product integral as a Taylor expansion one could also use an eigenvalue decomposition. This method is especially useful for slowly varying parameters. We must choose a segment size such that one can assume constant parameters within a segment, i.e.

$$\bar{\mathbf{P}}^{(0)}(\zeta) = \bar{\mathbf{P}}^{(0)}(\zeta_{c_m}) \quad \text{for } \zeta_m \leq \zeta < \zeta_{m+1}. \quad (4.27)$$

Then the product integral in (4.11) becomes the matrix exponential:

$$\mathcal{M}_{\zeta_{c_m}}^{\zeta'} \left\{ -j\omega \bar{\mathbf{P}}^{(0)} \right\} = e^{-j\omega(\zeta' - \zeta_{c_m}) \bar{\mathbf{P}}^{(0)}(\zeta_{c_m})} \quad (4.28)$$

The evaluation of this expression can be carried out by diagonalizing¹ the matrix $\bar{\mathbf{P}}^{(0)}(\zeta_m)$:

$$\bar{\mathbf{P}}^{(0)}(\zeta_m) = \bar{\mathbf{w}}_m^{-1} \bar{\mathbf{D}}_m \bar{\mathbf{w}}_m \quad (4.29)$$

$$= \sum_{n=1}^{2N} d_{m_n} (\bar{\mathbf{w}}_m^{-1})_n \bar{\mathbf{w}}_{m_n}^T \quad (4.30)$$

$$= \sum_{n=1}^{2N} d_{m_n} \bar{\mathbf{W}}_{m_n}. \quad (4.31)$$

The diagonal matrix $\bar{\mathbf{D}}_m$ contains the eigenvalues of $\bar{\mathbf{P}}^{(0)}(\zeta_m)$, the columns of $\bar{\mathbf{w}}_m$ are the corresponding eigenvectors, $\bar{\mathbf{w}}_{m_n}$ and $(\bar{\mathbf{w}}_m^{-1})_n$ are the n -th columns of this matrix and its inverse, respectively. $\bar{\mathbf{W}}_{m_n}$ is the dyadic product of these two vectors, i.e. a matrix, and d_{m_n} is the n -th eigenvalue.

For the matrix exponential we can now write:

$$\mathcal{M}_{\zeta_{c_m}}^{\zeta'} \left\{ -j\omega \bar{\mathbf{P}}^{(0)} \right\} = \sum_{n=1}^{2N} e^{-j\omega(\zeta' - \zeta_{c_m}) d_{m_n}} \bar{\mathbf{W}}_{m_n} \quad (4.32)$$

and thus

$$\lambda_{m_n} = \begin{cases} e^{-j\omega(\zeta' - \zeta_{c_m}) d_{m_n}} & 1 \leq n \leq 2N \\ 0 & \text{otherwise} \end{cases} \quad (4.33)$$

$$\bar{\mathbf{M}}_{m_n} = \begin{cases} \bar{\mathbf{W}}_{m_n} & 1 \leq n \leq 2N \\ \bar{\mathbf{0}} & \text{otherwise.} \end{cases} \quad (4.34)$$

¹The diagonalization of a matrix is not always possible. However, we assume that it is possible for our matrix. Otherwise we must use a different approach to calculate the integral.

Equation (4.15), for a transmission line in free space, becomes

$$I_{m_n j_i}^{(1)} = \int_{\zeta_m}^{\zeta_{m+1}} \frac{e^{-jkR_{ji}(\zeta, \zeta')} e^{-jk_{m_n}(\zeta' - \zeta_{c_m})}}{4\pi R_{ji}(\zeta, \zeta')} d\zeta'. \quad (4.35)$$

with $k_{m_n} = \omega d_{m_n}$. Unfortunately this expression can not be integrated in closed form, however, when $k \approx k_{m_n}$ a series expansion can be used:

$$e^{-jk_{m_n}(\zeta' - \zeta_{c_m})} = e^{-jk_{m_n}(\zeta' - \zeta)} e^{-jk_{m_n}(\zeta - \zeta_{c_m})} \quad (4.36)$$

$$= e^{-jk(\zeta' - \zeta)} e^{j(k - k_{m_n})(\zeta' - \zeta)} e^{-jk_{m_n}(\zeta - \zeta_{c_m})} \quad (4.37)$$

$$= e^{-jk(\zeta' - \zeta)} \left(\sum_{p=0}^{\infty} \frac{j^p}{p!} (k - k_{m_n})^p (\zeta' - \zeta)^p \right) e^{-jk_{m_n}(\zeta - \zeta_{c_m})} \quad (4.38)$$

Inserting this into the integral yields

$$I_{m_n j_i}^{(1)} = \frac{1}{4\pi} e^{-jk_{m_n}(\zeta - \zeta_{c_m})} \sum_{p=0}^{\infty} \frac{j^p}{p!} (k - k_{m_n})^p \int_{\zeta_m}^{\zeta_{m+1}} \frac{e^{-jkR_{ji}(\zeta, \zeta')} e^{-jk(\zeta' - \zeta)}}{R_{ji}(\zeta, \zeta')} (\zeta' - \zeta)^p d\zeta', \quad (4.39)$$

which has closed-form solutions, see Appendix C.2. For $k \approx k_{m_n}$ this series can be truncated after a few terms.

4.3 Discussion of the Numerical Methods

We showed two different methods for the calculation of the parameters, one is based on a Taylor series expansion and one is based on an eigenvalue decomposition. The truncation of the Taylor series of the first approach after a few terms requires the segment length to be small. The number of terms and the segment length are directly related to each other. The more terms one takes into account the longer the segment can be. In applications it turned out that terms up to a power of 3 and a segment length, such that the conductors are not longer than $\lambda/10$, produced very good results.

Unlike the Taylor series, the eigenvalue expansion is independent from the segment length. However, it requires almost constant parameters within a segment. Thus it is especially useful for long, almost uniform line sections. There it allows an efficient determination of the line parameters. An analytical variant of this technique is used for the first examples in the following chapter.

Chapter 5

Application

Abstract — *The application of the new transmission-line supertheory is the subject of this chapter. Here we will start with a rather simple example, a finite-length wire above ground plane, where analytical solutions for the parameters can be calculated. This is followed by considerations of the semi-infinite and the infinite line, where the radiated power and the field coupling are determined. Three additional practical examples are calculated numerically. The results of the TLST are validated with the aid of measured data as well as with solutions obtained with the method of moments. All are in very good agreement.*

5.1 The Straight, Finite-Length Wire Above Ground

At a first glance the setup shown in Figure 5.1 might appear to be a simple uniform transmission line. For low frequencies ($h \ll \lambda$) this indeed is true. Then the classical transmission-line theory can be successfully applied. However, at higher frequencies, additional effects occur due to the open ends at the terminals. These influence the per-unit-length parameters and make them position dependent. We will derive analytical formulae for these parameters with the aid of the transmission-line supertheory.

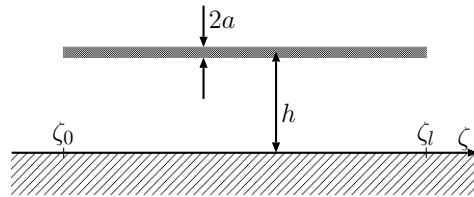


Figure 5.1: A transmission line consisting of a straight, finite-length wire parallel to a ground plane.

The exact geometry of our line is given in Figure 5.1, the line starts at ζ_0 and ends at ζ_1 . It has a radius of $a = 1$ mm and is at a height $h = 50$ mm above the ground plane.

With the aid of the image theory and the thin-wire approximation we can easily find the Green's function and the integral kernels, which are scalars in this case:

$$G(\mathbf{C}(\zeta), \mathbf{C}(\zeta')) = \frac{1}{4\pi} \left(\frac{e^{-jk\sqrt{(\zeta-\zeta')^2+a^2}}}{\sqrt{(\zeta-\zeta')^2+a^2}} - \frac{e^{-jk\sqrt{(\zeta-\zeta')^2+4h^2}}}{\sqrt{(\zeta-\zeta')^2+4h^2}} \right) \quad (5.1)$$

$$k_l(\zeta, \zeta') = \mu G(\mathbf{C}(\zeta), \mathbf{C}(\zeta')) \quad (5.2)$$

$$k_c(\zeta, \zeta') = \frac{1}{\varepsilon} G(\mathbf{C}(\zeta), \mathbf{C}(\zeta')) \quad (5.3)$$

Equation (3.57) then becomes:

$$\bar{\mathbf{I}}^{(0)} = \int_{\zeta_0}^{\zeta_l} \left[\begin{array}{cc} 0 & k_l(\zeta, \zeta') \\ k_c(\zeta, \zeta') & 0 \end{array} \right] \Big|_{\omega=0} d\zeta' \quad (5.4)$$

$$= \begin{bmatrix} 0 & \mu \\ \frac{1}{\varepsilon} & 0 \end{bmatrix} F_1(\zeta) \quad (5.5)$$

where the closed-form solution of the integral is

$$F_1 = \ln \frac{\sqrt{(\zeta_l - \zeta)^2 + a^2} + (\zeta_l - \zeta)}{\sqrt{(\zeta_l - \zeta)^2 + 4h^2} + (\zeta_l - \zeta)} - \ln \frac{\sqrt{(\zeta_0 - \zeta)^2 + a^2} + (\zeta_0 - \zeta)}{\sqrt{(\zeta_0 - \zeta)^2 + 4h^2} + (\zeta_0 - \zeta)}. \quad (5.6)$$

With (3.48) we eventually find the zeroth-order parameters for the finite-length transmission line:

$$\bar{\mathbf{P}}^{(0)} = \begin{bmatrix} \frac{1}{j\omega F_1} \frac{\partial F_1}{\partial \zeta} & \frac{1}{c_0^2} \\ 1 & 0 \end{bmatrix}. \quad (5.7)$$

The new quantity $c_0 = 1/\sqrt{\mu\varepsilon}$ indicates the propagation speed of the electromagnetic wave. In the following step we need to evaluate the product integral of (5.7). Unfortunately this is not possible in closed form. Because we are only dealing with the starting values for the iteration it is acceptable to simplify these parameters. If we are far away from the two termination regions the function F_1 becomes constant and its derivative vanishes. We can use those parameters everywhere on the line. They can be calculated by taking the following limit:

$$\bar{\mathbf{I}}^{(0)} = \lim_{\substack{\zeta_0 \rightarrow -\infty \\ \zeta_l \rightarrow \infty}} \int_{\zeta_0}^{\zeta_l} \left[\begin{array}{cc} 0 & k_l(\zeta, \zeta') \\ k_c(\zeta, \zeta') & 0 \end{array} \right] \Big|_{\omega=0} d\zeta' \quad (5.8)$$

$$= \begin{bmatrix} 0 & \mu \\ \frac{1}{\varepsilon} & 0 \end{bmatrix} \lim_{\substack{\zeta_0 \rightarrow -\infty \\ \zeta_l \rightarrow \infty}} F_1(\zeta) \quad (5.9)$$

with the solution

$$\lim_{\substack{\zeta_0 \rightarrow -\infty \\ \zeta_l \rightarrow \infty}} F_1 = F_1^\infty = 2 \ln \frac{2h}{a}. \quad (5.10)$$

Now the zeroth-order parameters are considerably simpler:

$$\bar{\mathbf{P}}^{(0)} = \begin{bmatrix} 0 & 1/c_0^2 \\ 1 & 0 \end{bmatrix}. \quad (5.11)$$

They are equivalent to the parameters from the classical transmission-line theory. The computation of the product integral can be carried out analytically:

$$\mathcal{M}_\zeta^{\zeta'} \left\{ -j\omega \bar{\mathbf{P}}^{(0)} \right\} = \begin{bmatrix} \cos k (\zeta' - \zeta) & -j \frac{1}{c_0} \sin k (\zeta' - \zeta) \\ -j c_0 \sin k (\zeta' - \zeta) & \cos k (\zeta' - \zeta) \end{bmatrix}. \quad (5.12)$$

This expression is now inserted into (3.51) and the elements of the $\bar{\mathbf{I}}^{(1)}$ matrix become:

$$I_{11}^{(1)} = I_{22}^{(1)} = -\frac{j}{4\pi} \sqrt{\frac{\mu}{\varepsilon}} G_1 \quad (5.13)$$

$$I_{12}^{(1)} = \frac{\mu}{4\pi} G_2 \quad (5.14)$$

$$I_{21}^{(1)} = \frac{1}{4\pi\varepsilon} G_2 \quad (5.15)$$

where

$$\begin{aligned} \begin{Bmatrix} G_1 \\ G_2 \end{Bmatrix} &= \int_{\zeta_0}^{\zeta_l} G(\mathbf{C}(\zeta), \mathbf{C}(\zeta')) \begin{Bmatrix} \sin k (\zeta' - \zeta) \\ \cos k (\zeta' - \zeta) \end{Bmatrix} d\zeta' \\ &= \begin{Bmatrix} -j/2 \\ 1/2 \end{Bmatrix} \left(\mathbf{E}_1(jkR_{1l-}) - \mathbf{E}_1(jkR_{10-}) - \mathbf{E}_1(jkR_{2l-}) + \mathbf{E}_1(jkR_{20-}) \right. \\ &\quad \left. \pm (\mathbf{E}_1(jkR_{1l+}) - \mathbf{E}_1(jkR_{10+}) - \mathbf{E}_1(jkR_{2l+}) + \mathbf{E}_1(jkR_{20+})) \right) \end{aligned} \quad (5.16)$$

and

$$R_{1\{0\}^\pm} = \sqrt{\left(\zeta_{\{l\}^\pm} - \zeta \right)^2 + a^2} \pm \left(\zeta_{\{l\}^\pm} - \zeta \right) \quad (5.17)$$

$$R_{2\{0\}^\pm} = \sqrt{\left(\zeta_{\{l\}^\pm} - \zeta \right)^2 + 4h^2} \pm \left(\zeta_{\{l\}^\pm} - \zeta \right). \quad (5.18)$$

The function E_1 is the exponential integral (see [AS72])

$$E_1(z) = \int_z^\infty \frac{e^{-t}}{t} dt. \quad (5.19)$$

With these results we can give a closed-form solution for the parameter matrix $\overline{\mathbf{P}}$ after one iteration:

$$\overline{\mathbf{P}}^{(1)} = \begin{bmatrix} \frac{1}{j\omega} \frac{1}{G_2} \frac{\partial G_2}{\partial \zeta} & \frac{1}{c_0^2} - \frac{1}{\omega c_0} \frac{1}{G_2} \frac{\partial G_1}{\partial \zeta} \\ 1 & 0 \end{bmatrix}. \quad (5.20)$$

In our setup, the current only has a component in the direction of the conductor, which is straight and in parallel to the ground plane. Then the vector potential is also in this direction and we can define the voltage in a plane perpendicular to the conductor as

$$v(\zeta) := \varphi(\zeta), \quad (5.21)$$

where φ is the scalar potential at this conductor. Hence, we can give the telegrapher equations in the voltage-current representation, as it is known from the classical theory:

$$\frac{\partial}{\partial \zeta} \begin{bmatrix} v \\ i \end{bmatrix} + j\omega \overline{\mathbf{P}}^{*(1)} \begin{bmatrix} v \\ i \end{bmatrix} = \mathbf{0}, \quad (5.22)$$

with

$$\overline{\mathbf{P}}^{*(1)} = \begin{bmatrix} -j \frac{1}{c_0} \frac{G_1}{G_2} & \frac{\mu}{4\pi} \left(G_2 + \frac{G_1^2}{G_2} \right) \\ 4\pi \varepsilon \frac{1}{G_2} & j \frac{1}{c_0} \frac{G_1}{G_2} \end{bmatrix}. \quad (5.23)$$

By solving the above equations with appropriate boundary conditions we can compute currents and voltages. However, it is almost not possible to compare these results with data from measurements or from computations with other methods, e.g. MoM. Real setups as well as MoM models require fixed boundary conditions at the terminals. This means, we have to connect a source and a load at the two ends of the transmission line. In our TLST setup, there is no connection from the wire to the ground plane. We would have to take this into account in the parameter computation. This means the MoM computation and measurements would refer to a different system than the one computed with the TLST. The results will be different and a comparison does not make sense. We can, however, compare the parameters from the classical transmission-line theory with our new parameters.

For this we investigate a line where the conductor is 50 mm above the ground plane, has a radius of 1 mm and is 1 m long. Figure 5.2 shows the per-unit-length inductance for different frequencies related to the per-unit-length inductance calculated with the classical transmission-line theory ($l_0 = \frac{\mu}{2\pi} \ln \frac{2h}{a}$). For low frequencies ($\lambda \gg h$) we see

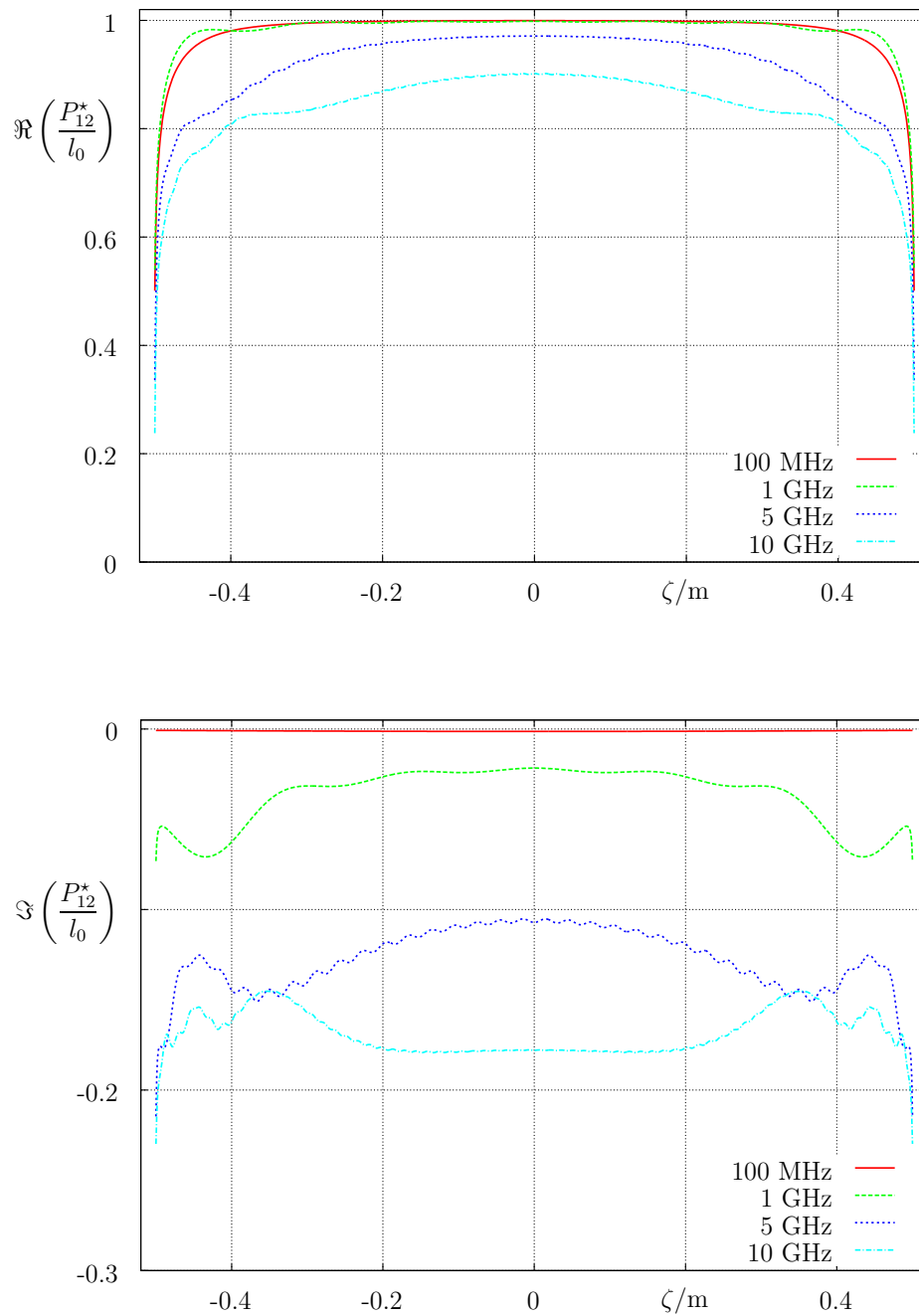


Figure 5.2: Per-unit-length inductance of the finite-length transmission line related to the corresponding parameter from the classical transmission-line theory (upper plot real part, lower plot imaginary part).

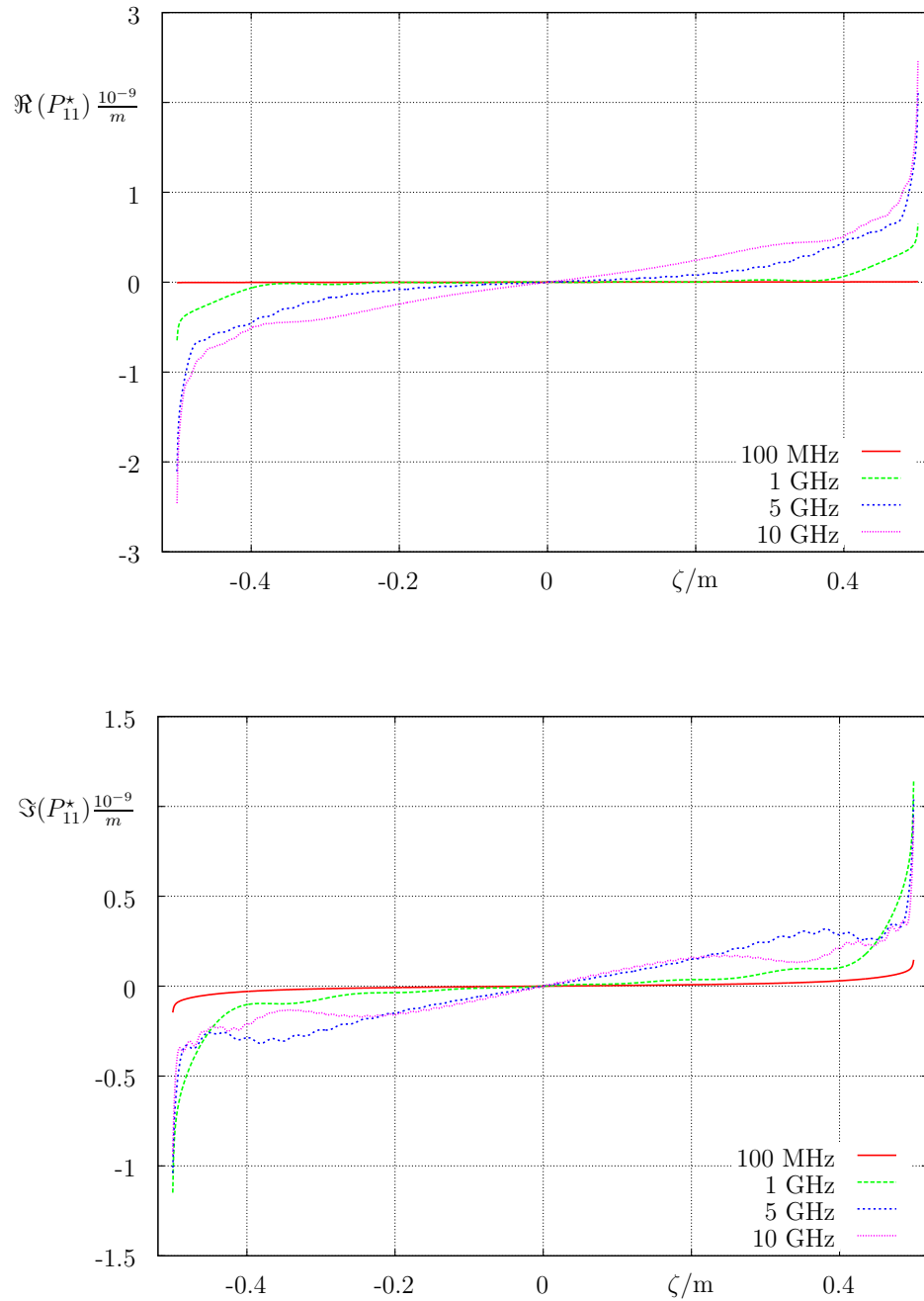


Figure 5.3: Per-unit-length parameter P_{11}^* of the finite-length transmission line (upper plot real part, lower plot imaginary part).

that in the central part of the line, this parameter is equal to the parameter from the classical theory. Compared to a point at the central part of the line where the wire is present at both sides, at the terminals the wire is only present at one side. Only this wire contributes to the inductance and consequently the value must decrease to one half of the value at the center.

As we increase the frequency and come into regions where the wavelength and the height are in the same order of magnitude, the real part of the parameters become smaller and an imaginary part occurs, which, multiplied with $j\omega$, becomes real and is a part of the radiation resistance. This effect is especially large at the terminals, but existent along the whole conductor. A similar behavior can be observed for the per-unit-length capacitance with the difference that it increases when getting closer to the terminals. Also the diagonal parameters P_{11}^* (see Figure 5.3) and P_{22}^* reflect this frequency-dependent behavior. The parameters almost vanish for low frequencies and become larger with higher frequencies. They show the largest values at the terminals. The “antisymmetric” progression with respect to ζ is caused by the antisymmetric definition of the current which always flows towards larger ζ .

To further concentrate on the open end, we move one open end to infinity. This end is then far enough away to not influence the other end and we can fix the boundary condition there. This leads to the semi-infinite line.

5.2 The Semi-Infinite Line

As noted before, to get from the finite line to the semi-infinite line we just have to let ζ_0 go to $-\infty$. Then G_1 and G_2 become

$$\begin{Bmatrix} G_1 \\ G_2 \end{Bmatrix} = \begin{Bmatrix} -j/2 \\ 1/2 \end{Bmatrix} \left(E_1(jkR_{1l-}) - E_1(jkR_{2l-}) \pm (E_1(jkR_{1l+}) - E_1(jkR_{2l+})) + 2 \ln \frac{2h}{a} \right). \quad (5.24)$$

The parameters are calculated with the aid of (5.20). They are very similar to the parameters of the finite line. At the open end they show the same behavior. If we move away from the open end the parameters approach the parameters of the classical transmission-line theory.

We can now go one step further and calculate currents and voltages on the line by solving the extended telegrapher equations numerically. A wave can be generated by connecting a voltage source ($v = 1$ V). The source should be far enough away from the open end. This is the case when the per-unit-length parameters are approximately the same as those of the classical transmission-line theory. Furthermore, the internal resistance of the source should match the characteristic impedance of the line to avoid reflections.

When a wave, that travels along the line, comes into the region, where the parameters start to change due to the influence of the open end, at every position a small fraction of the wave will be reflected. Additionally, a small part will be radiated and the remaining part travels further where again a small fraction will be reflected and radiated. When the wave eventually reaches the end, again a part of the energy travels further, and therefore, is radiated and the rest is reflected. This effect is small for low frequencies. Here almost all energy will be reflected and hence, the reflection factor is one. In this frequency region the classical transmission-line theory is still valid. For higher frequencies the radiation increases and less wave energy is reflected. This behavior can be observed in the reflection factor r vs. frequency. The magnitude of this quantity is presented in Figure 5.4. It was calculated from the actual voltages and currents from the transmission-line supertheory. Moreover, the plot shows the magnitude of the reflection factor calculated with the method of moments (MoM), which is a direct numerical solution of Maxwell's equations. For this computation the program CONCEPT was used. The line was modeled with a thin 5 m long wire. The discretization was chosen such that at least 20 segments per wavelength were used. At one end the line was connected to the ground plane and excited with a voltage source. The other end was left open. Then at the central part of the line, far away from the terminations, one can assume a TEM mode with forward and backward traveling waves. These waves were determined from the current distribution. Their quotient then gives the desired reflection factor. Practically, there is no difference between the two curves. Thus we can say that the TLST correctly models the physical conditions at the open end, and this only after one iteration.

5.3 Field Coupling to an Infinite Line

Now we move the remaining end of the semi-infinite line to infinity. This gives an infinitely long line. As long as there is no external excitation only a TEM mode can propagate. This statement is supported by the per-unit-length parameters, which can be calculated by setting ζ_l in (5.24) to infinity. The result is

$$G_1 = 0 \quad \text{and} \quad G_2 = 2 \ln \frac{2h}{a}, \quad (5.25)$$

which yields the parameters

$$\bar{\mathbf{P}}^{(1)} = \begin{bmatrix} 0 & \frac{1}{c_0^2} \\ 1 & 0 \end{bmatrix} \quad (5.26)$$

or, for the v - i representation

$$\bar{\mathbf{P}}^{*(1)} = \begin{bmatrix} 0 & \frac{\mu}{2\pi} \ln \frac{2h}{a} \\ 2\pi\epsilon \frac{1}{\ln \frac{2h}{a}} & 0 \end{bmatrix}. \quad (5.27)$$

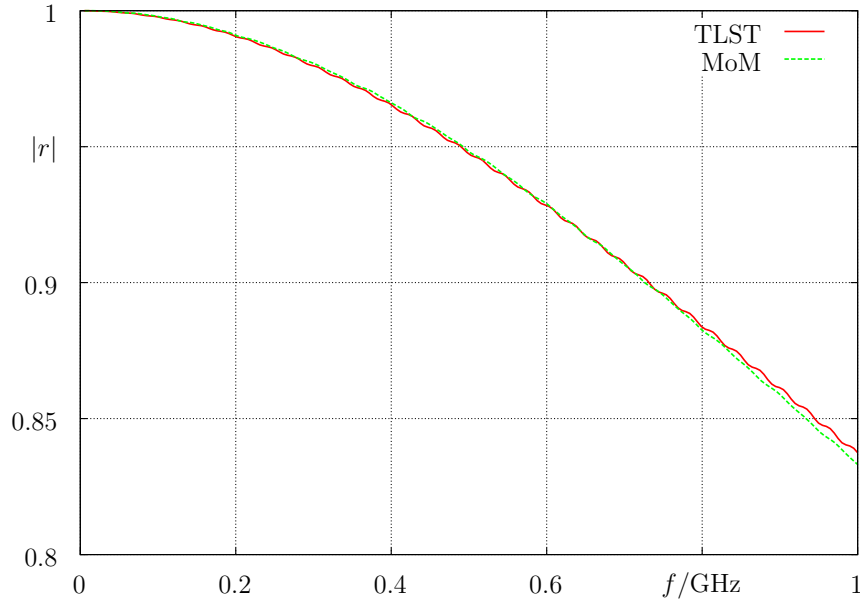


Figure 5.4: The reflection factor at the open end of the semi-infinite transmission line.

These are exactly the same as the zeroth-order parameters, which means, that the iteration already converged to the exact result. The parameters are frequency and position independent. The diagonal terms in the v - i representation as well as in the q - i representation vanish and the remaining parameters are real valued. This indicates that there is no radiation caused by the transmission line itself. However, when illuminated with an external field (see Figure 5.5) a non-TEM mode can be excited and radiation occurs (see also [NT04c]). This is not reflected in the per-unit-length parameters but in the source terms. With the TLST we are able to derive the correct expressions for this situation.

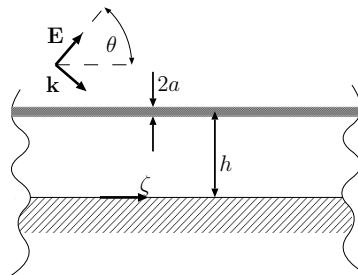


Figure 5.5: The infinitely long, uniform transmission line with field coupling.

The electric field strength along the wire for an incident plane-wave field as in Fig. 5.5

is given by

$$v^{(i)'}(\zeta) = E_0 e^{-jk\zeta \cos \theta}, \quad (5.28)$$

where E_0 is the magnitude that also takes into account the reflections from the ground plane. Normally one would use the iterative procedure (3.59) to determine q'_s . In this special case, however, a closed-form solution is possible. The dependence of the electric field on the spatial coordinate ζ implies the same dependence of the source term:

$$q'_s(\zeta) = q'_0 e^{-jk\zeta \cos \theta}. \quad (5.29)$$

Then with (3.46) we may write

$$I_{10} = -jc_0 q'_0 \int_{-\infty}^{\infty} k_l(\zeta, \zeta') \int_{\zeta}^{\zeta'} \sin(k(\zeta' - \xi)) e^{-jk\xi \cos \theta} d\xi d\zeta' \quad (5.30)$$

and

$$I_{20} = q'_0 \int_{-\infty}^{\infty} k_c(\zeta, \zeta') \int_{\zeta}^{\zeta'} \cos(k(\zeta' - \xi)) e^{-jk\xi \cos \theta} d\xi d\zeta'. \quad (5.31)$$

The inner integration is carried out first and yields

$$\int_{\zeta}^{\zeta'} \sin(k(\zeta' - \xi)) e^{-jk\xi \cos \theta} d\xi = \frac{e^{-jk\zeta \cos \theta}}{k \sin^2 \theta} \left[e^{-jk(\zeta' - \zeta) \cos \theta} - \cos(k(\zeta' - \zeta)) + j \sin(k(\zeta' - \zeta)) \cos \theta \right] \quad (5.32)$$

and

$$\int_{\zeta}^{\zeta'} \cos(k(\zeta' - \xi)) e^{-jk\xi \cos \theta} d\xi = -j \cos(\theta) \frac{e^{-jk\zeta \cos \theta}}{k \sin^2 \theta} \left[e^{-jk(\zeta' - \zeta) \cos \theta} - \cos(k(\zeta' - \zeta)) + j \sin(k(\zeta' - \zeta)) \frac{1}{\cos \theta} \right]. \quad (5.33)$$

Because k_l and k_c are even functions, and the sine is an odd function the sine components in (5.32) and (5.33) do not contribute to the integrals in (5.30) and (5.31). Hence we may write

$$I_{10} = jc_0 q'_0 \frac{e^{-jk\zeta \cos \theta}}{k \sin^2 \theta} \int_{-\infty}^{\infty} k_l(\zeta, \zeta') (\cos(k(\zeta' - \zeta)) - \cos(k(\zeta' - \zeta) \cos \theta)) d\zeta' \quad (5.34)$$

and

$$I_{20} = j \cos \theta q'_0 \frac{e^{-jk\zeta \cos \theta}}{k \sin^2 \theta} \int_{-\infty}^{\infty} k_c(\zeta, \zeta') (\cos(k(\zeta' - \zeta)) - \cos(k(\zeta' - \zeta) \cos \theta)) d\zeta'. \quad (5.35)$$

These integrals can be solved (see Appendix C.3) and result in

$$I_{10} = j \frac{\mu}{4\pi} c_0 q'_0 \frac{e^{-jk\zeta \cos \theta}}{k \sin^2 \theta} (G_2 - G_3) \quad (5.36)$$

and

$$I_{20} = j \frac{1}{4\pi\epsilon} \cos \theta q'_0 \frac{e^{-jk\zeta \cos \theta}}{k \sin^2 \theta} (G_2 - G_3) \quad (5.37)$$

where

$$G_2 = 4\pi \int_{-\infty}^{\infty} g(\mathbf{C}(\zeta), \mathbf{C}(\zeta')) \cos(k(\zeta' - \zeta)) d\zeta' \quad (5.38)$$

$$= 2 \ln \frac{2h}{a}, \quad (5.39)$$

$$G_3 = 4\pi \int_{-\infty}^{\infty} g(\mathbf{C}(\zeta), \mathbf{C}(\zeta')) \cos(k(\zeta' - \zeta) \cos \theta) d\zeta' \quad (5.40)$$

$$= -j\pi \left(H_0^{(2)}(ak \sin \theta) - H_0^{(2)}(2hk \sin \theta) \right). \quad (5.41)$$

With the aid of (5.28) and (5.29) we can now solve (3.49) for q_0 giving the rather simple answer

$$q_0 = \frac{4\pi\epsilon}{G_3} E_0. \quad (5.42)$$

Then the **exact extended telegrapher equations** for a uniform, infinite long, ideally conducting transmission line with plane-wave field coupling become

$$\frac{\partial}{\partial \zeta} \begin{bmatrix} q \\ i \end{bmatrix} + j\omega \begin{bmatrix} 0 & \frac{1}{c_0^2} \\ 1 & 0 \end{bmatrix} \begin{bmatrix} q \\ i \end{bmatrix} = \begin{bmatrix} \frac{4\pi\epsilon}{G_3} E_0 e^{-jk\zeta \cos \theta} \\ 0 \end{bmatrix}. \quad (5.43)$$

We may also convert this to the v - i representation giving:

$$\frac{\partial}{\partial \zeta} \begin{bmatrix} v \\ i \end{bmatrix} + j\omega \begin{bmatrix} 0 & P_{12}^* \\ P_{21}^* & 0 \end{bmatrix} \begin{bmatrix} v \\ i \end{bmatrix} = \begin{bmatrix} \frac{G_2 - G_3 \cos^2 \theta}{G_2 \sin^2 \theta} E_0 e^{-jk\zeta \cos \theta} \\ -\sqrt{\frac{\epsilon}{\mu}} \frac{4\pi(G_2 - G_3) \cos \theta}{G_2 G_3 \sin^2 \theta} E_0 e^{-jk\zeta \cos \theta} \end{bmatrix}. \quad (5.44)$$

These equations are identical with the results obtained in [NT04c] with the aid of a spatial Fourier transformation. For small k , if $\lambda \ll h$, the function G_3 converges to

G_2 thus $G_3 \approx G_2$. In this case, the source terms can be simplified and the telegrapher equations become

$$\frac{\partial}{\partial \zeta} \begin{bmatrix} v \\ i \end{bmatrix} + j\omega \begin{bmatrix} 0 & P_{12}^* \\ P_{21}^* & 0 \end{bmatrix} \begin{bmatrix} v \\ i \end{bmatrix} = \begin{bmatrix} E_0 e^{-jk\zeta \cos \theta} \\ 0 \end{bmatrix}. \quad (5.45)$$

This is exactly the same result one gets from the classical transmission-line theory with Agrawal's field-coupling model (cf. Section 2.2.3).

5.4 The Skewed Wire Transmission Line

We now choose a more complicated configuration and take a closer look at a skewed wire transmission line. This line is built from a finite-length wire which is located above a ground plane. The wire is not parallel to this plane, as shown in Figure 5.6. Furthermore, at one end the wire is short circuited to the ground plane. This is the

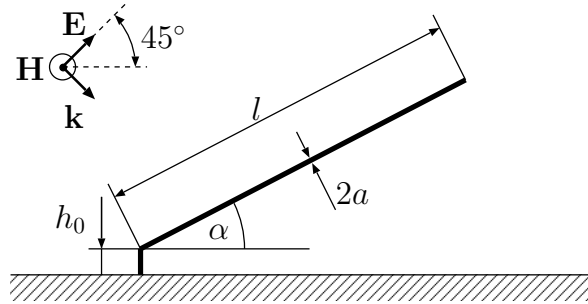


Figure 5.6: The setup of the skewed wire transmission line ($h_0 = 1$ mm, $l = 0.538$ m, $a = 0.2$ mm).

place where the line will be fed and the current is measured.

The current on this line consists of two components which are often referred to as the transmission-line-mode current and the antenna-mode current. In order to determine these two, we take into account the mirror image due to the ground plane. Furthermore, we know that the current is derived from a vector quantity and as such can be decomposed into mutually orthogonal (horizontal and vertical) components (see Figure 5.7). The horizontal parts have opposite directions, such that the fields that are caused by these currents partly compensate each other. This is a property of the transmission-line mode. The vertical components have the same direction and the field contributions add up. This indicates the antenna mode.

Thus for an angle of $\alpha = 0^\circ$ there are almost no antenna mode currents, (except for the riser) and the line behaves like a (classical) transmission line. For an angle of $\alpha = 90^\circ$

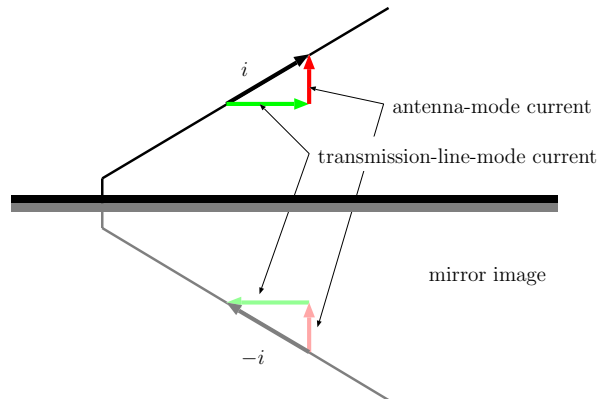


Figure 5.7: Transmission-line-mode current and antenna-mode current in the skewed transmission line.

there are no transmission-line-mode currents. The wire is an effective antenna. Both cases, and all in between, will be correctly modeled by the TLST.

Unfortunately, we can not easily define a voltage in this setup, because the vector potential does not only have components in the direction of the conductor. The v - i representation is not suitable here. We will rather use the q - i or φ - i representation. As stated before the quasivoltage has no physical meaning, except for parts of the line, that are very close ($\ll \lambda$) to the ground plane, e.g., the beginning of the vertical part. Then φ becomes the real voltage between the plane and the transmission line.

The per-unit-length parameters are calculated numerically. Figure 5.8 shows the P_{12} parameters of the q - i representation, related to the corresponding parameter of a uniform line. It was calculated for different angles at a frequency of 1 GHz. For other frequencies the parameter shows a very similar behavior.

When $\alpha = 0^\circ$ the line behaves almost like a uniform line because its distance to the ground plane is only 1 mm. This is much smaller than the wavelength. Only very close to the terminals a small deviation from the classical TLT parameters can be observed. The parameter P_{12} is real and has a value of almost $1/c_0^2$, just like a uniform line. When the angle increases, the value of the parameter starts to change, it becomes position dependent and complex. For a lossless system this indicates radiation. The biggest deviation can be observed for an angle of $\alpha = 90^\circ$, where the wire is an antenna.

To validate our TLST we compare the magnitude of the input impedance $|Z_i|$ of the transmission line with measured data. The measurement was performed on an actual setup of the line with an angle of $\alpha = 21.7^\circ$ with a network analyzer. The results are shown in Figure 5.9. The two currents show a reasonably good agreement. Both curves show the typical behavior of an open-ended transmission line. One can identify the resonances due to standing waves; their frequencies roughly correspond to the length

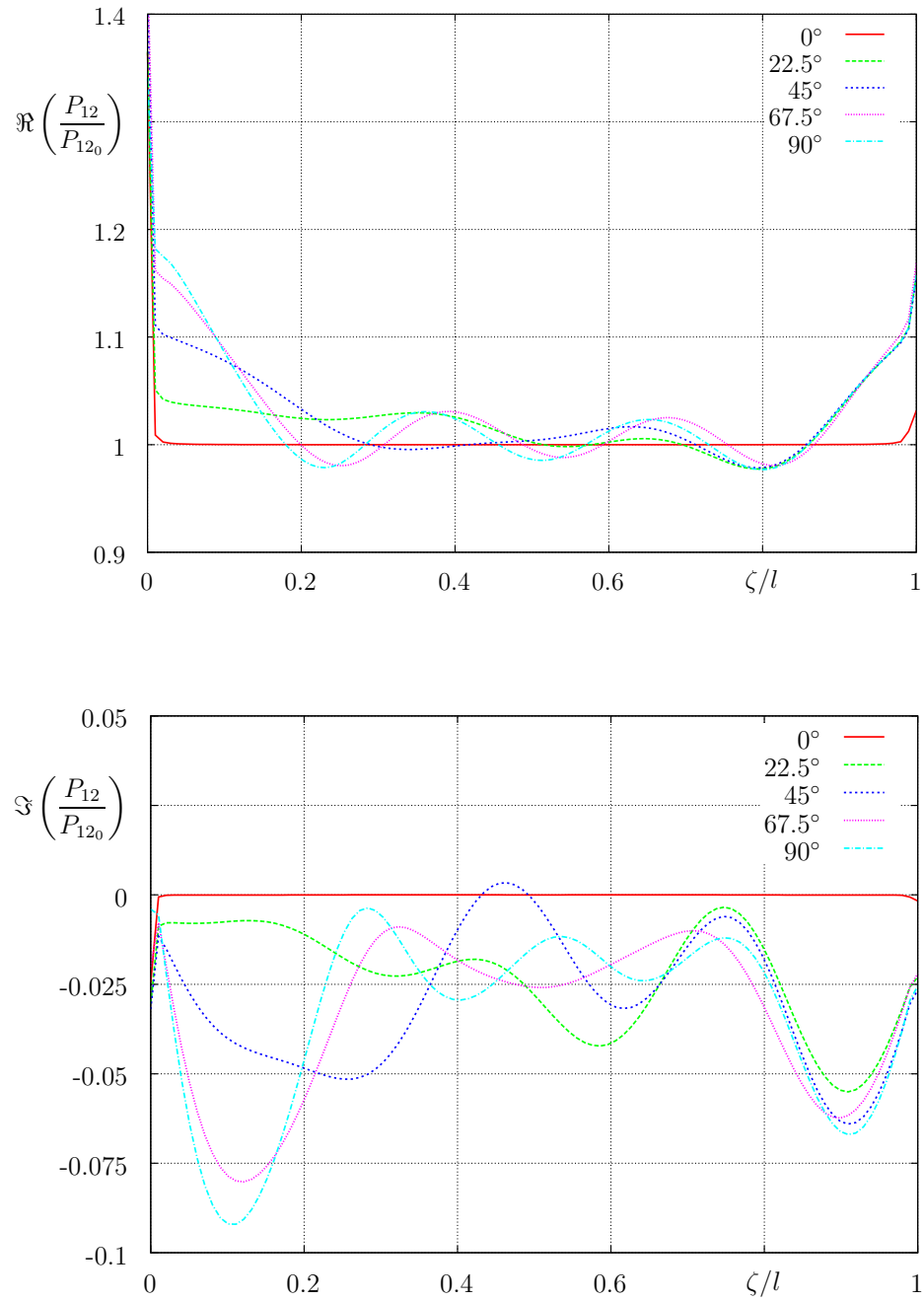


Figure 5.8: The real (upper) and imaginary (lower) parts of the parameter P_{12} for the skewed transmission line, related to the corresponding parameter of a uniform line ($P_{12_0} = 1/c_0^2$).

of the wire. For lower frequencies the resonances are very sharp and have very high or very low magnitudes, respectively. With increasing frequency they become smeared out and less sharp which is caused by losses. These are radiation losses, because the system is otherwise considered to be lossless. The input impedance looks very similar for other angles, up to 90° .

The validity can also be confirmed with MoM calculations. Also here the program CONCEPT was used. The line was modeled with a thin wire and the discretization was chosen to have more than 20 segments per wavelength. A 1 V voltage source was used as the excitation at the beginning of the line. Then the current distribution along the skewed wire was determined for a frequency of 0.974 GHz, which is very close to a resonance frequency. The results from the TLST are compared with the MoM solution in Figure 5.9. Again we have a very good agreement between the two results.

Eventually, we can also excite the skewed transmission line with an external field, i.e., use the line as a receiving antenna. The vectors \mathbf{E} and \mathbf{k} were directed as shown in Figure 5.6. As can be seen in Figure 5.10 one gets a perfect match between the MoM and the TLST solution.

5.5 The Periodic Transmission Line

Realistic transmission lines often have a periodic structure. Some examples are lines that are tied together in periodic distances, lines that are placed above a periodic structure, or helically-shaped lines that are placed above a ground plane. These periodic lines exhibit a very interesting behavior, e.g., they block certain frequency bands. These effects can be computed with the classical transmission-line theory for nonuniform lines and are not of interest here. We will present strong effects that can not be seen with this theory.

For this we investigate a rather canonical structure, a sinusoidally-shaped line like the one shown in Figure 5.11. It is 0.8 m long and has 8.5 periods with an amplitude of 5 cm. The zero-line of the sine is 6 cm above the ground plane and the wire has a radius of 0.2 mm. At both terminals the line is connected to the ground plane via a resistor roughly the size of the low-frequency wave resistance ($R = 304 \Omega$). Furthermore a voltage source of 1 V is connected at the beginning of the line.

Figure 5.12 shows the input and output current of the transmission line as a function of frequency. Up to 1 GHz the transmission line shows a rather typical behavior. The resistor of 304Ω is not a perfect match, such that some reflections occur at the terminals. This causes the ripples on the current. The input and output currents are almost equal and close to $1 \text{ V} / (2 \cdot 304 \Omega) = 1.6 \text{ mA}$, just as it should be for a matched transmission line. There are some irregularities which are caused by the nonuniformity, they occur above 500 MHz.

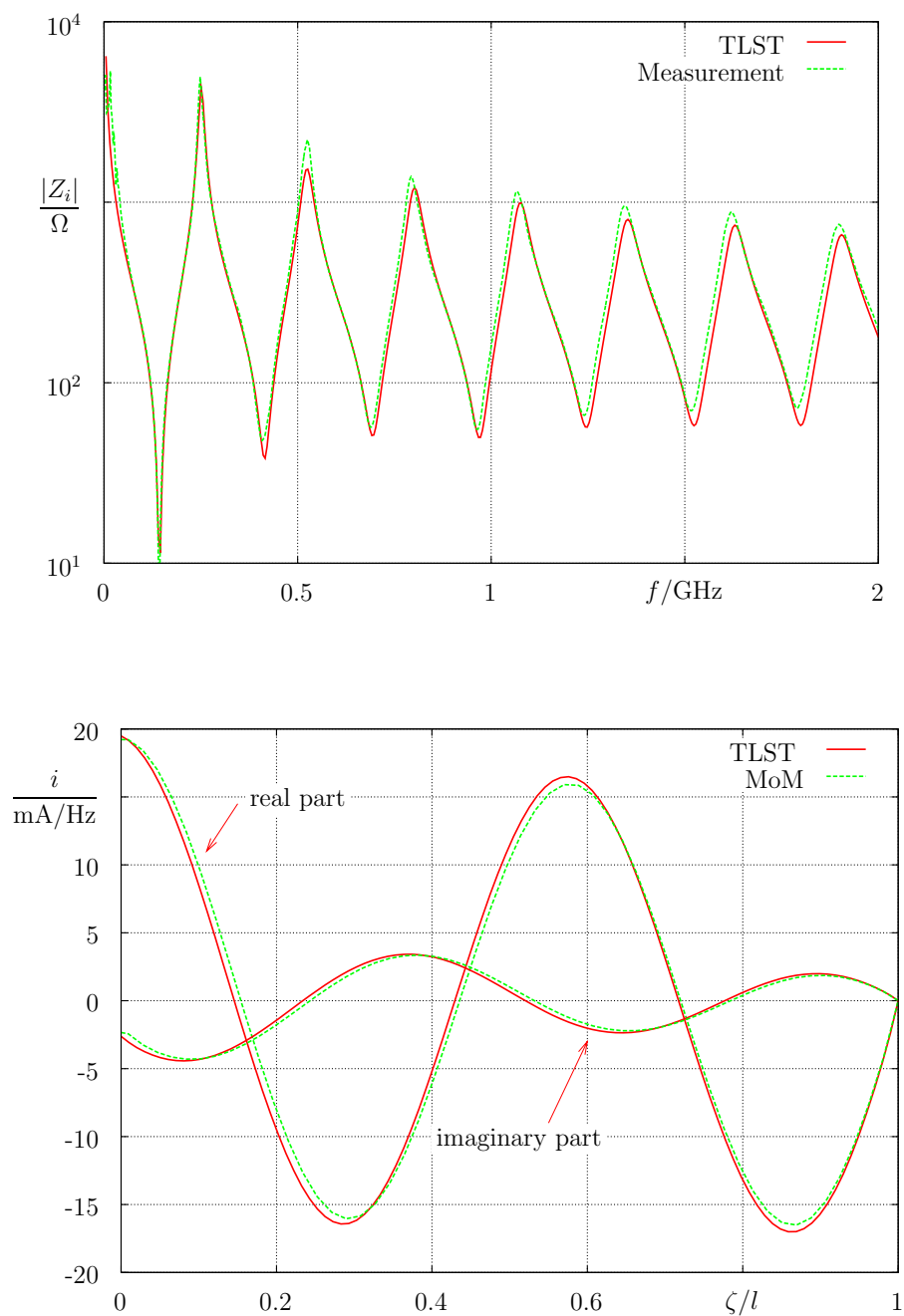


Figure 5.9: The magnitude of the input impedance Z_i vs. frequency (upper) and the current distribution at 0.974 GHz (lower) of the skewed transmission line ($\alpha = 21.7^\circ$).

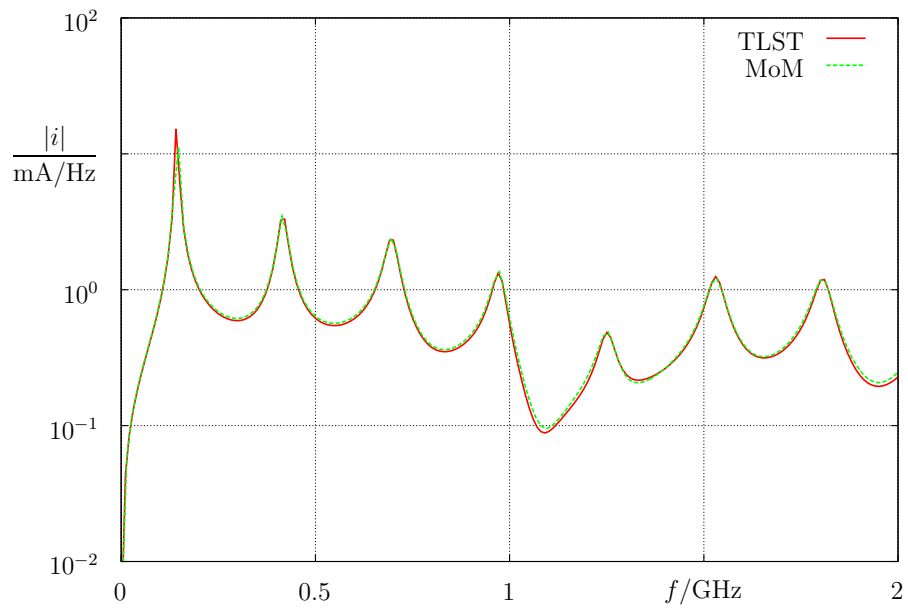


Figure 5.10: The magnitude of the field excited current to the ground plane vs. frequency of the skewed transmission line ($\alpha = 21.7^\circ$).

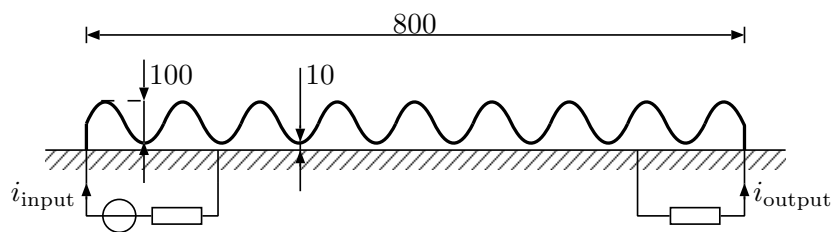


Figure 5.11: The mechanical and electrical setup of the sinusoidal transmission line.

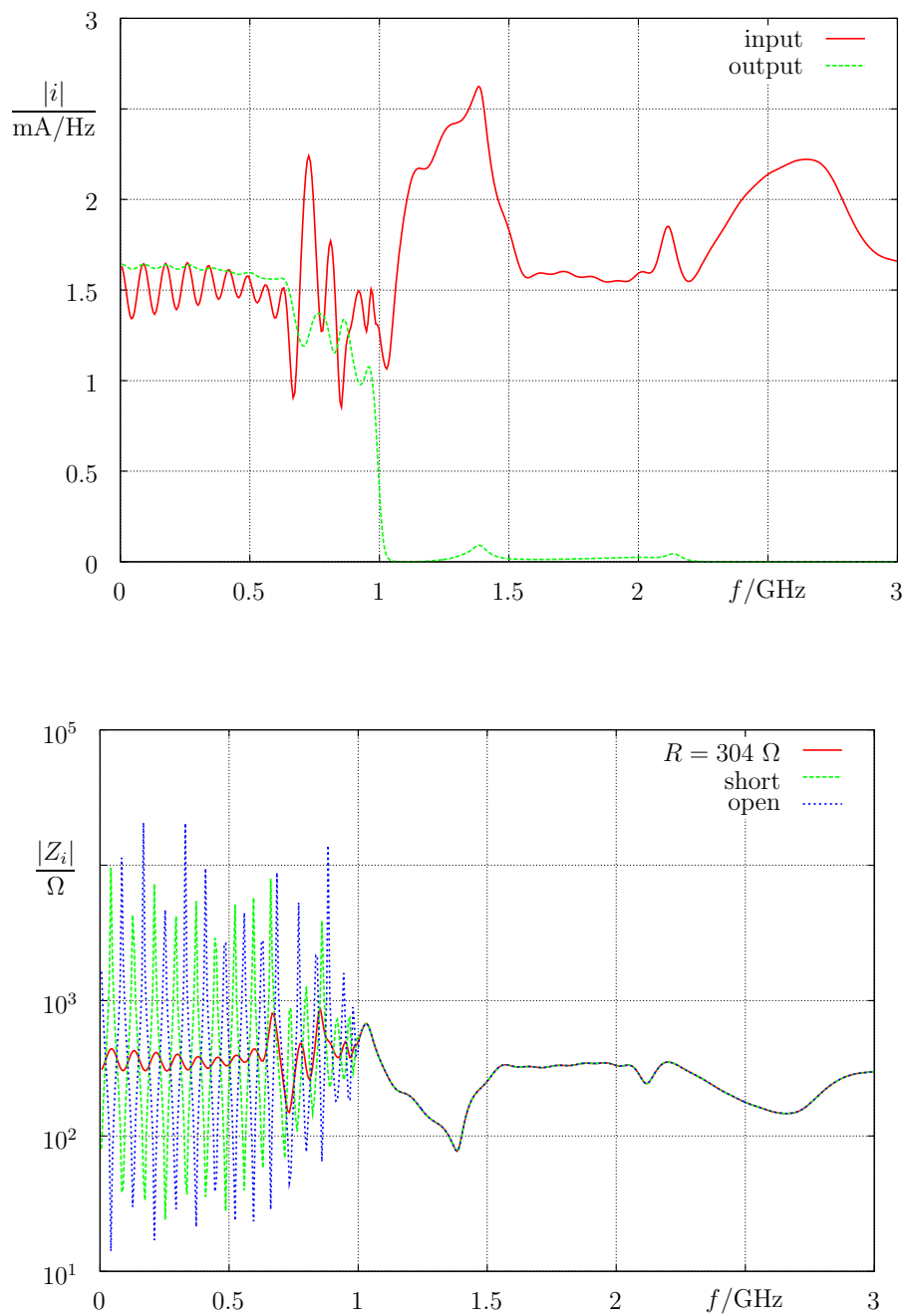


Figure 5.12: The magnitude of the input current vs. frequency (upper) and the input impedance for three different terminations (lower) of the periodic transmission line ($\alpha = 21.7^\circ$).

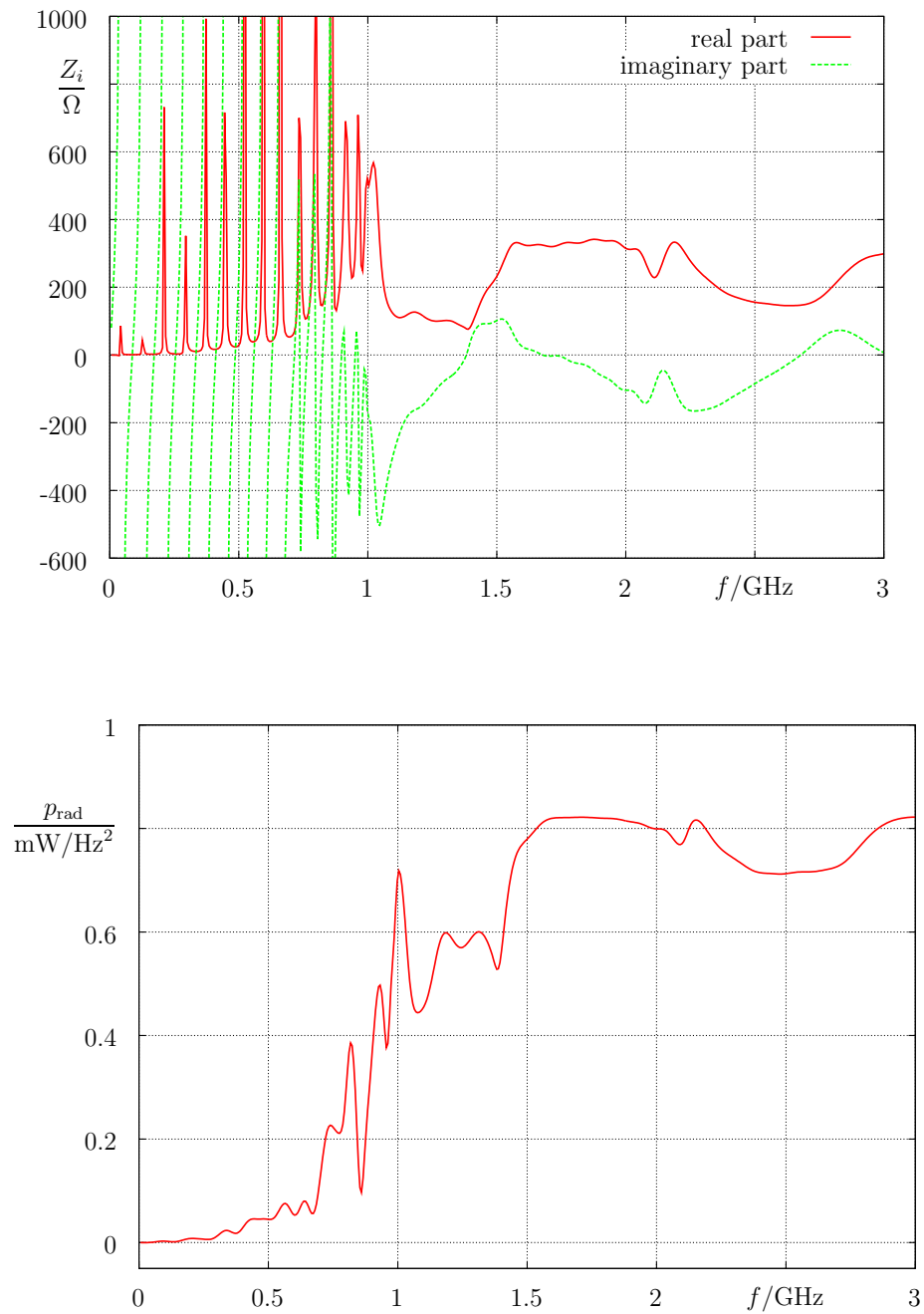


Figure 5.13: The real and imaginary part of the input impedance of the sinusoidal line when short circuited to the ground (upper) and the radiated power (lower).

Above 1 GHz the behavior dramatically changes. This is the frequency, where approximately 8 to 9 periods of the wave are on the line. The output current decreases rapidly and stays very close to zero for all frequencies. Thus a signal that propagates along the line does not reach the end. The vanishing current at the end suggests the assumption that the input impedance is independent from the termination resistor above 1 GHz. This is indeed the case as can be seen in Figure 5.12, where the magnitudes of the input impedances for the open, shorted and “almost matched” far end are shown.

Below 1 GHz all three configurations show the typical transmission-line input impedance. We see the transformation of the termination resistor to the beginning of the line. Above 1 GHz, all three input impedances are exactly equal. Hence, the input impedance of the line is independent from the actual termination. Furthermore, above this frequency the input impedance has a large real part (see Figure 5.13) and a rather small imaginary part. The line acts almost like a resistor. This must be due to the radiation, because the transmission line itself is perfectly conducting.

We can also calculate the time averaged radiated power by subtracting the power dissipated in the termination resistors from the power generated by the source. The result is shown in Figure 5.13 as well. The line is a quite good wide band radiator at frequencies above 1.5 GHz. Practical applications of this might be possible, however, further investigations are necessary, e.g., the radiation pattern must be analyzed.

5.6 Cross Talk in a Nonuniform Multiconductor Transmission Line

In this final example we examine the crosstalk in a nonuniform multiconductor transmission line. Figure 5.14 shows the V-shaped wires which are placed above a ground plane. One wire is at a constant height of 20 mm, the height of the other wire changes from 10 mm to 20 mm. Furthermore, the wires are bent at the ends in order to reach the termination resistors which are located below the ground plane.

The wire that changes its height is driven by a voltage source of 1 V with an internal resistance of 50Ω . All other ends are terminated with 50Ω resistors.

Figure 5.15 shows the cross talk current flowing into the termination resistor at the far end of the passive wire. The plot presents the solutions from the TLST with the parameters after one iteration. Additionally, the current, measured with a network analyzer on a real setup of the wire structure is shown for validation. Also here one finds a very good agreement between the measurement and the TLST prediction for the cross talk current. Similar results can be obtained for all other currents which agree equally well with the measured data.

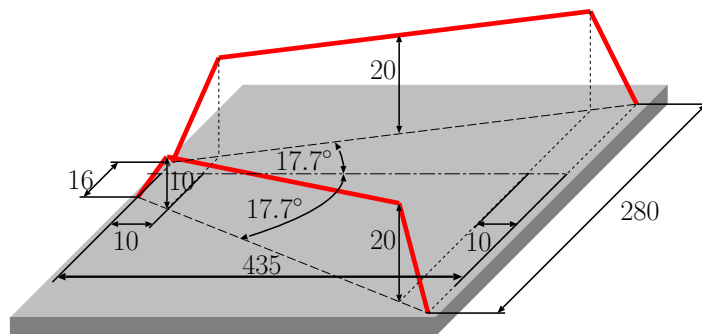


Figure 5.14: A nonuniform multiconductor transmission-line.

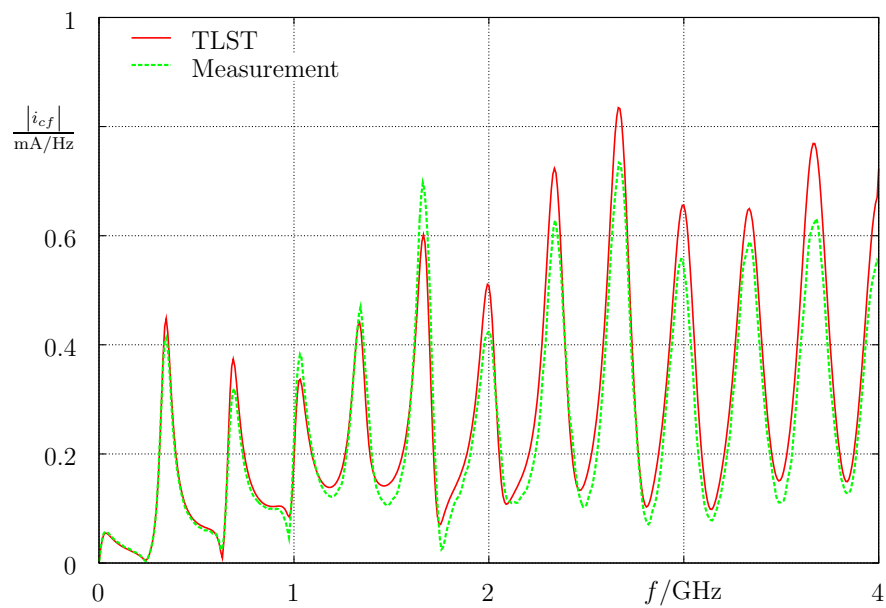


Figure 5.15: The far end cross talk current of the passive wire of the NMTL.

Chapter 6

Conclusion and Perspectives

The focus of this thesis is the full-wave description of the interactions between nonuniform multiconductor transmission lines and electromagnetic fields with the aid of an extended transmission-line theory, the transmission-line supertheory. It covers not only the derivation of this novel theory but also the application to canonical and realistic examples.

For the derivation, first an integral equation is formulated based on the general solution of Maxwell's equations and the boundary condition at the surface of the conductors. This rather general expression is then adapted to the geometry of the nonuniform transmission line, which is described with the aid of space curves and polar coordinate systems. The unknown quantities in these equations are the current and the per-unit-length charge along the conductors.

Based on the assumption that the current is governed by a second-order differential equation, a trial function is formulated and inserted into the adapted integral equation. Together with the continuity equation the integral equation can then be cast into a system of first-order differential equations for the unknown currents and per-unit-length charges. The equations are the extended telegrapher equations of the transmission-line supertheory. The remarkable result is that this conversion is possible without any additional assumptions or simplifications.

Moreover, in the course of the derivation one gets integral equations for the determination of the coefficients of the differential equations, i.e. the per-unit-length parameters, and for the distributed source terms. Because there are no known general analytical solutions for these equations iterative procedures are suggested which give very good results even after one iteration.

The position-dependent per-unit-length parameters become complex and frequency dependent. The extended telegrapher equations with these parameters correctly model the propagation of electromagnetic waves along nonuniform multiconductor transmission lines, the radiation of electromagnetic energy, and the coupling of external fields

for all frequencies. There is no restriction to the quasi-TEM mode like in the classical transmission-line theory.

The capabilities of the new theory are demonstrated in detail for several examples. First a finite length transmission line is considered and the parameters are computed. This setup is then modified to a semi-infinite line and the radiated power and reflection coefficient is calculated at the finite terminal. Both are found to be in perfect agreement with MoM calculations. Then this line is again modified to an infinitely long transmission line, and the distributed sources for a plane-wave incident field are calculated. After this a skewed transmission line is investigated. Also here for different excitations all results show a reasonable good agreement with measurements and comparative MoM calculations. In the next application a periodical transmission line is analyzed and very interesting properties are found. For instance, above a certain frequency the input impedance of the line is independent from the termination. In the final example the cross talk in a multiconductor line is calculated and agrees very well with measurements.

Future enhancements of the theory include modifications of the derivation to predict the cross-sectional current and charge distribution. This would allow not only to take into account, but also to calculate the skin and proximity effects in the conductors. As mentioned in Chapter 3 this could be done by introducing appropriate series expansions for the distribution functions.

The consideration of dielectric coating of the wires is also of particular interest. Here ideas from [Pop91] could be applied.

For the determination of the per-unit-length parameters and the source terms the solution of integral equations is required. These solutions are obtained iteratively. The convergence of this iteration has not been proven for the general case. Further investigations are necessary.

Appendix A

Adaption of the Integral Equations to the Conductor Geometry

Here we discuss the manipulations of the integral equation (2.39), that are necessary to adapt this equation to the geometry of a nonuniform multiconductor line. The original equation (see also (2.39)) reads:

$$\text{grad} \frac{1}{\varepsilon} \int_V G(\mathbf{x}, \mathbf{x}') \varrho(\mathbf{x}') dv' + j\omega\mu \int_V G(\mathbf{x}, \mathbf{x}') \mathbf{J}(\mathbf{x}') dv' + \frac{\mathbf{J}(\mathbf{x})}{\sigma} = \mathbf{E}^{(i)}(\mathbf{x}). \quad (\text{A.1})$$

First the volume integrals are split into a sum of integrals over the individual conductor volumina. Moreover, the observation position \mathbf{x} is placed at the surface of one conductor (e.g. j) at ζ , i.e. $\mathbf{x} = \hat{\mathbf{x}}_j(\zeta, \alpha)$:

$$\begin{aligned} \text{grad} \frac{1}{\varepsilon} \sum_{i=1}^N \int_{V_i} G(\hat{\mathbf{x}}_j, \mathbf{x}'_i) \varrho(\mathbf{x}'_i) dv' \\ + j\omega\mu \sum_{i=1}^N \int_{V_i} G(\hat{\mathbf{x}}_j, \mathbf{x}'_i) \mathbf{J}(\mathbf{x}'_i) dv' + \frac{\mathbf{J}(\hat{\mathbf{x}}_j)}{\sigma} = \mathbf{E}^{(i)}(\hat{\mathbf{x}}_j). \end{aligned} \quad (\text{A.2})$$

Now we dot multiply this expression with the tangential unit vector \mathbf{T}_j^u at the observation point. This extracts the tangential component along the conductors, all other components are small and, therefore, neglected.

$$\begin{aligned} \mathbf{T}_j^u(\zeta) \cdot \text{grad} \frac{1}{\varepsilon} \sum_{i=1}^N \int_{V_i} G(\hat{\mathbf{x}}_j, \mathbf{x}'_i) \varrho(\mathbf{x}'_i) dv' \\ + \mathbf{T}_j^u(\zeta) \cdot j\omega\mu \sum_{i=1}^N \int_{V_i} G(\hat{\mathbf{x}}_j, \mathbf{x}'_i) \mathbf{J}(\mathbf{x}'_i) dv' + \mathbf{T}_j^u(\zeta) \cdot \frac{\mathbf{J}(\hat{\mathbf{x}}_j)}{\sigma} = \mathbf{T}_j^u(\zeta) \cdot \mathbf{E}^{(i)}(\hat{\mathbf{x}}_j) \end{aligned} \quad (\text{A.3})$$

Eventually, this expression is averaged over the surface by integration over the angle α :

$$\begin{aligned} & \frac{1}{2\pi} \int_0^{2\pi} \mathbf{T}_j^u(\zeta) \cdot \text{grad} \frac{1}{\varepsilon} \sum_{i=1}^N \int_{V_i} G(\hat{\mathbf{x}}_j, \mathbf{x}'_i) \varrho(\mathbf{x}'_i) dv' d\alpha \\ & + \frac{1}{2\pi} \int_0^{2\pi} \mathbf{T}_j^u(\zeta) \cdot j\omega\mu \sum_{i=1}^N \int_{V_i} G(\hat{\mathbf{x}}_j, \mathbf{x}'_i) \mathbf{J}(\mathbf{x}'_i) dv' d\alpha \\ & + \frac{1}{2\pi} \int_0^{2\pi} \mathbf{T}_j^u(\zeta) \cdot \frac{\mathbf{J}(\hat{\mathbf{x}}_j)}{\sigma} d\alpha = \frac{1}{2\pi} \int_0^{2\pi} \mathbf{T}_j^u(\zeta) \cdot \mathbf{E}^{(i)}(\hat{\mathbf{x}}_j) d\alpha. \end{aligned} \quad (\text{A.4})$$

We may now replace the current and charge density with (3.25) and (3.26) and investigate the individual terms of the expression. After some reordering and the application of

$$\mathbf{T}_j^u \cdot \text{grad} = \frac{1}{u_{jj}} \frac{\partial}{\partial \zeta} \quad (\text{A.5})$$

the first term of the right hand side can be written as

$$\begin{aligned} & \frac{1}{2\pi} \int_0^{2\pi} \mathbf{T}_j^u(\zeta) \cdot \text{grad} \frac{1}{\varepsilon} \sum_{i=1}^N \int_{V_i} G(\hat{\mathbf{x}}_j, \mathbf{x}'_i) \varrho(\mathbf{x}'_i) dv' d\alpha = \\ & \frac{1}{u_{jj}} \frac{\partial}{\partial \zeta} \sum_{i=1}^N \int_{\zeta_0}^{\zeta_i} k_{c_{ji}}(\zeta, \zeta') q_i(\zeta') d\zeta', \end{aligned} \quad (\text{A.6})$$

where

$$k_{c_{ji}}(\zeta, \zeta') = \frac{1}{2\pi\varepsilon} \int_0^{2\pi} \int_{S_i(\zeta')} G(\hat{\mathbf{x}}_j, \mathbf{x}'_i) d_{\varrho_i}(\mathbf{x}'_i) f_{c_i} da' d\alpha. \quad (\text{A.7})$$

The second term can be treated in a very similar way resulting in

$$\frac{1}{2\pi} \int_0^{2\pi} \mathbf{T}_j^u(\zeta) \cdot j\omega\mu \sum_{i=1}^N \int_{V_i} G(\hat{\mathbf{x}}_j, \mathbf{x}'_i) \mathbf{J}(\mathbf{x}'_i) dv' d\alpha = \frac{1}{u_{jj}} \sum_{i=1}^N \int_{\zeta_0}^{\zeta_i} k_{l_{ji}}(\zeta, \zeta') i_i(\zeta') d\zeta', \quad (\text{A.8})$$

with

$$k_{l_{ji}}(\zeta, \zeta') = \frac{\mu}{2\pi} u_{jj}(\zeta) u_{ii}(\zeta') \mathbf{T}_j^u(\zeta) \cdot \mathbf{T}_i^u(\zeta') \int_0^{2\pi} \int_{S_i(\zeta')} G(\hat{\mathbf{x}}_j, \mathbf{x}'_i) d_{\mathbf{J}_i}(\mathbf{x}'_i) f_{c_i} da' d\alpha. \quad (\text{A.9})$$

Evaluating the third term is rather easy and yields

$$\frac{1}{2\pi} \int_0^{2\pi} \mathbf{T}_j^u(\zeta) \cdot \frac{\mathbf{J}(\hat{\mathbf{x}}_j)}{\sigma} d\alpha = \frac{1}{u_{jj}} z_{jj} i_j, \quad (\text{A.10})$$

where z_{jj} is the surface impedance defined as

$$z_{jj}(\zeta) = u_{jj}(\zeta) \frac{1}{2\pi} \int_0^{2\pi} \frac{d_{\mathbf{J}_i}(\hat{\mathbf{x}}_i)}{\sigma} d\alpha. \quad (\text{A.11})$$

Finally, the term on the left hand side, multiplied with u_{jj} , will be assigned to a new variable, i.e.,

$$v_j^{(i)'}(\zeta) = \frac{1}{2\pi} u_{jj}(\zeta) \int_0^{2\pi} \mathbf{T}_j^u(\zeta) \cdot \mathbf{E}^{(i)}(\hat{\mathbf{x}}_j) d\alpha. \quad (\text{A.12})$$

We can now combine these results to the new adapted integral equation

$$\frac{\partial}{\partial \zeta} \sum_{i=1}^N \int_{\zeta_0}^{\zeta_i} k_{c_{ji}}(\zeta, \zeta') q_i(\zeta') d\zeta' + j\omega \sum_{i=1}^N \int_{\zeta_0}^{\zeta_i} k_{l_{ji}}(\zeta, \zeta') i_i(\zeta') d\zeta' + z_{jj} i_j = v_j^{(i)'}(\zeta). \quad (\text{A.13})$$

Appendix B

The Product Integral

B.1 The Differential Equation and its Solution

Many processes in nature can be described with the aid of a system of first-order ordinary differential equations of the form

$$\frac{\partial}{\partial \zeta} \mathbf{X}(\zeta) - \mathbf{C}(\zeta) \mathbf{X}(\zeta) = \mathbf{X}'_s(\zeta) \quad (\text{B.1})$$

where \mathbf{X} is an N -element column vector containing the unknown physical quantities, \mathbf{C} the known $N \times N$ coefficient matrix, characterizing the physical system and $\mathbf{X}'_s(\zeta)$ the known excitation. The solution is constructed with the product integral $\mathcal{M}_{\zeta_0}^{\zeta} \{\mathbf{C}\}$ [Gan84, DF79],

$$\mathbf{X}(\zeta) = \mathcal{M}_{\zeta_0}^{\zeta} \{\mathbf{C}\} \mathbf{X}(\zeta_0) + \int_{\zeta_0}^{\zeta} \mathcal{M}_{\xi}^{\zeta} \{\mathbf{C}\} \mathbf{X}'_s(\xi) d\xi. \quad (\text{B.2})$$

The column vector $\mathbf{X}(\zeta_0)$ is determined by the boundary conditions. The product integral itself fulfills the equation

$$\frac{\partial}{\partial \eta} \mathcal{M}_{\zeta_0}^{\eta} \{\mathbf{C}\} = \mathbf{C}(\eta) \mathcal{M}_{\zeta_0}^{\eta} \{\mathbf{C}\}, \quad (\text{B.3})$$

and the boundary condition

$$\mathcal{M}_{\zeta_0}^{\zeta_0} \{\mathbf{C}\} = \mathbf{1}. \quad (\text{B.4})$$

B.2 The Determination of the Product Integral

One way to calculate the product integral is to integrate (B.3)

$$\mathcal{M}_{\zeta_0}^{\zeta} \{\mathbf{C}\} = \mathbf{1} + \int_{\zeta_0}^{\zeta} \mathbf{C}(\eta) \mathcal{M}_{\zeta_0}^{\eta} \{\mathbf{C}\} d\eta \quad (\text{B.5})$$

and successively replace $\mathcal{M}_{\zeta_0}^\eta \{\mathbf{C}\}$ on the right hand side with (B.5). This yields Picard's series

$$\mathcal{M}_{\zeta_0}^\zeta \{\mathbf{C}\} = \mathbf{1} + \int_{\zeta_0}^\zeta \mathbf{C}(\eta) d\eta + \int_{\zeta_0}^\zeta \mathbf{C}(\eta) \int_{\zeta_0}^\eta \mathbf{C}(\xi) d\xi d\eta + \dots \quad (\text{B.6})$$

Volterra developed a different formula for the product integral. He divided the interval $[\zeta_0, \zeta]$ into k subintervals, with $\zeta_i, i = 0 \dots k$ being the interval boundaries. Then by letting the number of subintervals go to infinity and the subinterval size to zero, the product integral is given by

$$\mathcal{M}_{\zeta_0}^\zeta \{\mathbf{C}\} = \lim_{k \rightarrow \infty} \prod_{i=0}^{k-1} e^{(\zeta_{i+1} - \zeta_i) \mathbf{C}(\zeta_i)} \quad (\text{B.7})$$

$$= \prod_{\zeta_0}^\zeta e^{\mathbf{C}(\eta) d\eta}. \quad (\text{B.8})$$

It was this operation that inspired the name product integral, because it is similar to the ordinary integral, but instead of the summation there is a multiplication. This formula is also suitable for a numerical evaluation of the product integral, in this case k is kept finite. There are many more methods for numerical calculations, the most important are discussed in [HNS03].

A third way to determine the product integral is to develop its Taylor series at ζ_0 :

$$\mathcal{M}_{\zeta_0}^\zeta \{\mathbf{C}\} = \mathbf{M}_0 + \mathbf{M}_1 (\zeta - \zeta_0) + \frac{1}{2} \mathbf{M}_2 (\zeta - \zeta_0)^2 + \dots + \frac{1}{n!} \mathbf{M}_n (\zeta - \zeta_0)^n + \dots \quad (\text{B.9})$$

With the aid of (B.3) and corresponding derivatives, it is easy to find a recursive expression for the coefficient matrices:

$$\mathbf{M}_0 = \mathbf{1} \quad (\text{B.10})$$

$$\mathbf{M}_n = \sum_{i=0}^{n-1} \binom{n-1}{i} \left(\frac{\partial^{n-i-1}}{\partial \zeta^{n-i-1}} \mathbf{C}(\zeta) \right) \Big|_{\zeta=\zeta_0} \mathbf{M}_i \quad (\text{B.11})$$

For a commuting parameter matrix function, i.e. $\mathbf{C}(\eta_1) \mathbf{C}(\eta_2) = \mathbf{C}(\eta_2) \mathbf{C}(\eta_1)$, the product integral simplifies to the matrix exponential and one gets

$$\mathcal{M}_{\zeta_0}^\zeta \{\mathbf{C}\} = e^{\int_{\zeta_0}^\zeta \mathbf{C}(\eta) d\eta}. \quad (\text{B.12})$$

B.3 Inverse Operation

The inverse operation of product integration is product differentiation. The product derivative is defined by

$$\mathcal{D}_\zeta \{\mathbf{C}\} := \frac{\partial \mathbf{C}(\zeta)}{\partial \zeta} \mathbf{C}(\zeta)^{-1}. \quad (\text{B.13})$$

Thus we may write

$$\mathcal{D}_\zeta \left\{ \mathcal{M}_{\zeta_0}^\zeta \{\mathbf{C}\} \right\} = \mathbf{C}. \quad (\text{B.14})$$

B.4 Calculation Rules for the Product Integral

There are several rules that can be applied to the product integral, the most important are:

$$\mathcal{M}_{\zeta_0}^\zeta \{\mathbf{C}\} = \mathcal{M}_{\zeta_1}^\zeta \{\mathbf{C}\} \mathcal{M}_{\zeta_0}^{\zeta_1} \{\mathbf{C}\} \quad (\text{B.15})$$

$$\mathcal{M}_{\zeta_0}^\zeta \{\mathbf{C}\} = \left(\mathcal{M}_\zeta^{\zeta_0} \{\mathbf{C}\} \right)^{-1} \quad (\text{B.16})$$

$$\mathcal{M}_{\zeta_0}^\zeta \{\mathbf{X}\mathbf{C}\mathbf{X}^{-1}\} = \mathbf{X} \mathcal{M}_\zeta^{\zeta_0} \{\mathbf{C}\} \mathbf{X}^{-1} \quad (\mathbf{X} = \text{const.}) \quad (\text{B.17})$$

$$\mathcal{M}_{\zeta_0}^\zeta \{\mathbf{C} + \mathcal{D}_\eta \mathbf{X}\} = \mathbf{X}(\zeta) \mathcal{M}_{\zeta_0}^\zeta \{\mathbf{X}^{-1} \mathbf{C} \mathbf{X}\} \mathbf{X}(\zeta_0)^{-1} \quad (\mathbf{X} = \mathbf{X}(\zeta)). \quad (\text{B.18})$$

Appendix C

Solutions for Some Important Integrals

C.1 Integrals Involving Powers of $\sqrt{x^2 + b^2}$

For the numerical evaluation of the parameters the following integral must be solved:

$$I_{np} = \int \frac{\left(\sqrt{x^2 + b^2} - \sqrt{x_c^2 + b^2}\right)^p}{\sqrt{x^2 + b^2}} (x - x_c)^n dx. \quad (\text{C.1})$$

It is possible to derive a general solution involving the hypergeometric function [AS72], which, however, is rather complicated. We will give simpler solutions for individual numbers n and p . We can distinguish between two cases here, namely $b > 0$ and $b = 0$. The table below shows the results for $n = 0, 1, 2$ and $p = 0, 1, 2$ for the first case. These and higher order terms can be easily obtained with a computer algebra system or with the aid of integral tables and partial integration.

n	p	I_{np}
0	0	$\operatorname{arcsinh} \frac{x}{b}$
1	0	$\sqrt{x^2 + b^2} - x_c \operatorname{arcsinh} \frac{x}{b}$
2	0	$\left(\frac{1}{2}x - 2x_c\right) \sqrt{x^2 + b^2} + \left(x_c^2 - \frac{1}{2}b^2\right) \operatorname{arcsinh} \frac{x}{b}$
n	1	$\frac{(x - x_c)^{n+1}}{n + 1} - \sqrt{x_c^2 + b^2} I_{n0}$

n	p	I_{np}
0	2	$\frac{1}{2}x\sqrt{x^2+b^2} + \left(\frac{3}{2}b^2 + x_c^2\right) \operatorname{arcsinh}\frac{x}{b} - 2(x-x_c)\sqrt{x_c^2+b^2}$
1	2	$\left(\frac{1}{3}x - \frac{1}{2}xx_c + x_c^2 + \frac{4}{3}b^2\right) \sqrt{x^2+b^2} - x_c\left(\frac{3}{2}b^2 + x_c^2\right) \operatorname{arcsinh}\frac{x}{b} - (x-x_c)^2\sqrt{x_c^2+b^2}$
2	2	$\left(\frac{1}{4}x^3 - \frac{2}{3}x^2x_c + xx_c^2 - 2x_c^3 - b^2\left(\frac{5}{8}x - \frac{8}{3}x_c\right)\right) \sqrt{x^2+b^2} +$ $\left(x_c^4 - \frac{5}{8}b^4 + x_c^2b^2\right) \operatorname{arcsinh}\frac{x}{b} - \frac{2}{3}(x-x_c)^3\sqrt{x_c^2+b^2}$

If $b = 0$ the integral becomes

$$I_{np} = \int \frac{(x-x_c)^{p+n}}{x} dx \quad (\text{C.2})$$

and the solution is much simpler. The results are given in the table below.

$n+p$	I_{np}
0	$\ln x$
1	$x - x_c \ln x$
2	$\frac{1}{2}x^2 - 2xx_c + x_c^2 \ln x$
3	$\frac{1}{3}x^3 - \frac{3}{2}x^2x_c + 3xx_c^2 + x_c^3 \ln x$
4	$\frac{1}{4}x^4 - \frac{4}{3}x^3x_c + 3x^2x_c^2 - 4xx_c^3 + x_c^4 \ln x$

C.2 Integrals Involving Exponential and Power Functions

The solution of the integral

$$\int \frac{e^{-jk(\sqrt{(\zeta'-\zeta)^2+b^2}+\zeta'-\zeta)}}{\sqrt{(\zeta'-\zeta)^2+b^2}} (\zeta'-\zeta)^p d\zeta', \quad (\text{C.3})$$

can be found by substituting

$$t = -jk \left(\sqrt{(\zeta' - \zeta)^2 + b^2} + \zeta' - \zeta \right) \tag{C.4}$$

giving:

$$\int \frac{e^t}{t} \left(\frac{(jkb)^2 + t^2}{2jkt} \right)^p dt. \tag{C.5}$$

For the first three values of p the results are summarized in the table below.

p	$\int \frac{e^t}{t} \left(\frac{(jkb)^2 + t^2}{2jkt} \right)^p dt$
0	$-E_1(-t)$
1	$\frac{e^t}{2jk} - (jkb)^2 E_1(-t)$
2	$\frac{e^t(t-1)}{(2jk)^2} + jkb^2 e^t - (jkb)^4 E_1(-t)$
3	$\frac{e^t(t^2-2t+2)}{(2jk)^3} + \frac{3}{2}(jk)^3 b^4 e^t + \frac{3}{4}b^2 e^t(t-1) - (jkb)^6 E_1(-t)$

C.3 Integrals Involving Trigonometric and Exponential Functions

$$\int_{-\infty}^{\infty} \frac{\cos \left(k \sqrt{\zeta^2 + b^2} \right)}{\sqrt{\zeta^2 + b^2}} \cos(k_1 \zeta) d\zeta = \begin{cases} -\pi Y_0 \left(b \sqrt{k^2 - k_1^2} \right) & k > k_1 > 0 \\ 2K_0 \left(b \sqrt{k_1^2 - k^2} \right) & k_1 > k > 0 \end{cases} \tag{C.6}$$

$$\int_{-\infty}^{\infty} \frac{\sin \left(k \sqrt{\zeta^2 + b^2} \right)}{\sqrt{\zeta^2 + b^2}} \cos(k_1 \zeta) d\zeta = \begin{cases} -\pi J_0 \left(b \sqrt{k^2 - k_1^2} \right) & k > k_1 > 0 \\ 0 & k_1 > k > 0 \end{cases} \tag{C.7}$$

Then:

$$\begin{aligned} & \int_{-\infty}^{\infty} \frac{e^{-jk\sqrt{(\zeta'-\zeta)^2+b^2}}}{\sqrt{(\zeta'-\zeta)^2+b^2}} e^{-jk_1(\zeta'-\zeta)} dz' \\ &= \begin{cases} -\pi Y_0 \left(a \sqrt{k^2 - k_1^2} \right) - j\pi J_0 \left(a \sqrt{k^2 - k_1^2} \right) \\ +\pi Y_0 \left(2h \sqrt{k^2 - k_1^2} \right) + j\pi J_0 \left(2h \sqrt{k^2 - k_1^2} \right) & k > k_1 > 0 \\ 2K_0 \left(a \sqrt{k_1^2 - k^2} \right) - 2K_0 \left(2h \sqrt{k_1^2 - k^2} \right) & k_1 > k > 0 \end{cases} \end{aligned} \tag{C.8}$$

with $H_0^{(2)}(z) = J_0(z) - jY_0(z)$

$$\int_{-\infty}^{\infty} \frac{e^{-jk\sqrt{(\zeta' - \zeta)^2 + b^2}}}{\sqrt{(\zeta' - \zeta)^2 + b^2}} e^{-jk_1(\zeta' - \zeta)} d\zeta' = \begin{cases} -j\pi \left[H_0^{(2)} \left(a\sqrt{k^2 - k_1^2} \right) - H_0^{(2)} \left(2h\sqrt{k^2 - k_1^2} \right) \right] & k > k_1 > 0 \\ 2 \left[K_0 \left(a\sqrt{k_1^2 - k^2} \right) - K_0 \left(2h\sqrt{k_1^2 - k^2} \right) \right] & k_1 > k > 0 \end{cases} \quad (\text{C.9})$$

The function J_0 is the Bessel function of first kind, Y_0 the Bessel function of second kind, K_0 the modified Bessel function of second kind, and $H_0^{(2)}$ the Hankel function of second kind.

In free space we have $k_1 = k$, thus the limits of the above formulae must be taken. For both of the above cases the result is:

$$\lim_{k_1 \rightarrow k} \int_{-\infty}^{\infty} \frac{e^{-jk\sqrt{(\zeta' - \zeta)^2 + b^2}}}{\sqrt{(\zeta' - \zeta)^2 + b^2}} e^{-jk_1(\zeta' - \zeta)} d\zeta' = 2 \ln \frac{2h}{a} \quad (\text{C.10})$$

Bibliography

- [APG79] A. K. Agrawal, H. J. Price, and S. H. Gurbaxani. Transient response of multi-conductor transmission line excited by a nonuniform electromagnetic field. Interaction Note 367, www-e.uni-magdeburg.de/notes, July 1979.
- [Arf85] G. Arfken. *Mathematical Methods for Physicists*. Academic Press, Orlando, FL, 3 edition, 1985.
- [AS72] M. Abramowitz and I. A. Stegun, editors. *Handbook of Mathematical Functions with Formulas, Graphs, and Mathematical Tables*. Dover, 9th printing edition, 1972.
- [Bal89] Constantine A. Balanis. *Advanced engineering electromagnetics*. Wiley, New York, NY, 1989.
- [Bau02] Carl E. Baum. About the name of the new transmission-line theory. private communication, 2002.
- [Bau04] Carl E. Baum. About the name of the scalar potential/voltage in the transmission-line supertheory. private communication, 2004.
- [BLT78] C. Baum, T.K. Liu, and F.M. Tesche. On the Analysis of General Multi-conductor Transmission-line Networks. Interaction Note 350, www-e.uni-magdeburg.de/notes, November 1978.
- [BNS96] C. E. Baum, J. Nitsch, and R. Sturm. Analytical solution for uniform and nonuniform multiconductor transmission lines with sources. In W. R. Stone, editor, *Review of Radio Science*, pages 433–464. Oxford University Press, 1996. ISBN 0-19-856531-3.
- [BNS97] C. E. Baum, J.B. Nitsch, and R. J. Sturm. Nonuniform multiconductor transmission lines and networks. In *Progress in electromagnetic research symposium PIERS*, Hong Kong, January 1997. ISBN 962-442-097-1, 962-442-098-X.

- [BS03] C. E. Baum and T. Steinmetz. An interpolation technique for analyzing sections of nonuniform multiconductor transmission lines. In *15th International Zurich Symposium and Technical Exhibition on Electromagnetic Compatibility, February 18 - 20, 2003*, pages 593–596, Zurich, Switzerland, February 2003.
- [Col91] R.E. Collin. *Field theory of guided waves*. IEEE Press, New York, 1991.
- [DF79] J.D. Dollard and C.N Friedman. *Product Integration with Application to Differential Equations*. Addison-Wesley Publishing Company, Reading, Massachusetts, 1979.
- [DSH87] A.R. Djordjevic, T.R. Sarkar, and R.F. Harrington. Time domain response of multiconductor transmission lines. *Proceedings IEEE*, 75(6):743–764, 1987.
- [Dud94] Donald G. Dudley. *Mathematical foundations for electromagnetic theory*. IEEE Press, New York, NY, 1994.
- [DZ88] P. Degauque and A. Zeddani. Remarks on the Transmission-Line Approach to Determining the Current Induced on Above-Ground Cables. *IEEE Transactions on EMC*, 30(1):77, February 1988.
- [Fra97] G. Franceschetti. *Electromagnetics*. Plenum Press, New York, 1997.
- [GA94] P. Graneau and A. K. T. Assis. Kirchhoff on the motion of electricity in conductors. *Apeiron*, 19:19–25, 1994.
- [Gan84] F.R. Gantmacher. *The theory of matrices*, volume 2. New York: Chelsea Publishing Company, 1984.
- [GC86] H.E. Green and J.D. Cashman. End Effect in Open-Circuited Two-Wire Transmission Lines. *IEEE Transactions on MTT*, 34(1):180, January 1986.
- [GCT78] D.V. Giri, S.K. Chang, and F.M. Tesche. A coupling model for a pair of skewed transmission lines. Interaction Note 349, www-e.uni-magdeburg.de/notes, September 1978.
- [Get93] W.J. Getsinger. End-Effects in Quasi-TEM Transmission Lines. *IEEE Transactions on MTT*, 41(4):666, April 1993.
- [GN99] F. Gronwald and J. Nitsch. The physical origin of gauge invariance in electrodynamics. *Electrical Engineering*, 81:363–367, 1999.
- [Haa02] H. Haase. Berechnung der Störeinkopplung in komplexe Leitungssysteme, 1. Zwischenbericht. October 2002.

- [Har67] R.F. Harrington. Matrix methods for field problems. *Proc. IEEE*, 55(2):136–149, February 1967.
- [Hea25] O. Heaviside. *Electromagnetic Theory*, volume II. Ernest Benn LTD, London, 1925. First published in 1899.
- [Hea51] O. Heaviside. *Electromagnetic Theory*. E.&F.N. SPON LTD, London, 1951.
- [HKWN04] H. Haase, S. Kotchetov, G. Wollenberg, and J. Nitsch. Einkopplung externer Störfelder in ungleichförmige Leitungen – Analyse im Frequenz- und Zeitbereich – (Coupling of external fields to nonuniform transmission lines – analysis in time and frequency domain–). In *EMV2004*, Düsseldorf, February 2004.
- [HN00a] H. Haase and J. Nitsch. HPM coupling to wire structures including radiation effects. In *Euro Electromagnetics EUROEM 2000*, page 14/8.1, Edinburgh, 2000.
- [HN00b] H. Haase and J. Nitsch. Parameter ungleichförmig geführter Leitungen. In *EMV 2000*, pages 119–126, Düsseldorf, February 2000.
- [HN01a] H. Haase and J. Nitsch. Feldeinkopplung in dreidimensionalen Leitungsstrukturen mittels einer Full-Wave Leitungstheorie. In *Kleinheubacher Berichte*, volume 44, pages 117–124. T-Nova, Deutsche Telekom Innovationsgesellschaft mbH, 2001. ISSN 0343-5725.
- [HN01b] H. Haase and J. Nitsch. Full-Wave Telegraphengleichungen (FWTLT) für dreidimensionale Leitungsstrukturen. In *EMC Kompendium*, page 121. publish-industry Verlag, GmbH, München, ISBN 3-934698-02-6, 2001.
- [HN01c] H. Haase and J. Nitsch. Full-wave transmission line theory (FWTLT) for the analysis of three-dimensional wire-like structures. In *14th International Zurich Symposium and Technical Exhibition on Electromagnetic Compatibility*, pages 235–240, Zurich, February 2001.
- [HN01d] H. Haase and J. Nitsch. Generalized transmission-line theory for the treatment of nonuniform multiconductor transmission lines. In *XI. International Symposium on Theoretical Electrical Engineering*, August 2001.
- [HN02a] H. Haase and J. Nitsch. Generalized telegrapher equations for radiating nonuniform transmission lines. In *PIERS*, page 739, Cambridge, Massachusetts, USA, July 2002.

- [HN02b] H. Haase and J. Nisch. High frequency excitation of pcb structures. In *AMEREM*, page 17, Annapolis, Maryland, USA, June 2002.
- [HN03a] H. Haase and J. Nitsch. Generalized transmission-line theory for the treatment of nonuniform multiconductor transmission lines. *Journal of Applied Electromagnetics and Mechanics*, 17(1-3):149–156, 2003.
- [HN03b] H. Haase and J. Nitsch. Investigation of nonuniform transmission line structures by a generalized transmission–line theory. In *15th International Zurich Symposium and Technical Exhibition on Electromagnetic Compatibility*, pages 597–602, Zurich, February 2003.
- [HNS03] H. Haase, J. Nitsch, and T. Steinmetz. Transmission–Line Super Theory: A new Approach to an Effective Calculation of Electromagnetic Interactions. *URSI Radio Science Bulletin (Review of Radio Science)*, 307:33–60, December 2003.
- [HOR99] F.W. Hehl, Y.N. Obukhov, and G.F. Rubilar. Classical Electrodynamics, A Tutorial on its Foundations. Festschrift für W.E. Grafarend, available at <http://www.lane.gov/as/physics/9907046>, July 1999.
- [HSN01] H. Haase, T. Steinmetz, and J. Nitsch. Effects of nonuniform cables on the propagation and coupling processes at high frequencies. In *Proceedings of the International Conference on Electromagnetics in Advanced Applications*, September 2001.
- [HSN02] H. Haase, T. Steinmetz, and J. Nitsch. Wirkung ungleichförmiger Leitungsführung auf die Ausbreitung- und Kopplungsvorgänge in komplexen ausgedehnten Leitungsnetzwerken bei hohen Frequenzen. In *Tagungsbeitrag 8. Internationale Fachmesse und Kongreß für EMV, Düsseldorf, 09.–1. April 2002*, pages 615–624, EMV 2002, ISBN 3-8007-2684-X, VDE-Verlag, April 2002.
- [HSN04] H. Haase, T. Steinmetz, and J. Nitsch. New propagation models for electromagnetic waves along uniform and nonuniform cables. *Electromagnetic Compatibility, IEEE Transactions on*, 46(3):345–352, August 2004.
- [Jac98] J.D. Jackson. *Classical Electrodynamics*. John Wiley & Sons, Inc., New York, 3 edition, 1998.
- [Kel55] W.T. Kelvin. On the theory of the electric telegraph. *Proc. Roy Soc.*, 7:382–399, 1855.
- [Kin55] Ronald P.W. King. *Transmission Line Theory*. McGraw-Hill Book Company, 1955.

- [Kir57a] Gustav Kirchhoff. On the motion of electricity in wires. *Philosophical Magazine*, 13:393–412, 1857.
- [Kir57b] Gustav Kirchhoff. Ueber die Bewegung der Electricität in Drähten. *Annalen der Physik (Poggendorfs Annalen)*, 100, 1857.
- [Kir57c] Gustav Kirchhoff. Ueber die Bewegung der Electricität in Leitern. *Annalen der Physik (Poggendorfs Annalen)*, 102, 1857.
- [Kra99] S. G. Krantz. *Handbook of Complex Variables*. Birkenäuser, Boston, MA, 1999.
- [KS64] P. I. Kuznetsov and R. L. Stratonovich. *The Propagation of Electromagnetic Waves in Multiconductor Transmission Lines*. Pergamon Press, Oxford, London, New York, Paris, 1964. translated from Russian original.
- [Lam76] J. Lam. Equivalent lumped parameter for a bend in a two-wire transmission line: Part I. inductance. Interaction Note 303, www-e.uni-magdeburg.de/notes, December 1976.
- [Lam77] J. Lam. Equivalent lumped parameter for a bend in a two-wire transmission line: Part II. capacitance. Interaction Note 304, www-e.uni-magdeburg.de/notes, January 1977.
- [Lin95] I.V. Lindell. *Methods For Electromagnetic Field Analysis*. NY: Oxford University Press/NJ: IEEE Press, 1992/95.
- [LK99] Weikun Liu and Yoshio Kami. Vertical Riser Effects of a Finite-Length Transmission Line. In *International Symposium on EMC Tokyo, EMC'99 Tokyo*, 1999.
- [Lor67a] L. Lorenz. On the identity of the vibrations of light with electrical currents. *Philosophical Magazine and Journal of Science*, 43:287–301, July-December 1867. Translated from *Annalen der Physik und Chemie*, June 1867.
- [Lor67b] L.V. Lorenz. Über die Identität der Schwingungen des Lichtes mit den elektrischen Strömen. *Poggendorffs Annalen der Physik*, 131:243–263, 1867.
- [Max65] J. C. Maxwell. A dynamical theory of the electromagnetic field. *Philosophical Transactions of the Royal Society of London*, 155:459–512, 1865. This article accompanied a December 8, 1864 presentation by Maxwell to the Royal Society.
- [Max73] J.C. Maxwell. *A Treatise on Electricity and Magnetism*. Clarendon Press, Oxford, 1873.

- [Mei03] Kenneth K. Mei. Theory of maxwellian circuits. *Radio Science Bulletin*, 305:6–13, September 2003.
- [MF53] P. M. Morse and H. Feshbach. *Methods of Theoretical Physics, Part I*. McGraw-Hill, New York, 1953.
- [Mie00] G. Mie. Elektrische Wellen an zwei parallelen Drähten (Electrical waves along two parallel wires). *Annalen der Physik*, 2(6):201, 1900.
- [NBS92] J. Nitsch, C. E. Baum, and R. Sturm. Analytical treatment of circulant nonuniform multiconductor transmission lines. *IEEE Trans. Electromagn. Compat.*, 34:28–38, 1992.
- [NG99] J. Nitsch and F.: Gronwald. Analytical solutions in multiconductor transmission line theory. *IEEE Transactions on Electromagnetic Compatibility*, 4(41):469–479, November 1999.
- [NHFY95] T. Nakamura, N. Hayashi, H. Fukuda, and S. Yokokawa. Radiation from the transmission line with an acute bend. *IEEE Transactions on EMC*, 37(3):317–325, 1995.
- [Nit98] J. Nitsch. Exact analytical solution for nonuniform multiconductor transmission lines with the aid of the solution of the corresponding matrix Riccati equation. *Electrical Engineering*, 81(2):117–120, May 1998.
- [NR95] C.A. Nucci and F. Rachidi. On the contribution of the electromagnetic field components in field-to-transmission line interaction. *IEEE Transactions on Electromagnetic Compatibility*, 37(4):505 – 508, November 1995.
- [NS01] R. Nevels and C.-S. Shin. Lorenz, Lorentz, and the gauge. *IEEE Antennas and Propagation Magazine*, 43(3):70–72, 2001.
- [NT02] J. Nitsch and S. Tkachenko. Source dependent transmission line parameters – plane wave vs tem excitation. Interaction Note 577, October 2002.
- [NT04a] J. Nitsch and S. Tkachenko. Newest developments in transmission-line theory and applications. Interaction Note 592, www-e.uni-magdeburg.de/notes, September 2004.
- [NT04b] J. Nitsch and S. Tkachenko. Telegrapher equations for arbitrary frequencies and modes: Radiation of an infinite, lossless transmission line. *Radio Science*, 39, 2004.
- [NT04c] J.B. Nitsch and S.V. Tkachenko. Complex-valued transmission-line parameters and their relation to the radiation resistance. *Electromagnetic Compatibility, IEEE Transactions on*, 46(3):477–487, August 2004.

- [NT05] J.B. Nitsch and S.V. Tkachenko. Global and Modal Parameters in the Generalized Transmission Line Theory and their Physical Meaning. *URSI Radio Science Bulletin*, 2005. (submitted).
- [OKH97] M. Omid, Y. Kami, and M. Hayakawa. Field Coupling to Nonuniform and Uniform Transmission Lines. *IEEE Transactions on EMC*, 39(3):201–211, August 1997.
- [O’N66] B. O’Neill. *Elementary Differential Geometry*. Academic Press Inc., New York, 1966.
- [Pau94] C.R. Paul. *Analysis of Multiconductor Transmission Lines*. John Wiley & Sons, New York, 1994.
- [Pop91] B. D. Popovic. *CAD of wire antennas and related radiating structures*. John Wiley & Sons, 1991.
- [Rac93] F. Rachidi. Formulation of the field-to-transmission line coupling equations in terms of magnetic excitation field. *IEEE Transactions on EMC*, 35(3):404–407, August 1993.
- [Rei02] A. Reibiger. Field theoretic description of TEM waves in multiconductor transmission lines. In F. Maio I. Canavero, editor, *Proc. 6th IEEE Workshop on Signal Propagation on Interconnects*, pages 93–96, Torino, Politecnico di Torino, 2002.
- [RW44] Simon Ramo and John Whinnery. *Fields and Waves in modern Radio*. J. Wiley, New York, 1944.
- [Sch55] S.A. Schelkunoff. Conversion of maxwell’s equations into generalised telegraphists’s equations. *Bell Syst. Tech. J.*, pages 995–1043, 1955.
- [SHN02a] T. Steinmetz, H. Haase, and J. Nisch. Field coupling into a network of nonuniform transmission line tubes – measurements inside an eurofighter wing. In *AMEREM*, page 19, Annapolis, Maryland, USA, June 2002.
- [SHN02b] T. Steinmetz, H. Haase, and J. Nitsch. Die Effekte ungleichförmiger Leitungsführung in komplexen ausgedehnten Leitungsnetzwerken. In *EMC Kompendium*, page 95. publish-industry Verlag, GmbH, München, ISBN 3-934698-07-7, 2002.
- [Som64] A. Sommerfeld. *Electrodynamics*. Academic Press, New York, 1964.

- [Ste05] T. Steinmetz. *Analyse dominanter elektromagnetischer Vorgänge in komplexen Systemen unter besonderer Berücksichtigung von ausgedehnten Verbindungsstrukturen*. PhD thesis, Otto-von-Guericke-Universität Magdeburg, 2005.
- [Stu98] R.J. Sturm. On the Theory of Nonuniform Multiconductor Transmission Lines: an Approach to Irregular Wire Configurations. Interaction Note 541, www-e.uni-magdeburg.de/notes, June 1998.
- [Stu99] R.J. Sturm. The treatment of multiconductor nonuniform transmission lines; a comparison of high and low characteristic impedance lines. In *International Symposium on EMC, Magdeburg*, pages 231–234, October 1999.
- [TB94] F.M. Tesche and B.R. Brändli. Observations on the Adequacy of Transmission-Line Coupling Models for Long Overhead Cables. In *International Symposium on EMC*, page 374, Rome, Italy, September 1994.
- [Tes95] F.M. Tesche. Principles and Application of EM Field Coupling to Transmission Lines. In *International Zurich Symposium and Technical Exhibition on EMC*, March 1995.
- [TIK97] F.M. Tesche, M. V. Ianoz, and T. Karlsson. *EMC Analysis Methods and Computational Modells*. NY: John Wiley & Sons, Inc., 1997.
- [TN02] S. Tkachenko and J. Nitsch. Investigation of high-frequency coupling with uniform and non-uniform lines: comparison of exact analytical results with those of different approximations. In *XXVIIth General Assembly of the International Union of Radio Science*, Maastricht, Netherlands, August 2002.
- [TRI99] S. Tkatchenko, F. Rachidi, and M. Ianoz. On the theory of high-frequency wave propagation along nonuniform transmission lines. In *International Symposium on Electromagnetic Compatibility*, Magdeburg, October 1999.
- [TRI01] S. Tkatchenko, F. Rachidi, and M. Ianoz. High-frequency electromagnetic field coupling to long terminated lines. *IEEE Transactions on Electromagnetic Compatibility*, 43(2):117–129, May 2001.
- [TRNS03] S. Tkachenko, F. Rachidi, J. Nitsch, and T. Steinmetz. Electromagnetic field coupling to nonuniform transmission lines: Treatment of discontinuities. In *15th International Zurich Symposium and Technical Exhibition on Electromagnetic Compatibility, February 18 - 20, 2003*, pages 603–608, Zurich, Switzerland, February 2003.

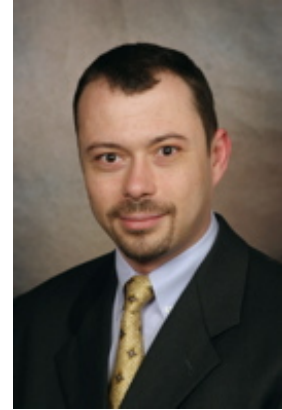
- [TSH65] C. D. Taylor, R. S. Satterwhite, and C. W. Jr. Harrison. The response of a terminated two-wire transmission line excited by a nonuniform electromagnetic field. Interaction Note 66, www-e.uni-magdeburg.de/notes, November 1965.
- [Ung96] H.-G. Unger. *Elektromagnetische Wellen auf Leitungen*. Hüthig Buch Verlag, Heidelberg, 4 edition, 1996. ELTEX.
- [vB91] J. van Bladel. Lorenz or Lorentz. *IEEE Antennas and Propagation Magazine*, 33(2):69, 1991.
- [Wat46] William Watson. Experiments and observations tending to illustrate the nature and properties of electricity. In one letter to Martin Folkes and two to the Royal Society. The 2nd ed. London, Printed for C. Davis, 1746.
- [Wat48] William Watson. In order to discover whether the electrical power would be sensible at great distances. with an experimental inquiry concerning the respective velocities of electricity and sound. Communicated to the Royal Society. London, Printed for C. Davis, 1748.
- [WtH97] D.O. Wendt and J.L. ter Haseborg. Description of electromagnetic effects in the transmission line theory via concentrated and distributed linear elements. In *IEEE AP-S International Symposium and URSI North American Radion Science Meeting*, volume 4, pages 2330–2333, Montréal, Québec, Canada, July 1997.
- [Zur84] Rudolf Zurmühl. *Praktische Mathematik für Ingenieure und Physiker*. Springer-Verlag Berlin, Heidelberg, New York, Tokyo, 1984.

Curriculum Vitae

Dipl.-Ing. Heiko Haase

born on Januar, 30th 1974 in Magdeburg
unmarried

Arndtstr. 49
39108 Magdeburg
Germany
Phone: 0391-811-2306
Mobile: 0179-714-1853



Professional Experience

- 1998 – now **Otto-von-Guericke-University Magdeburg** and
Helmut-Schmidt-University – University of the Federal Armed Forces Hamburg
Research Assistant
Doctorate in March 2005
- 2000 **Amundsen-Scott South Pole Station**
Freelance Job at DESY Zeuthen
Extension of the Data Acquisition System for the Antarctic Muon and Neutrino Detector
Arrays (AMANDA)

Education

- 1992 – 1998 **Otto-von-Guericke-University Magdeburg**
Electrical Engineering
Achievement: German Diplom (*summa cum laude*)
- 1988 – 1992 **Extended Secondary School “Gymnasium Kleinmachnow”**
Achievement: German Abitur (1.7)
- 1980 – 1988 **School “Polytechnische Oberschule Förderstedt”**

Stay Abroad

- 2002 **University of New Mexico**, Albuquerque, New Mexico, USA
Research stay and collaboration with the Air Force Research Lab
- 1995 – 1996 **University of Southern Colorado**, Pueblo, Colorado, USA
Achievement: Bachelor of Science (*summa cum laude*)

Practical Training

- 1997 **DESY Zeuthen**
Development of a Data Acquisition System for the Antarctic Muon and Neutrino Detector
Array

Foreign Languages

English business fluent
Russian basic knowledge

Awards

- 2002 Best HPE Paper Award
- 2001 Summa Foundation Award
- 2001 Antarctica Service Medal
- 1998 Outstanding Diploma Thesis